

https://dspace.org/

Mutations prevalent in fusion protein signal peptides from African RSV strains

Mogawane, Thathego

2025
University of the Witwatersrand, Johannesburg
https://hdl.handle.net/10539/49887
Mogawane, Thathego . (2025). Mutations prevalent in fusion protein signal peptides from African RSV strains [Master's dissertation, University of the Witwatersrand, Johannesburg]. WIReDSpace. https://hdl.handle.net/10539/49887

Downloaded from a DSpace repository. https://dspace.org/

Mutations prevalent in fusion protein signal peptides from African RSV strains



UNIVERSITY OF THE
WITWATERSRAND,
JOHANNESBURG

THATHEGO MOGAWANE

(1614804)

MSc (Medicine)

Division of Medical Virology, School of Pathology

Faculty of Health Sciences

Supervisor: Dr Florette Treurnicht (PhD)

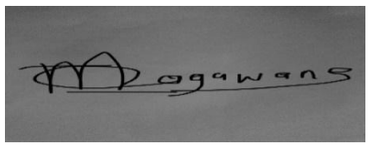
Co-Supervisor: Hloniphile Mthiyane (MSc)

2025

Declaration

I, Thathego Mogawane, hereby declare and confirm that the work on this dissertation is my own original work and other sources were acknowledged where relevant. This dissertation is submitted for the degree of MSc Medicine (Virology) at the University of the Witwatersrand. This work as a whole or in part has not been submitted for any other degree at this or any other institution.

Student Number: 1614804

Signature:  **Date:** **19/08/2025**

Dedication

I dedicate this research to my grandparents (Thabitha and Elias Mogawane) and my mother, aunt, and sister (Nelly, Margaret and Kgothatso Mogawane) respectively.

Conferences proceedings

Presentation at conferences

1. **Mogawane T**.; Mthiyane, H.; Treurnicht, F.K. Signal peptide mutations prevalent among RSV-A and RSV-B strains from Africa. **Virology Africa Conference 2024** (15^{th}-18^{th} April 2024) (Poster Presentation).

2. **Mogawane T**.; Mthiyane, H.; Treurnicht, F.K. Signal peptide mutations prevalent among RSV-A and RSV-B strains from Africa. **University of the Witwatersrand, Faculty of Health Sciences Research Day 2024** (05 September 2024) (Oral presentation).

Acknowledgements

I would like to thank God for the gift of wisdom and the strength he bestowed upon me which enabled me to complete this research. I wouldn't have done it without his guidance, grace and presence in my life.

Secondly, I would like to express my sincere gratitude to my supervisor Dr FK Treurnicht and Ms. Hloniphile Mthiyane for their great support, kindness, guidance, and patience in assisting me with my research. I thank God every day to have been granted the opportunity to work with them. They are such good teachers and care a lot about their students. May God bless them abundantly and forevermore. To my fellow students (Shiba Mbongiseni Smart and Makhene Tshedimoso) as well, thank you so much for taking your time to offer support and assistance in the lab, whenever I struggled.

This research wouldn't have been successful without the financial aid of the National Research Fund (NRF) and Poliomyelitis Research Fund (PRF). From the bottom of my heart, I express my gratitude to these funding schemes.

Finally, I would like to thank my family for their unwavering support in my studies. Their prayers and encouragement kept me going and sustained me thus far and for that I am eternally grateful. May God bless their souls. Finally, I would like to thank myself for not giving up when it was hard but instead kept on pushing until I completed this project. I am so proud of myself.

Funding

This study was funded by NHLS Research trust development-grant. Ms. Mogawane received bursaries towards her MSc degree studies from the National Research Foundation (2022-2024) and the Poliomyelitis Research Foundation (2022-2023).

Abstract

Background: Two subgroups of RSV are recognized namely, RSV-A and RSV-B. There are two major glycoproteins found on the surface of the virion, F and G glycoprotein. The F protein which is the more conserved major glycoprotein is the main target for vaccine development. The F protein comprises of a signal peptide which is the N terminal extension that targets the F protein to the different secretary pathways in the cytoplasm. Mutations found in the signal peptide may affect the control of gene expression, replication and pathogenicity. This study aimed to investigate the diversity and impact of the most prevalent signal peptide mutations on the expression of F proteins from African RSV strains.

Methods: 4876 African RSV genome and F gene sequences were retrieved from GenBank and GISAID. Nextclade was used to align F protein sequences and to construct phylogenetic trees. 3841 sequences were excluded due to lack of full complete RSV F genome, and the remaining 1035 were compared to the RSV-A A2 long strain and RSV-B B1 reference strains using BioEdit and AliView. These two software tools were also used to edit and trim the sequences and further assessed the positional amino acid frequency in signal peptides alignment. The identified mutations on the signal peptide were introduced into the RSV F protein sequence using site-directed mutagenesis and western blot was done to detect the expressed RSV F proteins.

Results: Among 1035 African RSV F sequences from 2007-2022, the most prevalent subtype was RSV-B at 89,9% (930/1035). The dominant genotypes among RSV-A strains were GA2.3.5 prevalent at 47.6% (50/105) and GA2.3.3 was 34.3% (36/105). Both belong to clade A23. While for RSV-B, GB5.0.5a was prevalent at 66.9% (622/930) and GB5.0.2 at 28.9% (269/930) and belongs to clade B6. Mutations in RSV-A F signal peptides were identified at four amino acid positions (I5T, A8T, T12A/I and L15F) at frequencies of <3%. T12A/I and T8I/A mutations were found in genotype GA2.3.5 (clade A23) South African sequences from 2018 and 2020. The I5T and L15F mutations were among Egyptian strains from 2018-2019. L4P, H6Y, F12L and L15F mutations were observed in RSV-B strains. The RSV F protein was expressed in the HEK-293T cells. The soluble protein fractions contained proteins of 18kDa that corresponded to the expected size of the F2 subunit for mutants that contain the T12I substitution. The I5T mutant protein appeared as a band between 45-55kDa, corresponding to the size of the cleaved F1 subunit. However, subsequent sequencing revealed that none of the expressed proteins have the expected amino acid substitutions. This ultimately meant that our site-directed mutagenesis experiments to introduce the mutations of interest failed.

Discussion: RSV-A mutations were identified at 7/15 amino acid positions and 4/7 positions (5, 8, 12, 15) were the most prevalent, and globally T12I and L15F were the most prevalent. In RSV-B, 7/15 mutations were identified on the signal peptide and 4/7 positions (4, 6, 12, 15) were the most prevalent. F12L and L4P were the most prevalent mutations globally. In general, we

observed that RSV-B signal peptide mutations occurred at a lower frequency. However, we were unable to recover F proteins with mutated signal peptides.

Contents

Declaration 2

Dedication 3

Conferences proceedings 4

Funding 5

Abstract 6

Contents 8

List of figures 10

Figure 3.1. 10

List of tables 11

List of Abbreviations 12

CHAPTER 1 15

INTRODUCTION AND LITERATURE REVIEW 15

1.1.2 Study Rationale 16

1.1.3 Aim and Objectives of the study 16

Aim 16

Objectives 16

1.2.2 Viral structure and Genome 17

1.2.2.1 Signal Peptides 18

1.2.2.2 G Protein 20

1.2.2.3 RSV Fusion protein 20

1.2.2.4 NS1 and NS2 22

1.2.2.5 N Protein 22

1.2.2.6 P protein 23

1.2.2.7 L protein 23

1.2.2.8 M protein 24

1.2.2.9 M2-1 protein 24

1.2.2.10 M2-2 protein 25

1.2.2.11 SH Protein 25

1.2.3 RSV genetic diversity 25

1.2.3.3. Impacts of genetic diversity on disease severity and clinical outcomes 27

1.2.3.4. Molecular understanding of RSV biology 28

1.2.11 Vaccine Development (RSV prevention) 34

1.2.12 Recent developments on RSV vaccine development 37

1.2.13 Challenges in RSV vaccine development 38

1.2.14 Laboratory diagnostics methods 38

1.2.15 Factors affecting the sensitivity and specificity of the assay 40

1.15. Summary 40

CHAPTER 2 42

MATERIALS AND METHODS 42

2.1. Study setting. 42

2.2. RSV F gene sequence data 42

2.3. F gene and SP sequence analysis 42

2.4. Laboratory Methods 43

2.4.3. Plasmid DNA purification 44

2.6.5. Mini Plasmid DNA purification 47

2.12. SDS-PAGE and Western Blotting to detect mutated F clone expression. 51

2.14. Ethics 52

CHAPTER 3 53

RESULTS 53

CHAPTER 4 67

DISCUSSION 67

REFERENCES 70

Appendices 82

Appendix A: Media, buffer and reagent 82

APPENDIX B: General information of the RSV-A fusion glycoprotein ORF mammalian expression plasmid. 84

APPENDIX C: Control pCMV expression plasmid 86

APPENDIX D: Ethical clearance waiver approval letter 87

APPENDIX E: Word count and Plagiarism report 88

List of Figures

Figure 1.1. Virion structure of RSV

Figure 1.2. Structure of respiratory syncytial virus (RSV)F protein and RSV fusion/entry processes.

Figure 1.3. RSV clinical manifestations in Adults, Elderly, and Immunocompromised.

Figure 2.1. Overview of research methodology including all the laboratory procedures stepwise.

Figure 3.1. Nextclade construct phylogenetic tree for RSV-A with (a) showing the African sequences and reference global data combined whereas (b) shows *only* the African sequences (n=105) from this study.

Figure 3.2. Nextclade construct tree for RSV-B with (a) showing the African sequences and reference global data combined whereas (b) highlights *only* the African sequences (n=930) from this study.

Figure 3.3. Global data from GISAID shows geographic origin of RSV-A strains with mutations highlighted for the number of occurrences in different colors on the global maps.

Figure 3.4. Global data from GISAID shows geographic origin of the mutations found in RSV-B, with the number of occurrences.

Figure 3.5. Gel electrophoresis results of the mini & midi prep for RSV F site directed mutagenesis, analyzed by electrophoresis in 2% agarose gel.

Figure 3.6. The two transformants with mutations, P5 and P12 were sent for sequencing to confirm the insertions of mutations and check for variation between the transformants with mutations and RSV F protein wildtype.

Figure 3.7. Expression of the RSV F protein on SDS-PAGE using supernatants treated in HEK-293T cells and harvested 48 hours post to transfection.

Figure 3.8. The western blot analysis of RSV F protein expression in HEK 239T cells treated with human plasma samples as primary antibody.

Figure 3.9. BCA protein assay. BSA standard curve using the standard microplate well protocol.

List of tables

Table 2.1. List of primers for the identified mutations for site directed mutagenesis.

Table 2.2. Exponential amplification (PCR) reagents.

Table 2.3. Thermocycling conditions for a routine PCR in site directed mutagenesis.

Table 2.4. BSA standard dilution scheme for the 96 well microplate procedure to determine protein quantification.

Table 2.5. Pipetting protocol for ELISA, with the hepatitis C plasma antibodies and calibrators.

Table 3.1. Summary RSV-A F genes clades detected in Africa with their genotypes and the period they were detected.

Table 3.2. Summary RSV-B F genes clades detected in Africa with their genotypes and the period they were detected.

Table 3.3. Positional amino acid frequencies in RSV-A signal peptide (N=105).

Table 3.4. Summary of genotype, geographic location, and year of detection of RSV-A strains with key signal peptide mutations.

Table 3.5. Global frequency of select signal peptide sequence mutations for RSV-A determined using RSVsurver GISAID.

Table 3.6. Positional amino acid frequencies in RSV-B signal peptide, (N=287).

Table 3.7. Summary of the most prevalent mutations in RSV-B with their genotypes, geographic locations, and the period they were detected.

Table 3.8. Global sequence data of mutations that occurred in RSV-B signal peptide acquired from GISAID.

Table 3.9. Summary of the results from ELISA with ratios values calculated to identify positive/negative samples.

Table 3.10. Absorbance of standards and samples concentrations.

List of Abbreviations

ATF6: Activated transcription factor 6

BA: Buenos Aires

Bcl-2: B-cell lymphoma type 2

CMJAH: Charlotte Maxeke Johannesburg Academic Hospital

CD8+T cell: Cytotoxic T cell

CDC: Centers for Disease Control and Prevention

COVID-19: Coronavirus disease of 2019

COPD: Chronic obstructive pulmonary disease

CMV: Cytomegalovirus

CX3CR1: CX3C motif chemokine receptor 1

CP: Cytoplasm domains

DC: Dendritic cells

DMEM: Dulbecco's modified Eagle medium

DNA: Deoxyribonucleic acid

DR4/5: Death receptor 4 and 5

EBOV: Ebolavirus

ERD: Enhanced respiratory disease

F: Fusion protein

FBS: Fetal bovine serum

FCS: Furin cleavage site

FDA: Food and drug administration

FI-RSV: Formalin inactivated respiratory syncytial virus vaccine

FP: Fusion peptide

GAGs: glycosaminoglycans

HEK293T: Human embryonic kidney SV40 large T antigen cell line

HCL: Hydrochloric acid

hMPV: Human metapneumovirus

HRA: Heptad repeat A

HRB: Heptad repeat B

HRC: Heptad repeat C

HSCT: Hematopoietic stem cell transplantation

HPLC: High performance liquid chromatography

IBs: Inclusion bodies

IDT: Integrated DNA technologies

IFN: Interferon

IGF1R: Insulin growth factor 1 receptor

IgA: Immunoglobulin A

IgG: Immunoglobulin G

IgM: Immunoglobulin M

IPTG: Isopropyl β-d-1 thiogalactopyranoside

IRE 1: Inositol-requiring enzyme

IV:	Intravenous
G:	glycoprotein G
GISAID:	Global Initiative on Sharing Avian Influenza Data
Gly:	Glycine
Gm:	Membrane bound G protein
GSK:	GlaxoSmithKline
L:	Large polymerase protein
LAV:	Live-attenuated vaccine
LB:	Luria broth
LRTI:	Lower respiratory tract illness
M2:	Matrix protein 2
mAb:	Monoclonal antibody
MALRTI:	Medically attended lower respiratory tract infections
MDA5:	Melanoma differentiation-associated gene
MAVS:	Mitochondrial antiviral signaling
N:	Nucleoprotein
NaCl:	Sodium Chloride
NAT:	Nucleic acid amplification testing
NmPCR:	nested multiplex PCR
NOX2:	NADPH oxidase 2
NHLS:	National Health Laboratory Service
NF-κb:	Nuclear factor κB
NRLs:	NOD-like receptors
NS:	Nonstructural
ON1:	Ontario 1
PAGE:	Polyacrylamide gel electrophoresis
P:	Phosphoprotein
PBS:	Phosphoproteins buffered saline
P27:	protein 27
PICU:	Pediatric intensive care unit
Post:	F- post-fusion
Pre-f:	Prefusion
PZMB:	Palivizumab
RdRp:	RNA-dependent RNA polymerase
RNA:	Ribonucleic Acid
RNP:	Ribonucleoprotein complex
RIG-1:	Retinoic acid-inducible gene I
RSV:	Respiratory Syncytial Virus
RSV-A:	Respiratory syncytial Virus subtype A
RSV-B:	Respiratory syncytial Virus subtype B
RT-PCR:	Reverse transcriptase-mediated polymerase chain reaction
ROS:	Reactive oxygen species

sG:	Secreted G protein
SH:	Small hydrophobic
SOC:	Super optimal broth with catabolite repression
SDS:	Sodium dodecyl sulfate
SP:	Signal peptide
SPase:	Signal peptidase
SPAG-2:	small-particle aerosol generator model 2
TAE:	Tris-Acetate EDTA
Tat:	Twin-arginine protein translocation
TBST:	Tris buffered saline with tween 20
TBS:	Tris buffered saline
Th:	Helper T lymphocytes
TLR4:	Toll-Like Receptor 4
TM:	Transmembrane
TMB:	Tetramethylbenzidine
TNF:	Tumor necrosis factor
TRAIL:	Tumor necrosis factor-related apoptosis inducing ligand
USA:	United States of America
VR:	Viral replication
WHO:	World Health Organization
WtRSV:	wildtype RSV

CHAPTER 1

INTRODUCTION AND LITERATURE REVIEW

1.1 INTRODUCTION

Respiratory Syncytial Virus (RSV) is one of the frequent causes of hospitalization in infants and the elderly, including other susceptible patients such as those who are immunocompromised, transplant recipients, and those with chronic lung and heart conditions, those receiving active cancer treatment, and people with COPD/asthma (Nowalk *et al*., 2022). Annually, around 33 million RSV-associated lower respiratory tract infections (LRTIs) in children below the age of five result in 3.6 million hospital admissions and roughly 101,400 deaths globally (Li *et al*., 2022). Similarly, before the COVID-19 (Coronavirus disease of 2019) pandemic caused by the severe acute respiratory syndrome coronavirus type 2 (SARS-CoV-2), high-income countries recorded RSV disease burden estimates of 5.2 million illnesses, 470,000 hospitalizations, and 33,000 in-hospital deaths among persons aged 60 and over (Savic *et al*., 2023).

The burden of disease is larger in low- and middle-income countries, indicating that future treatments may be most beneficial to these populations (Savic *et al*., 2023). Greater than 95% of lower respiratory infections and 97% of deaths in all age groups from low income and middle-income countries was associated with RSV as supported by the following estimates: 1,4 million (uncertainty range [UR] 1,0–2,0 million) RSV-associated acute lower respiratory infection hospital admissions, 13 300 (UR 6 800–28 100) RSV-associated acute lower respiratory infection in hospital deaths, and 45 700 (UR 38 400–55 900) RSV-attributable overall deaths with 2,0% (UR 1,6–2,4) of deaths in children aged 0–60 months and 3,6% (UR 3,0–4,4) of deaths in children aged 28 days to 6 months (Li *et al*., 2022).

The RSV season is an annual period where the circulation of RSV increases and presents as distinct epidemic peaks which are commonly seen during autumn and winter in both hemispheres (Staadegaard *et al*., 2024). Children under 2 years may experience RSV infection during these RSV seasons, however RSV reinfections are common in children under 5 years during subsequent RSV seasons (Nduaguba *et al*., 2023). Palivizumab (Synagis) and nirsevimab (Beyfortus) are monoclonal antibodies that are approved to prevent RSV disease in all infants who will be experiencing their first RSV season, which is usually during their first year of life when they have risk of RSV infection due limited or no preexisting immunity. Palivizumab and nirsevimab may also be administered to high-risk newborns (born prematurely or with chronic lung or heart disease) for severe RSV disease in their second RSV season, which usually occurs in the year following their first exposure (Staadegaard *et al*., 2024). Both therapeutics showed 40% to 80% efficacy in prophylaxis based on the risk factors for hospitalization (Jones *et al*., 2023).

Two RSV vaccines, Arexvy (GSK) and Abrysvo (Pfizer), were licensed in 2023. Abrysvo is approved for vaccination of women in their third trimester of pregnancy to protect newborns less

than 6 months old against RSV disease through passively acquired maternal antibodies (Wise., 2023). Both Abrysvo and Arexvy are approved for use in persons 60 years and older to prevent severe RSV outcomes (Wise., 2023). Recently, the US government also approved mRESVIA, Moderna's mRNA-1345 vaccine, for use in elderly people (Mullard *et al*., 2024). This makes it the third vaccine. Only ribavirin, oral or aerosolized, is, however, authorized for use as a therapy in several countries, despite complicated efficacy and safety issues (Tejada *et al*., 2022). As a result, RSV therapy clearly demonstrates an unmet medical need.

1.1.2 Study Rationale

Several studies have reported on the sequence variability of the RSV fusion gene; however, they did not investigate the impact of these changes on the F-protein (Day *et al*., 2006; Hause *et al*., 2017; Tapia *et al*., 2014). Tapia *et al* hypothesized that a study beyond genotype classification is needed because the sequence diversity might have an impact on the biology of infection and disease by providing the virus with possible survival advantage in a partially immune protected community (Tapia *et al*., 2014). Therefore, in this study, I aim to investigate the impact of F protein signal peptide mutations prevalent among African RSV strains on *in vitro* expression.

The results of this may provide insight on the impact of signal peptide mutations on F protein expression levels which may contribute to future studies to determine impact on F protein cleavage, oligomerization, and glycosylation. Therefore, our research question is what the extent of diversity among RSV-A & B F proteins' signal peptides is and how these differences impact protein expression. We hypothesize that the mutations found in the signal peptides of RSV-F introduce changes in the expression of F *in vitro* and this may indicate the potential of F incorporation into virus progeny which in turn may impact on the ability to induce lasting protective immune responses.

1.1.3 Aim and Objectives of the study

Aim: The aim is to investigate the diversity and impact of the most prevalent signal peptide mutations on the expression of F-proteins from African RSV strains.

Objectives:

- To retrieve RSV F gene sequences from GenBank/GISAID online databases and perform multiple sequence alignment to determine the amino acid diversity of the signal peptides.
- To use site-directed mutagenesis to introduce the most prevalent signal peptide mutations into an RSV-F clone.
- To assess the impact of mutations on F-protein expression *in vitro*.

1.2 LITERATURE REVIEW

1.2.1 History and Epidemiology

RSV was initially identified in 1956 in throat swabs collected from chimpanzees with symptoms such as nasal discharge, coughing, and sneezing, as has also been shown in other investigations (Carvajal *et al*., 2019; Chanock *et al*., 1962). The other monkeys in the colony soon began to exhibit identical symptoms, indicating that the infection was extremely contagious (Carvajal *et al*., 2019). The viral agent was formerly known as Chimp Coryza agent because of its origins (Chanock *et al*., 1962). But later in 1957, a related virus known as RSV was discovered in the throats of newborns suffering from croup and pneumonia (Carvajal et *al*., 2019; Chanock *et al*., 1962). Over sixty years later, RSV remains the primary cause of bronchiolitis in infants and is a frequent cause of life-threatening respiratory illnesses in children <5 years old (Kaler *et al*., 2023). Later, when reports of cases among the elderly began to emerge, the bimodal pattern of RSV was identified. As previously stated, RSV infection is a seasonal illness, with slight variations in duration and severity from nation to nation and from one year to next (Law *et al*., 2002).

Although the precise peak of the season varies by place, RSV infection usually peaks in the winter in temperate regions (Mihaltan., 2022). RSV typically peaks in the hottest months of the rainy season in tropical regions (Mihaltan., 2022). Prior to 2020, these seasonal trends were remarkably stable. Still, the circulation after the COVID-19 pandemic began in early 2020, RSV and other widespread respiratory virus patterns have changed (Mihaltan., 2022). RSV circulation peaked in July 2021 after starting to increase in the southern United States during spring of that year (Olsen *et al*., 2021). Since RSV is so widely dispersed, almost 50% of children in the US have acquired it, and nearly all children have done so by the time they reach two years (Olsen *et al*., 2021).

RSV causes severe lower respiratory tract infections in the first six months of life. Low- and middle-income nations account for most RSV-associated deaths (Regassa *et al*., 2023). Most of these deaths (99%) took place in developing nations, although the true death rate from RSV infection is higher than what is commonly known. The prevalence of RSV in 2023 was reported in the following regions: Northern Africa (30%; 95% confidence interval [CI]: 24%-36%), Southern Africa (23%; 95% CI: 19%-26%), and Eastern Africa (22%; 95% CI: 18%-26%) had the highest RSV prevalence. In Western Africa, the prevalence was 17%, while in Central Africa, it was 9% (Regassa *et al*., 2023).

1.2.2 Viral structure and Genome

RSV is a ribonucleic acid (RNA) virus with a negative sense single stranded RNA genome characteristic of the genus *Orthopneumovirus* and family *Pneumoviridae*. It is enveloped with ten genes that are transcribed into eleven proteins in a sequential order from 3'to 5' (Figure 1.1) (Cao *et al*., 2024), encoded by a 15.2-kb genome. There are ten functional genes (3′ NS1-NS2-N-P-M-SH-G-F-M2-L) present in the 15,191–15,226 nucleotides. M2-1 and M2-2 are encoded by two different ORFs that slightly overlap with each other, and are regulatory proteins

required for transcription (Shishir *et al*., 2023). The large polymerase protein [L], phosphoprotein[P], and nucleocapsid protein [N] are the proteins needed for viral replication (Krisna *et al*., 2023).

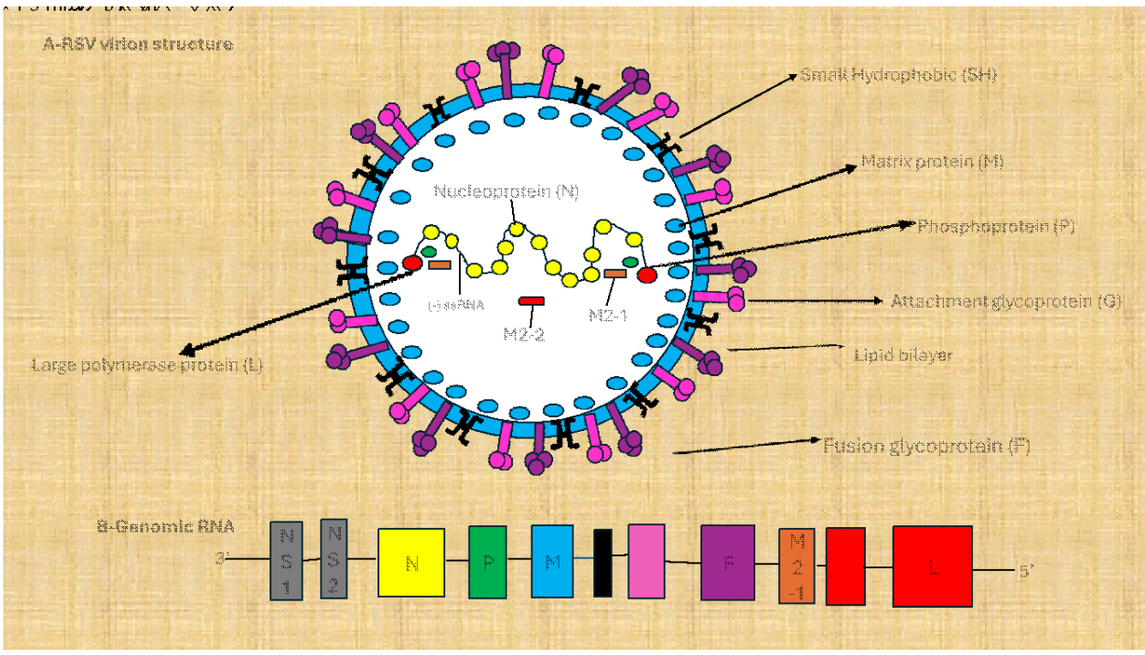


Figure 1.1. (A) Virion structure of RSV. The G(attachment) glycoprotein, F(fusion) glycoprotein, and SH (small hydrophobic) proteins are the three surface glycoproteins that facilitate binding to host cell membrane, mediates membrane fusion for viral entry and involved in ion channel activity, respectively. As the inner envelope protein, the matrix (M) protein forms a layer beneath the envelope. N-Nucleoprotein, forms the nucleocapsid which encapsulates the -ssRNA. The genome is a single-stranded, negative-sense RNA (-ssRNA) associated with several additional proteins: P (phospho-) protein, a polymerase factor, L (large polymerase) protein, responsible for viral RNA synthesis. Lastly, M2-1 and M2-2 are regulatory proteins involved in transcription and genome replication. (B) Diagram of the genomic RNA indicating the order and location of coding gene regions (Adapted from Taleb *et al*., 2018).

The following proteins: fusion glycoprotein [F], structural matrix protein [M], the attachment glycoprotein [G] are utilized by viruses during their assembly (Jha *et al*., 2016). The G and F proteins, along with small hydrophobic protein [SH], are necessary for attachment and entrance into host cells (Jha *et al*., 2016; Krisna *et al*., 2023). The non-structural proteins-1 and −2 [NS1 and NS2] are responsible for evading the host immune responses. They also reduce interferon activity (Krisna *et al*., 2023). Additionally, the G protein's shortened secretory form serves as a decoy for the neutralizing antibodies that target lymphocytes that carry Fc receptors (Collins *et al*., 2013; Jha *et al*., 2016).

1.2.2.1 Signal Peptides

N-terminal signal peptides (SPs) facilitate directing secretory proteins into the secretory route through interacting with chaperones, the membrane-embedded protein-conducting SecYEG channel, and by keeping the translocated protein in an unfolded translocation-competent condition (Kaushik *et al*., 2022). Since these omnipresent targeting signals were studied for so

long, it is well understood what their structural characteristics are. In essence, signal peptidase (SPase) recognition sites (SPases) consist of three regions: a positively charged N-region, a hydrophobic α-helical H-region, and a more polar C-region that often begins with a helix-breaking residue (Peng *et al*., 2019).

Comprehensive studies utilizing site-directed mutagenesis, which involve the deletion or substitution of specific amino acids within the SPs of a variety of distinct exported proteins, have revealed the functions of these three areas as well as the limits of sequence variation within them (Pugsley *et al*., 1989; Grasso *et al*., 2023). Therefore, it has been demonstrated that positively charged residues in the N-region activate the start of protein translocation, which explains why the introduction of negative charge in this area prevents protein translocation (Inouye *et al*., 1982; Grasso *et al*., 2023). A turn-inducing residue like Gly is frequently present in the centre of the H-region, which explains why deletion of the hydrophobic residues or insertion of charged residues interferes with productive protein export (Grasso *et al*., 2023; Peng *et al*., 2019). The H-region also facilitates loop-like insertion of SPs into the membrane.

Additionally, investigations on SPs that target proteins to the alternative twin-arginine protein translocation (Tat) pathway have demonstrated that the presence of positively charged residues at the C-terminal end of the H-region obstructs successful protein translocation via Sec (Tullman-Ercek *et al*., 2007). The generally conserved SPase recognition site Ala–3–X–Ala–1, where X can be any amino acid and −3 and −1 describe the residue locations relative to the SPase cleavage site, was identified via amino acid substitutions in the polar C-region (Peng *et al*., 2019). These investigations demonstrated the significance of a turn-inducing Pro residue in the C-region for SP cleavage by SPase (Peng *et al*., 2019). This defines the exported protein's N-terminus and is necessary for its consequent release from the membrane into the extracellular setting (Peng *et al*., 2019).

Like other signal peptides at the N-terminal of secretory proteins, the amino acid signal peptide carried by the RSV-F protein serves as a guide to identify the location and protein secretion pathway (Owji *et al*., 2018). Although they can be as large as 60 amino acids, signal peptides, also known as protein leader sequences, are typically 15 to 25 amino acids long (Kapp *et al*., 2013). According to Owji *et al*. (2018), mutations in the mRNA leader sequences are essential for controlling gene expression, replication, and pathogenicity. The HRSV F mRNA translates the precursor protein F0, which has 574 amino acids and a signal peptide sequence at the N-terminus that is broken off by a signal peptidase in the endoplasmic reticulum.

HIV-1 envelope signal peptide mutations can delay cleavage of the glycoprotein precursors, which affects the process of viral maturation which ultimately affects viral infectivity (Snapp *et al*., 2017). Regarding the lymphocytic choriomeningitis virus, a similar finding was reported (Smyth *et al*., 2021). It was discovered that the glycosylation of the viral surface glycoprotein is influenced by the signal peptide of the negative RNA strand Ebolavirus (EBOV) belonging to the Filoviridae family (Marzi *et al*., 2006). Genetic diversity in F protein signal peptides for RSV has

been documented (Hause *et al*., 2017; Tapie *et al*., 2014). Nevertheless, no research was done to determine how these mutations affected the expression or functionality of the F protein. Assessing the effect of signal peptide mutations on F protein glycosylation was not within the scope of this study.

1.2.2.2 G Protein

Among the most important proteins that the RSV virus has encoded is the G protein. The structure of the G protein varies the greatest between RSV strains and was used for antigenic classification of RSV into RSV-A and RSV-B subgroups (Battles and McLellan., 2019). The G protein is a glycoprotein with 298 amino acids that aids in the virus's adhesion to the host cell (Bohmwald *et al*., 2016; Collins *et al*., 2013). For virion attachment, the G protein selectively focuses on the nasal epithelium of ciliated human airway epithelial cells (Nam and Ison., 2019; Van Royen *et al*., 2022). G protein comprises two forms: secreted (sG) and membrane-bound (mG) (Van Royen *et al*., 2022). About 80% of the total released G protein is present as sG. It has been demonstrated that sG obstructs antibody-mediated neutralization by functioning as an antigen decoy and preventing immune cells with Fc receptors from neutralizing RSV by cell-mediated means (Van Royen *et al*., 2022).

The secreted G proteins contribute to immune evasion through its binding of neutralizing antibodies and thus reducing the host's ability to induce antibody-mediated neutralization of RSV (Bukreyev *et al*., 2012). The G protein has the important ability to inhibit the function of chemokines and cytokines since CX3C chemokine-like motif can mimic these molecules and influence CD8+ T cell responses, (Bohmwald *et al*., 2016). It has been observed that the CX3C motif decreases the number of immune cells that enter the lungs of mice infected with RSV (Collins *et al*., 2013). It is therefore expected to interact with members of the TNF family of cytokines, leading to an imbalance in the inflammatory response facilitated by these molecules (Bohmwald *et al*., 2016; Collins *et al*., 2013; Van Royen *et al*., 2022). These findings indicate that the G protein plays a variety of roles. In addition to the function of viral adherence to the host, G proteins are essential for controlling the immunological response that the RSV infection causes in cells. The RSV-induced immune system modification eventually makes the immune system incapable of fighting the virus (Van Royen *et al*., 2022).

1.2.2.3 RSV Fusion protein

The subsequent protein of the RSV genome's two viral neutralization antigens is the F protein. With less than 10% sequence variation between RSV-A and RSV-B, the F protein is highly conserved (Bohmwald *et al*., 2016). Like a conventional F protein, the 574 amino acid F protein (Figure 1.2) facilitates viral fusion and syncytium formation (Collins *et al*., 2013). F protein needs to cleave at two polybasic sites that are separated by 27 amino acids to fuse the viral particles with the host cells. Two subunits are produced by this proteolysis: the carboxy-terminal F1 subunit and the amino-terminal F2 subunit (Bohmwald *et al*., 2016).

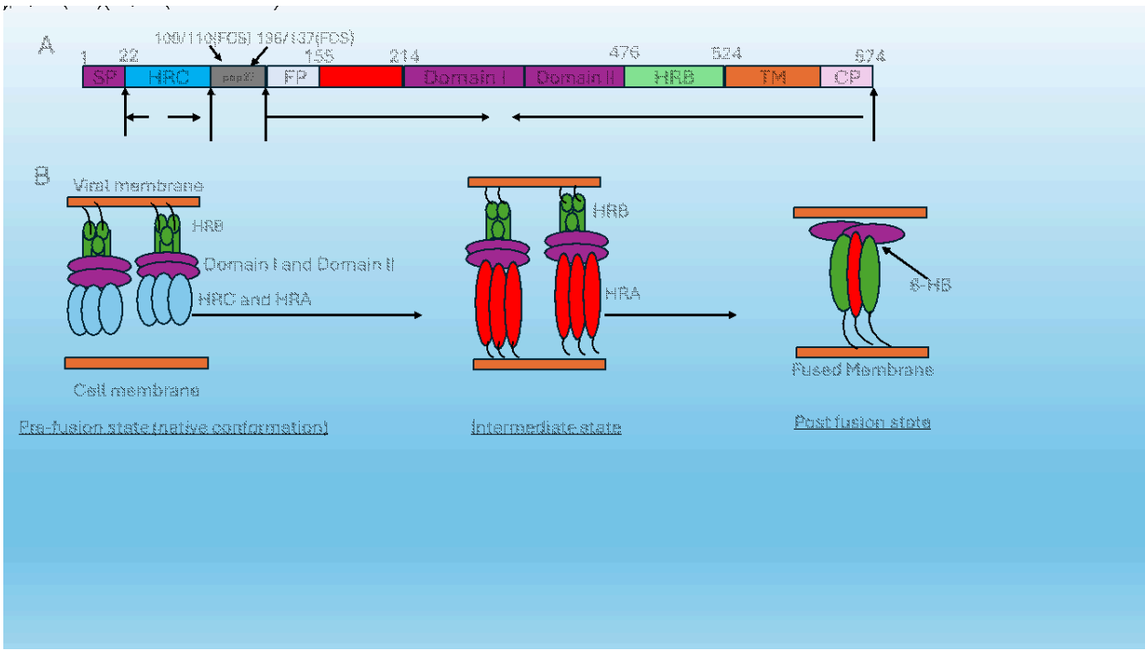


Figure 1.2. Structure of respiratory syncytial virus (RSV)F protein and RSV fusion/entry processes. (**A**) Schematic representation of RSV F protein. Proteolytic cleavage of the precursor F0 produces the F1 and F2 subunits. Signal peptide (SP), heptad-repeat C (HRC), furin cleavage site (FCS), 27-mer fragment (pep27), putative fusion peptide (FP), domain I and II, heptad-repeat A (HRA), heptad-repeat B (HRB), transmembrane (TM) and cytoplasm (CP) domains are indicated. (**B**) A model of RSV F protein-mediated membrane fusion. In the prefusion state, the FP is buried in the F protein. Once the G protein binds to its receptor(s) on the target cell, the F protein changes conformation into a long HRA helix, at the end of which is FP that inserts into the target cell membrane, and the three HRA domains form a coiled-coil trimer (in red). Subsequently, the HRB helices (in green) associate with the HRA trimer to form a 6-HB (6 helix bundle), pulling the cell membrane and viral membrane into proximity for fusion. (Adapted from Sun *et al*., 2013).

When two disulfide linkages covalently join the F1 and F2 subunits, a heterodimeric promoter is produced. Together, these three promoters produce the F protein's mature trimeric form (Falsey *et al*., 2000; Mitra *et al*., 2012). The trimer in a prefusion shape makes up the active F protein of the viral particle (Bohmwald *et al*., 2016). The F protein will undergo a conformational change to a post-fusion form in this trimeric state upon binding with the receptor, mediating the fusion of the viral envelope with the host membrane (Bohmwald *et al*., 2016; Van Royen *et al*., 2022).

Viral entry is facilitated by RSV-F binding to a major signalling receptor. The insulin growth factor 1 receptor (IGF1R) is a major signalling receptor for RSV-F and induces the expression of the fusion receptor, nucleolin, on the cell surface. This is followed by fusion of the viral envelope and cell membrane through the dynamic conformational change of RSV-F which is induced by

the interaction (Oraby *et al*., 2024; Rezende *et al*., 2023). There are two distinct conformational forms of RSV-F: prefusion and post-fusion (McLellan *et al*., 2013). Prefusion RSV-F has seven potent neutralisation sites (Ø, I, II, III, IV, V, and the recently discovered VI site) that make it highly antigenic. Of these, fusion results in the loss of sites Ø, I, and V. Nirsevimab and clesrovimab bind to epitopes in sites Ø and IV, respectively. (Oraby *et al*., 2024; Rezende *et al*., 2023).

Most of the RSV F protein is highly conserved except for the signal peptide and p27 domains, which constantly exhibit high levels of sequence variability between RSV isolates. Nevertheless, some RSV-F positions exhibit greater variability than others. Examples of these places are positions 206 and 209, which are both slightly outside and within binding site Ø, and positions 172 and 173 at site V. Furthermore, amino acid changes at positions 272 and 276 were linked with palivizumab (PZMB) resistance previously (Oraby *et al*., 2024; Rezende *et al*., 2023). The highly conserved antigenic site II of the pre- and post-fusion of the F protein are both palivizumab targets (Luna *et al*., 2020).

1.2.2.4 NS1 and NS2

NS1 and NS2 are known as non-structural proteins, therefore, the mature virion does not include either of them. The existence of these non-structural proteins sets RSV apart from the other viruses in the Mononegavirales order, such as the closely related hMPV. Moreover, NS1 and NS2 have developed into proteins with a variety of new roles to prevent the generation of type I interferon (IFN) and signaling (Liljeroos *et al*., 2013). Like other RNA viruses, RSV causes an infection that sets off a signal cascade by activating the retinoic acid-inducible gene I (RIG-I) and toll-like receptors (TLRs). It causes type 1 IFN to be produced (Thornhill and Verhoeven., 2020). Interferon-gamma (IFN-γ) is the main interferon that the nasal epithelium produces against the RSV infection (Van Royen *et al*., 2022). One way in which the RSV viral proteins subdue the host's innate immune system is by suppressing IFN synthesis and signaling.

Type III IFN-γ is thought to be the main IFN that shields the epithelial cells of the airways combating any respiratory illness (Thornhill and Verhoeven., 2020). Moreover, dendritic cell (DC) maturation is inhibited by NS1 and NS2 protein interference with type I IFN response. The ability of DCs to activate T lymphocytes may be inhibited by this effect (Van Royen *et al*., 2022). The presence of NS1 and NS2 proteins suppresses the synthesis of IFN, making airway epithelial cells more vulnerable to increased damage from respiratory infections of any kind. Furthermore, NS1 protein and NS2 protein-expressing human bronchial epithelial cells reduce T cell polarization towards Th1, Th2, and Th17 phenotypes, and Th2 and Th17 polarization, respectively (Van Royen *et al*., 2022). These two non-structural proteins are important components of virulence that influence the host's immune response directly.

1.2.2.5 N Protein

The 391 amino acid N protein binds firmly around the RNA genome to create helical nucleocapsids, which can be used as a template transcription and replication (Van Royen *et al*., 2022). The binding of N protein to the RNA genome inhibits recognition by host pattern recognition receptors, thereby protecting the viral RNA from degradation through host immune recognition (Van Royen *et al*., 2022). Additionally, the N protein is involved in the sequestration of signaling proteins from the innate immune system into inclusion bodies (IB) (Thornhill and Verhoeven., 2020; Van Royen *et al*., 2022). The N protein interacts with the M1, P, and L proteins while being contained by cytoplasmic IBs (Van Royen *et al*., 2022). These IBs are locations of viral replication and transcription, where all viral proteins of the VR complex are found.

N protein also plays a crucial role in initiating apoptosis and suppressing the interferon-signaling response in cell stress responses (Thornhill and Verhoeven., 2020; Van Royen *et al*., 2022). Moreover, it plays a part in opposing the host's natural immunity. The innate immune response is aided by the N protein's association within the IBs with melanoma differentiation-associated gene 5 (MDA5) and mitochondrial antiviral signaling (MAVS) after the initial hours of RSV infection (Thornhill and Verhoeven., 2020). IFN would be less effective if these molecules were sequestered because nucleic acid sensors would find it more difficult to identify the viral genome (Thornhill and Verhoeven., 2020). N protein expression reduces DCs' capacity to activate T cells by blocking the connection between peptide-major histocompatibility complexes (pMHCs) and the T-cell receptor (Thornhill and Verhoeven., 2020). The function of the N protein provides critical information on how RSV infection frequently impairs the development of protective T-cell responses.

1.2.2.6 P protein

The 241-amino acid viral P protein is known to be a cofactor of the VR complex and a necessary protein for the L protein to function (Collins *et al*., 2013). To facilitate interactions within the VR complex, the extremely stable P protein serves as an adaptor by binding to the N, L, and M2 proteins (Bohmwald *et al*., 2016). Within the VR complex the P protein is essential for both RNA transcription and replication. Without the P protein, viral transcription and replication could be hampered. The P protein is a significant phosphorylated RSV protein that has phosphates at over 10–12 locations. (Bohmwald *et al*., 2016; Collins *et al*., 2013). Research indicates that reducing P protein phosphorylation through mutation or the use of a cellular kinase inhibitor confirmed that phosphorylation is essential for RSV replication. In addition, to stop N from self-aggregating or adhering to nonviral RNA, the P protein binds to any unbound N protein monomers and assists their transfer to antigens (Collins *et al*., 2013).

1.2.2.7 L protein

The primary function of the 2,165 amino acid L protein, which is controlled and maintained by the VR complex, is the transcription and replication of the viral genome (Bohmwald *et al*., 2016; Collins *et al*., 2013). RSV has a negative-sense genomic RNA, thus, to express the L protein, the P protein transcribes it into messenger RNA (mRNA) every RSV gene (Collins *et al*., 2013). The L protein initiates each gene's transcription in this process by identifying a promoter region at the 3' extremity of the negative sense RNA strand (Bohmwald *et al*., 2016; Collins *et al*., 2013). During replication, the L protein subsequently transfers the viral genome from a negative sense RNA into a positive sense RNA, creating the antigenome. The antigenome is subsequently used as a template to make new negative sense RNA (Collins *et al*., 2013), after that, genomes will be enclosed in the infectious virions that are created.

1.2.2.8 M protein

The 256 amino acid M protein is crucial to the virion morphogenesis process (Collins *et al*., 2013). Additionally, because it facilitates viral assembly, the M protein is essential for replication of the RSV genome (Bian *et al*., 2012; Bohmwald *et al*., 2016; Collins *et al*., 2013). The M protein is found in the nucleus during the initial phases of infection, and it plays an important function in lowering the host cells' genes' transcriptional activity (Bian *et al*., 2012; Collins *et al*., 2013). The M protein is reported to be connected to the cytoplasmic viral inclusion bodies (IBs) later in the infection (Collins *et al*., 2013).

In human bronchial epithelial cells, the M protein also has the function of stopping the G1 and G2/M phases of the cell cycle (Collins *et al*., 2013). G1 is the stage in which initiation of proliferation of stem cells occurs. Viral proteins such as non-structural proteins cause cell cycle arrest in G1 or G2 phase through p53 or p21 accumulation (Wang *et al*, 2010). RSV replication is accelerated by the p53-dependent activities of the M protein (Bohmwald *et al*., 2016). Additionally, the viral filaments' direct maturation has been linked to the M protein. It is believed that viral filaments assist with the infectious virus's attachment to host cells (Reimers *et al*., 2005). The M protein may not be necessary to start the development of viral filaments, but when it is absent, the filaments stay immature and cannot facilitate attachment to host cell receptors (Bohmwald *et al*., 2016). According to additional research, IBs express the M protein, which interacts with the M2-1 protein to engage with the VR complex (Bohmwald *et al*., 2016; Tran *et al*., 2009). Moreover, the M protein interacts with the G and F proteins to signal the formation of the virions and can block viral transcription (Bohmwald *et al*., 2016; Collins *et al*., 2013).

1.2.2.9 M2-1 protein

As a component of the VR complex, the M2-1 protein is engaged in the transcription process. It helps the L protein continue the transcription of the viral genes by functioning as an extension factor that promotes the transcription of all RSV genes (Tran *et al*., 2009). The length of the M2-1 protein is 194 amino acids (Bohmwald *et al*., 2016; Reimers *et al*., 2005). M2-1, found in this RNA-binding protein, which can be found in either phosphorylated or unphosphorylated

form in infected cells, interacts with other elements of the VR complex (Bohmwald *et al*., 2016; Reimers *et al*., 2005).

This connection is specifically controlled through connections of the viral RNA, as RNases break the association between the M2-1 protein and the N protein (Reimers *et al*., 2005). The M2-1 protein also can activate NF-κβ, or nuclear factor-kappa β (Bohmwald *et al*., 2016). NF-κβ is one of the essential regulators of pro-inflammatory gene expression and stimulates transcription of pro-inflammatory adhesion molecules, chemokines, and cytokines, among other things. The M2-1 protein must exist as tetramers to fully function as an elongation factor possible. The protein cannot function properly without oligomerization, and this is corroborated using a mutant virus for the M2-1 protein that is unable to tetramer production (Bohmwald *et al*., 2016). The M2-1 protein, like the other proteins that make up the VR complex, is essential for controlling transcription and RSV RNA replication.

1.2.2.10 M2-2 protein

The M2-2 protein has a length of roughly 88–90 amino acids and is only slightly expressed in infectious cells (Collins *et al*., 2013). It is unknown how the M2-2 protein functions as a component of a virion, yet M2-2 deletion from recombinant RSV causes a virus to have decreased and delayed RNA replication (Collins *et al*., 2013). The M2-2 protein may also control transcription and viral polymerase-based replication (Cheng *et al*., 2005). More study and focus are needed on the M2-2 protein's overall significance in the RSV viral genome.

1.2.2.11 SH Protein

The SH protein is a surface membrane protein on the RSV virion that was demonstrated to exhibit two distinct forms and varied sizes, whether it is found in RSV-A or RSV-B (Bohmwald *et al*., 2016; Fuentes *et al*., 2007. The length of SH in RSV-A and RSV-B are 64 and 65 amino acids, respectively (Fuentes *et al*., 2007; Rixon *et al*., 2004). It was stated that the SH protein is a viroporin that can produce ion membrane channels seen in cells (Bohmwald *et al*., 2016; Fuentes *et al*., 2007; Rixon *et al*., 2004). The SH protein may function as a virulence factor during an RSV infection, although it is not involved in the virus's entrance into host cells.

1.2.3 RSV genetic diversity

In 1985, complementary deoxyribonucleic acid (cDNA) probes and monoclonal antibodies were utilized to distinguish the two antigenic groups RSV-A and RSV-B, on several circulating strains (Mufson *et al*., 1985). Further advancements in detailed sequencing techniques made it possible to characterize RSV diversity more thoroughly. Fourteen different genotypes of RSV-A (GA1 to GA7, SAA1, CB-A, NA1 to NA4 and ON1) and 37 recognized genotypes of RSV-B (Munoz-Escalante *et al*., 2021) (BA1 to BA12, BA-C, SAB1 to SAB4, GB1 to GB4, URU1 to URU2, CB-B, CB-1, BA-CCB and BA-CCA) have been found within these antigenic groupings. Both subtypes have different evolutionary rates; RSV-A is thought to have a lower rate (1.48×10^{-3} nucleotide substitutions/site/year) than RSV-B (1.92×10^{-3} substitutions/site/year) (Yu *et al*., 2021).

RSV-A was found to have lower intra-host variation and higher consensus diversity than RSV-B in previous investigations evaluating diversity within antigenic groupings (Lin *et al*., 2021). The attachment glycoprotein (G), which is under significant evolutionary pressure as a factor in viral transmission and as the focus of the humoral response, has the highest nucleotide substitution rates throughout the genome. Short duplication occurrences in G have been found in RSV-A (genotype ON1) and RSV-B (genotype BA1), and it has been hypothesized that these selection pressures are responsible for their convergent evolution. Targeted sequencing of the G ORF has been the mainstay of conventional RSV genotyping methods due to the high degree of variability in this region (Guzman and Hultquist., 2022). For phylogenetic analysis and viral genotype categorization, targeted sequencing of G, and more especially of the second hypervariable region, is generally used in most of the current molecular epidemiology research (Goya *et al*., 2020; Goya *et al*., 2024; Guzman and Hultquist., 2022).

RSV seasonality varies in tropical countries and close to the equator, even though cases usually follow a seasonal pattern with the peak of infections taking place in the Northern Hemisphere from late December to late February (Tang and Loh., 2014). RSV seasonality was not found to be caused by environmental factors like temperature or humidity, and subtropical regions showed year-round RSV cases (Hsu *et al*., 2014). Subtype switching occurs year to year, with a single genotype dominating a geographic area (RSV-A followed by RSV-B and back), notwithstanding the possibility of a heterogeneous population of genotypes co-circulating in populations throughout one RSV season. For instance, during 11 recurrent epidemics, local circulating genotypes were gradually replaced during RSV epidemics in Kilifi, Kenya (Agoti *et al*., 2015). The following genotypes: GA2, GA5, and GA7 being outcompeted by NA1, NA2, and ON1 genotypes were seen in Malaysia, Canada, and India, (Choudhary *et al*., 2013; Eshaghi *et al*., 2012; Khor *et al*., 2013).

Recent studies have shown that the two most common genotypes in China are BA9 RSV-B and ON1 RSV-A (Chen *et al*., 2022). This is because RSV and other RNA viruses have high rates of mutation (10^{-3} to 10^{-4} substitutions/site/year). *In vitro* evidence suggests that both the G and SH genes are more prone to spontaneous mutations than any other region of the RSV genome (Shishir *et al*., 2023) only the G gene was shown to have mutated in vivo study. Circulating RSV appears to consistently change in sequence and antigenicity in response to immunological pressure, especially in the G protein (Shishir *et al*., 2023). Moreover, an RSV outbreak was reported in Australia affecting the ON1 genotype especially during the COVID-19 timeframe of 2020–2021, with several point mutations found in the attachment (G) glycoprotein's C-terminal region, in addition to the nucleocapsid and small hydrophobic proteins (Shishir *et al*., 2023).

1.2.3.1 RSV seasonality and diversity in South Africa

Prior to the COVID-19 pandemic, South Africa reported an estimated 6,000 RSV-associated deaths annually (Cohen *et al*., 2018). Use of non-pharmaceutical interventions to combat the spread of SARS-CoV-2 during the pandemic resulted in a substantial reduction in RSV

circulation during the 2020-2021 winter seasons in South Africa (Olsen *et al*., 2021; Tempia *et al*., 2021). Subsequently, following relaxation of lockdown limitations off-season outbreaks of RSV were observed (Agha and Avner, 2021; van Summeren *et al*., 2021). The changed epidemiology and recovery of RSV was possibly due to waned immunity from decline or absence of exposure to the virus during the pandemic period (Reicherz *et al*., 2022).

RSV-A and -B strains detected in 2021 and 2022 in the Free State Province of South Africa were lineages GA2.3.5 (previously ON1) and GB5.0.5a (previously BA9) (Sondlane *et al*., 2024). Other studies supported these findings, highlighting that GA2.3.5 and GB5.0.5a were the dominant RSV lineages that circulated before and after the COVID-19 pandemic (Goya *et al*., 2023; Jallow *et al*., 2022; Redlberger-Fritz *et al*., 2023). The RSV-A ON1 (GA2.3.5) lineage has been leading infections worldwide since its discovery in Ontario, Canada, in 2010 (Eshaghi *et al*., 2012; Lu *et al*., 2019; Eden *et al*., 2022; Jia *et al*., 2022; Lee *et al*., 2023). The BA genotype has increased global dominance since its emergence and is presently the leading RSV-B genotype that circulates (Gaymard *et al*., 2018; Trento *et al*., 2010).

In contrast to RSV-A, GB5.0.2 circulated in Africa and South Africa as the leading variant from the mid-2000s to 2015 and GB5.0.5a arose as the leading from 2018 onwards (Sondlane *et al*., 2024; Pretorius *et al*., 2013; Van Niekerk and Venter, 2011). The leading lineage in South African, GB5.0.5a that rotated before the COVID-19 pandemic was rarely observed post 2020 (Sondlane *et al*., 2024).

1.2.3.2 HRSV lineage nomenclature

From 2020, Goya *et al.* introduced a hierarchical classification scheme for HRSV phylogenies, which includes genotypes, sub-genotypes, and lineages based on the G gene (Goya *et al*., 2020). This lineage nomenclature includes the RSV subgroup letter and ascending ordinal numbers, separated by dots to indicate nested lineages. They also established a distinctive designation, D, for the G-gene duplications which have been reported since 2017 (Goya *et al*., 2023; Liang *et al*., 2019; Streng *et al*., 2019). For example, A.D refers to the historical ON1 genotype of RSV-A and B.D designates the BA genotype of RSV-B and subsequent addition of ordinal numbers in sequence for new nested lineages. Aliases beginning with E are limited to three numbered layers of nested lineages, preventing indefinite accumulation of numbers (Goya *et al*., 2024). For instance, the B.D.4.1.1 lineage contains descendant lineages designated B.D.E.1-B.D.E.4, rather than B.D.4.1.1.1-B.D.4.1.1.4, where E represents 4.1.1. The nomenclature described is based on tree topology, with no regard for date of collection or the most recent common ancestor of each lineage (Goya *et al*., 2024).

1.2.3.3. Impacts of genetic diversity on disease severity and clinical outcomes

Variations in the viral genotype can affect the presentation, severity, and clinical prognosis of a disease by altering the viral load, immune evasion, and cell tropism. Distinct influenza virus

subtypes and SARS-CoV-2 have been linked to severe or moderate illness, with a comparable trend shown in patient outcomes (Avni *et al*., 2020; Giles *et al*., 2021). Some studies have looked at the connection between clinical severity and RSV genotype, but with contradictory outcomes (Avni *et al*., 2020; Giles *et al*., 2021). There are probably several factors contributing to the contradictory results, including variations in the inclusion criteria, cohort demography, prior immunity and sample size.

Most studies have used G sequencing to clarify genotypes in conjunction with severity metrics like intubation, duration of hospitalization and use of severity scores from medical records (Avni *et al*., 2020; Giles *et al*., 2021; Vandini *et al*., 2017). Studies conducted in Italy and Germany showed that RSV-A genotype ON1 exacerbates the clinical severity of bronchiolitis in hospitalized babies, especially during the RSV seasons of 2016–2017 and 2017–2018 (Midulla *et al*., 2020; Streng *et al*., 2019). Similarly, in a multicenter prospective study conducted in the United States, transcriptome analysis, genotyping and clinical data were combined, and it was discovered that genotype GA5 (RSV-A) was linked to a distinct host immune response and greater disease severity in five consecutive RSV seasons (Rodriquez-Fernandez *et al*., 2018). Subtypes RSV-A or RSV-B, however, have not been linked to any clinical outcomes in hospitalized patients or patients with severe bronchiolitis, according to other investigations (Rodriquez-Fernandez *et al*., 2018).

1.2.3.4. Molecular understanding of RSV biology

Understanding the molecular virology and selective pressures that affect RSV replication, and evolution is essential to comprehending the process by which modifications to the RSV genome affect viral propagation, disease etiology, and treatment efficacy. Over time, selection will favor mutations that increase a virus's capacity to replicate in a certain location, or that increase viral fitness, and vice versa (Wargo *et al*., 2012). For instance, changes that boost immune evasion, increase transmission, or confer resistance to an antiviral treatment could improve viral fitness in specific cellular settings, giving the viruses that carry them an advantage (Irwin *et al*., 2016).

RSV entry receptors and attachment factors are diverse. These include nucleolin, the epidermal growth factor receptor (EGFR), IGF1R, and ICAM-1 that interact with F, as well as CX3CR1 and heparan sulphate proteoglycans (HSPGs) that interact with G. In the end, receptor binding allows F to start membrane fusion and introduce the genetic material of the virus into the cell (Feng *et al*., 2022). F and G are important proteins in immune evasion in addition to their function in viral entry, because they are common targets of the humoral immune response, which includes neutralizing antibodies that prevent receptor interaction (Krzyzaniak *et al*., 2013). To evade immune detection, the G protein is firstly heavily glycosylated, masking its immune epitopes, and secondly G is released in a soluble form that acts as a decoy which binds neutralizing antibodies thus reducing the levels of antibodies available to neutralize actual viral particles (Guzman and Hultquist., 2022). G is therefore under a lot of selective pressure and is one of the most diverse ORFs in RSV.

Numerous mutations in RSV G and F have been documented to impact on how well they interact with their corresponding host factors, which in turn affects how well cells connect to one another and fuse their membranes (Guzman and Hultquist., 2022). Like this, it has been discovered that several escape mutations discovered in F after in vitro selection for fusion inhibitor resistance have secondary effects on cell entry. For instance, mutations in the F protein of RSV-A strains 2–20 and A2 have been found to change interaction with EGFR, which has an impact on the production of airway mucin downstream (Guzman and Hultquist., 2022). In summary, the development of innovative therapeutic and preventive treatments targeting these proteins will be greatly aided by the application of in vitro techniques to clarify the effects of mutations on RSV replication, causing the viral fitness to drop.

1.2.4 RSV Pathogenesis

RSV enters the mouth or nose through the air or through direct contact with an infected person. Firstly, it affects the upper respiratory system's airway epithelium before going on to the lower respiratory system and the bronchioles, which are the sites of viral replication. The two main cell types impacted by RSV infection are type 1 pneumocytes in the alveolus and ciliated cells in the bronchial epithelia (Guzman and Hultquist., 2022). Using *in vitro* cultures, RSV was shown to infect basal epithelial cells and intraepithelial dendritic cells of the respiratory tract. RSV infection causes ciliation loss, sloughing and shedding of a particular apical epithelial cap with occasional syncytium formation and mucus hypersecretion as the infection progresses. This may result in the creation of thick plugs in the bronchiolar lumen *in vivo* (Guzman and Hultquist., 2022).

1.2.5 Innate and cell intrinsic immune response to RSV.

Numerous physiological reactions, including cell apoptosis, innate immune responses, and cell stress responses, can prevent the reproduction of the respiratory syncytial virus. RSV triggers the cell's intrinsic and extrinsic pathways, which in turn trigger caspase three activation and eventual cell death (Van Royen *et al*., 2022). These processes are aided by the B-cell lymphoma 2 (Bcl-2) protein family, which localises to the mitochondria, and the tumour necrosis factor-related apoptosis inducing ligand (TRAIL) and its death receptors 4 and 5 (DR4/5). The first step in the innate immune response to RSV is the virus's recognition by NOD-like receptors (NLRs), toll-like receptors (TLRs), and RIG-I like receptors (RLRs) (Van Royen *et al*., 2022).

These molecules stimulate nuclear factor-kB and interferon regulatory receptors (IFRs) through several adaptor proteins, which leads to synthesis of type 1/III interferons (IFNs) and cytokines. Nucleotide-binding domain and leucine rich repeat containing family, pyrin domain-containing 3 (NLRPI3) contributes to IFN and cytokine production, forms the inflammasome complex, and starts caspase 1 during RSV infection. Three types of stress are activated by RSV: transcriptional stress, oxidative stress, and ER stress (Van Royen *et al*., 2022).

When the endoplasmic reticulum (ER) is overloaded with RSV glycoproteins, the unfolded protein response is triggered, and virus replication is controlled. This is detected by the ER membrane protein inositol-requiring enzyme 1 (IRE 1) and activated transcription 6 (ATF6) (Van Royen *et al*., 2022). Stress granules, which are made up of stalled mRNAs to halt their translation and use several processes connected to inclusion bodies where RSV replicates to restrict the synthesis of SGs are activated by RSV infection. Reactive oxygen species (ROS) are produced by RSV infection through the action of NADPH oxidase 2 (NOX2). IRF3 and NF-kB are then activated because of NOX2-mediated ROS, which in turn triggers subsequent antiviral reactions (Van Royen *et al*., 2022).

1.2.6 Humoral response

Neonates develop antibodies to most RSV proteins, which strengthens their innate immune responses to the virus. IgM, IgA, and IgG antibody production is triggered by RSV infection in both blood and mucosa (da Silva *et al*., 2023). The host is protected from reinfections by these antibodies, which are made possible by the adaptive immune response to RSV. Although the basic immune response to RSV is ineffective, IgG and IgA antibody levels significantly increase when reinfection occurs, for example in newborns. To neutralise the virus, these antibodies are often directed against the F and G proteins of RSV. However, newborns under six months old have reduced antibody production against F protein, which results in weaker neutralising antibody responses to RSV (da Silva *et al*., 2023).

The induction of the IgM antibody, which is often identified within the first 5–10 days of the infection and remains in the blood for 1–3 months, is the main humoral immune response against RSV. However, the IgM response is still detectable for at least a year in certain studies. Conversely, most patients have RSV-specific IgG antibodies, which peak 20–30 days following the onset of symptoms (da Silva *et al*., 2023). It's interesting to note that levels of IgG antibodies specific to RSV start to decrease one year after the patient contracts the virus for the first time. Similarly, adults who are linked to a higher risk of developing symptoms from RSV infection have decreased levels of RSV-specific neutralising antibodies in their serum (da Silva *et al*., 2023).

1.2.7 Transmission of RSV

Just as other respiratory viruses, the transmission of RSV happens through big droplet inoculation in the eyes, nose, or mouth, needing close interaction with an RSV-infected individual or auto-inoculation to the face (nose, mouth, or eyes) via contaminated fomites or skin (Hussain *et al*., 2022). When an infected individual coughs or sneezes they release large droplets which are then transmitted. It is estimated that a single cough generates up to 3,000 droplets (Hussain *et al*., 2022). These droplets can spread on various kinds of surfaces or directly infect

another person. Varying on the surface type, the virus may be active and infectious for several periods (Tada *et al*., 2019).

According to research, RSV can survive for up to six hours on nonporous surfaces (Haber., 2018). Nonporous surfaces include hard surfaces like metal, plastic, glass, and worktops. Although varnished wood is regarded as a nonporous surface, RSV viability on varnished wood has not yet been investigated (Haber., 2018). RSV is viable for up to two hours on porous materials such as paper, cardboard, and textiles. Since the virus can remain active on gloves for up to five hours, it makes sense that RSV can spread as a nosocomial infection through hospital wards and other healthcare settings (Tada *et al*., 2019). RSV can spread by airborne droplets, just like any other respiratory infection, however it is unclear how long these airborne droplets will remain viable (Kaler *et al*., 2023).

It is believed that there are several ways that respiratory viruses might spread, which are sometimes categorized into three groups: contact, big respiratory droplets, and small respiratory droplets; the last of which is also known as aerosol or airborne transmission (Tada *et al*., 2019). Aerosol transmission involves particles smaller than 5 mm and in droplet transmission particles are larger than 5 mm (Kaler *et al*., 2023; Tada *et al*., 2019).

The respiratory droplets' dimensions are also significant because talking, sneezing, coughing, and breathing can all produce tiny respiratory droplets (Siegel *et al*., 2007; Thomas *et al.*, 2013). Large droplets, on the other hand, settle rapidly, whereas tiny aerosols can stay in the air and possibly travel farther due to airflow (Kaler *et al*., 2023; Tada *et al*., 2019). Additionally, smaller aerosols have a higher chance of being inhaled deeply into the lungs and infecting the lower respiratory tract's alveolar tissues. Larger droplets, on the other hand, have a higher chance of becoming stuck in the upper airways (Tada *et al*., 2019).

1.2.8 RSV replication

When RSV enters the upper respiratory system through mucous membranes like the mouth or nose, it damages airway epithelial cells (AECs). Following that, it enters the lower respiratory system and travels to the bronchioles, which are better sites for viral replication. Usually, the viral adherence site to the host cell is the nasal epithelium (Tada *et al*., 2019). The key cells that RSV infection targets are ciliated cells in the bronchial epithelia and type I pneumocytes in the alveolus. Following the virus's attachment to the polarized, ciliated margins of the apical surface of the AECs, they contract RSV infection (Kaler *et al*., 2023).

The G protein, which is connected to the cell surface factors, mediates the first attachment stage. GAGs (heparan sulphates and chondroitin sulphate B glycosaminoglycans) interact with the G protein. Following this connection, which assists the virus to get closer to the cell membrane to infect it, the F protein interacts with the nucleolin, its receptor (Kaler *et al*., 2023; Tada *et al*., 2019). The helical ribonucleoprotein complex (RNP) is released into the cytoplasm of the host

cell upon fusion. The replication of new negative-sense genomes to pack into virions is facilitated by the viral RNA-dependent RNA polymerase (RdRp) complex and requires the transcription of viral mRNA (Kaler *et al*., 2023; Tada *et al*., 2019).

The assembly of RSV virions will occur at or close to the plasma membrane upon completion of the replication process. According to previous research, F proteins attach to lipid rafts and use the F cytoplasmic tail to attract and concentrate M proteins (Kaler *et al*., 2023; Tada *et al*., 2019). Through actin-dependent membrane deformation directed outward, this process initiates filament budding. Nevertheless, some research has indicated that this process might be more complex, with filament formation beginning intracellularly as vesicles carrying viral proteins travel along microtubules and grow into filaments that are then loaded with nucleocapsids before merging by an unclear mechanism with the plasma membrane (Kaler *et al*., 2023; Tada *et al*., 2019).

Virion detaches from the polarized epithelial cells' apical membrane after budding, and then they mature into filamentous particles about 130 nm in size in an M-dependent process. Once replication of virion particles has taken place, the host is deemed contagious and has the capacity to infect more people (Kaler *et al*., 2023; Tada *et al*., 2019). People who have the virus will continue to spread if they are infected. Within a day or two of infection, the virus starts to shed, frequently before the appearance of significant symptoms. The degree of the infection, the age of the infected host, and whether the infected person has a weakened immune system all seem to have an approximate correlation with the very variable viral shedding (Kaler *et al*., 2023; Tada *et al*., 2019).

1.2.9 Clinical manifestations of RSV

1.2.9.1 RSV clinical manifestations in infants

The early symptoms of RSV are the same in all age groups, however, the duration of the infection varies. Several days post contact and transmission, patients normally go through mild to moderate nasal congestion and low-grade fever, followed by a consistent cough within a few days (Black, 2003; Jha *et al*., 2016). Patients with earlier RSV infections may encounter these symptoms for several weeks and then subside with no further episode (Black, 2003). Everyone will show symptoms imitating an upper respiratory tract infection; but the symptomatic profile later may vary. Lower respiratory tract infections are more commonly observed in newborns 2-3 days after upper respiratory tract infection symptoms are noted (Coultas *et al*., 2019). Infants and children with this infection can show different types of symptoms, varying from mild upper respiratory tract symptoms to severe lower airway involvement that needs hospitalization and mechanical ventilation (Jha *et al*., 2016).

Viral bronchiolitis is one of the greatest widespread infant viral infections that arise due to RSV infection. In almost a quarter of infants with viral respiratory infections, development to lower respiratory tract occurrence is seen. While bronchiolitis is the most frequent progression,

pneumonia and laryngotracheitis (croup) may also arise (Black, 2003; Jha *et al*., 2016). Bronchiolitis normally occurs post to a primary prodrome of nasal congestion, cough, and coryza persisting up to three days (Black, 2003; Jha *et al*., 2016). Successively, a low-grade fever, wheezing, and signs of enhanced respiratory difficulties arise, such as nasal flaring, chest wall retraction, and tachypnea (Black, 2003; Coultas *et al*., 2019; Jha *et al*., 2016).

RSV-associated apnea is also significantly seen in infants <6 months of age and is a very important gauge for hospitalization (Black, 2003; Coultas *et al*., 2019; Jha *et al*., 2016). In some infants, coughing may develop to become more severe and as such, vomiting is observed as being more abundant and thicker, resulting in the onset of pharyngitis. Pharyngitis is seen between at least one-third of infants. On investigation, rhinitis, and pharyngitis may be linked with conjunctival signs and erythema to the tympanic membrane (Black, 2003; Coultas *et al*., 2019; Jha *et al*., 2016). Vomiting is also frequently seen in about half of the infected individuals (Black, 2003; Coultas *et al*., 2019; Jha *et al*., 2016). Neonates may show only lethargy and poor feeding, which may result in hospitalization because of dehydration and potential malnutrition. Such infants normally show terrible hypoxemia and dehydration that may require hospital emergency rooms (Black, 2003; Coultas *et al*., 2019; Jha *et al*., 2016).

1.2.9.2 RSV clinical manifestations in adults

The symptom profile in older patients is comparable to that in newborns, but it is more severe and more likely to affect the lower respiratory tract (Coultas *et al*., 2019). This can be linked to a significant later identification of RSV in adults because people could mistakenly link the initial non-specific symptoms with colds or influenza. Adults with RSV infections typically have nasal congestion before developing a cough (Black, 2003; Coultas *et al*., 2019; Jha *et al*., 2016). A chest examination will also reveal audible crackles, and in up to half of the older patients, chest radiographs will show infiltration. Numerous non-specific symptoms of a viral respiratory tract infection, such as coryza, sore throat, fever, and malaise, are linked to RSV infection in older adults as well as lower respiratory tract symptoms such as cough, as noted in Figure 1.3 (Jha *et al*., 2016).

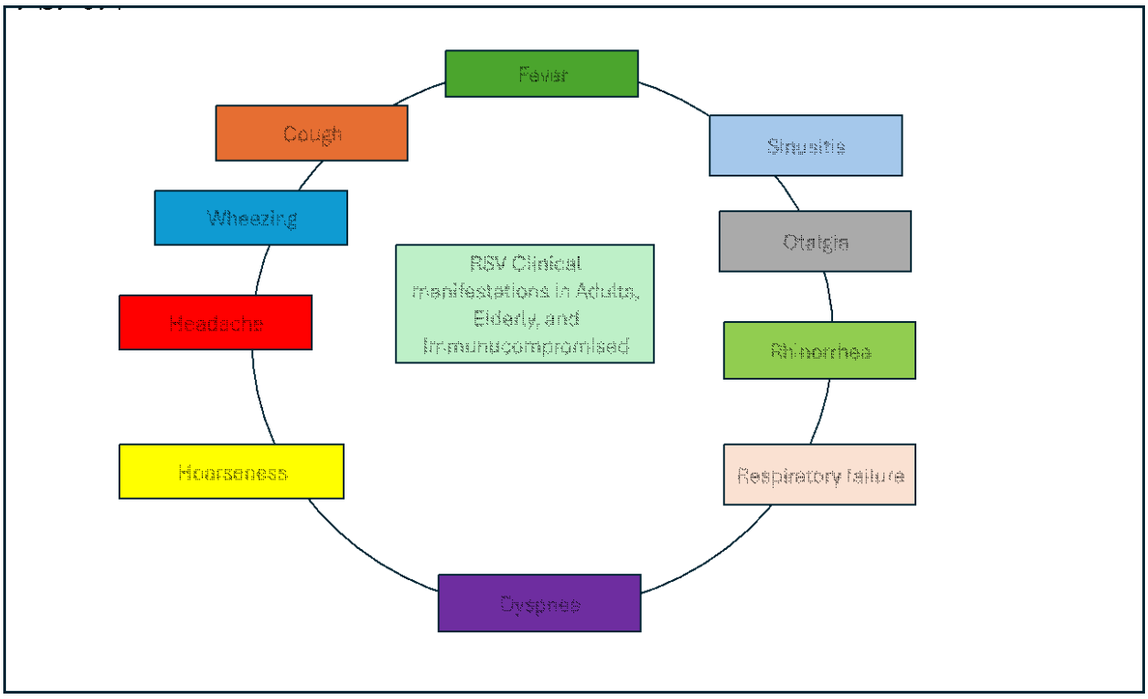


Figure 1.3. RSV clinical manifestations in Adults, Elderly, and Immunocompromised (Adapted from Kaler *et al*., 2023).

1.2.10 Clinical management and treatment

To stop transmission, there is a stronger focus on symptomatic management and supportive care to prevent transmission of RSV infections in recent years. RSV often has a self-limited duration and symptomatic presentation, and symptomatic therapy involves the path of action. However, depending on whether an adult or a child has an RSV infection, different clinical management protocols apply (Nam and Ison, 2019). Most RSV-infected newborns and kids receive effective outpatient treatment. RSV-targeted therapy has shown promise in a few pediatric populations, including recipients of lung and bone marrow transplants. These therapy measures' ultimate objectives are to reduce the likelihood of transmission, lessen the illness's duration and intensity, and soothe symptoms. Studies have been conducted on ribavirin, palivizumab, motavizumab, and RSV-immune globulin (RSV-IVIG) as treatment alternatives (Nam and Ison, 2019).

1.2.11 Vaccine Development (RSV prevention)

RSV vaccine candidates are primarily based on RSV-A GA1 genotype strains isolated in 1960 (Hause *et al*., 2017). Vaccines that incorporate the pre-fusion (pre-F) form of the RSV F protein were reported to be highly immunogenic (McLellan *et al*., 2013). Immunogenicity is linked to the more conserved nature of pre-F among RSV isolates (Lee *et al*., 2023).

1.2.11.1 Potential RSV vaccine candidates

Over the past decade, there has been a substantial rise in the number of trials assessing different RSV vaccination methods. (Mazur *et al*., 2022; Ramilo *et al*., 2023). Presently, a total of 34 different RSV vaccines are currently in development, with 21 advancing through clinical trials from phase 1 to phase 3. RSV has several surface proteins, but the fusion (F) and attachment (G)

proteins are the two primary glycoproteins that serve as targets for immunization. On the other hand, both are highly effective in inducing protective neutralizing antibodies and are essential for both viral pathogenesis and infectivity (Rodriguez-Fernandez *et al*., 2021).

Since the F protein is more conserved than the G protein, which is primarily what distinguishes RSV's two unique subtypes, RSV-A and RSV-B, from one another, the F protein is a preferred target for monoclonal antibodies (mAbs) and vaccine development. The F protein has emerged as the favored target for RSV-specific interventions since it was discovered that it exists in two conformational forms: "pre-fusion F" (preF) and "post-fusion F" (postF). It is also known that the preF conformation induces higher-potency neutralizing antibodies (McLellan *et al*., 2010; McLellan *et al*., 2013; Rodriguez-Fernandez *et al*., 2021). Currently available RSV vaccine candidates can be classified as protein-based, recombinant-vector-based, nucleic-acid-based, live-attenuated (LAV) or chimeric vaccines.

1.2.11.2 Active Immunization by various vaccines designed for infants and adults.

(a) **Recombinant-Vector-based Vaccines** transfer the genes of the relevant RSV proteins (antigens) into cells and humoral tissues through a modified replication-defective virus (Samy *et al*., 2020; Williams *et al*., 2020). Adenovirus-based vaccinations have shown good efficacy against severe disease in the recent SARS-COV-2 pandemic (Falsey *et al*., 2021), supporting the idea that comparable techniques for RSV may be successful. However, concerns have been raised regarding an increased risk of thrombo-embolic events (Greinacher *et al*., 2021; Klok *et al*., 2022). Three recombinant-vector-based vaccination candidates, intended for use in pediatric and geriatric populations, are presently undergoing phase 2-3 advanced clinical trials (Greinacher *et al*., 2021; Klok *et al*., 2022).

(b) **Nucleic acid vaccines mechanism** is based on the infection of cells with messenger RNA (mRNA) encoding RSV antigens. The potential of this strategy has been highlighted by the safety and great efficacy of mRNA vaccines against SARS-CoV-2 infection in recent years [Corbett *et al*., 2020; Polack *et al*., 2020; Regev-Yochay *et al*., 2022]. Only phase 1 trial of an adult RSV mRNA vaccine has been published (Aliprantis *et al*., 2021), even though the vaccine is still in development. However, given the information gathered from the SARS-CoV-2 vaccine, it is expected that more trials will be conducted.

(c) **Protein-based vaccine** strategies (such as vaccines containing particles, subunits, and whole-inactivated viruses) rely on the presentation of different antigens at higher densities to stimulate the immune system. The current contenders are intended to safeguard elderly individuals and to protect at-risk infants through immunization of pregnant women in their third trimester (Gatt *et al*., 2023). The primary aim of a reduction in the rate of medically relevant lower respiratory tract infections in the first ninety days of life was not met by the RSV F protein nanoparticle immunization that was recently evaluated in pregnant women receiving vaccination between 28 and 36 weeks. On the other hand, a possible advantage was discovered with respect

to other results, like a decline in hospitalization and a severe infection with hypoxemia. Other candidate vaccines based on RSV F protein are undergoing varying phases of clinical testing (Gatt *et al*., 2023) combining F and non-F antigens.

(d) **Live attenuated vaccines:** These vaccines imitate a real infection to elicit a strong immune response but attenuated for lowered pathogenicity. Achieving a favorable balance between safety (attenuation) and the induction of a robust immunogenic response is the primary problem with this class of vaccines (Karron *et al*., 2021). LAVs are regarded as safe and don't seem to increase the risk of vaccine-induced illness in young children. Good effectiveness rates were shown in a recent trial evaluating seven live-attenuated RSV vaccinations given intraperitoneally to children between the ages of 6 and 24 months (Karron *et al*., 2021).

An 88% success rate against medically attended acute lower respiratory illness was demonstrated by compiled data of the five most promising vaccinations (Karron *et al*., 2021). When the benefits of passive immunization fade after a while, older infants who are not adequately protected by a maternal vaccine or mAbs may benefit greatly from LAVs. A related tactic involves using chimeric live virus vaccine candidates to express RSV proteins in closely related attenuated viruses like the parainfluenza and Sendai viruses. Although there are currently few chimeric RSV vaccine candidates in development, chimeric vaccines have a high safety record (Abarca *et al*., 2020).

1.2.11.3 Passive Immunization with monoclonal antibodies

A combination of intravenous immunoglobulin (IVIG) and high quantities of RSV-protective antibodies was the first method devised to give passive immunization for the prevention of severe RSV infection. This approach was linked to a 40% decrease in RSV hospitalization, a 50% decrease in hospitalization days, and a 60% decrease in days requiring more oxygen in high-risk infants. However, 5% of the RSV IVIG infusions resulted in adverse effects, most of which were moderate (Brady *et al*., 2014).

Passive immunization with the humanized monoclonal antibody (mAb) palivizumab (Synagis®), inhibits RSV entry and is recommended for prophylactic treatment of infants at high risk for severe RSV illness. During the RSV season, monthly intramuscular administrations of palivizumab are performed (Brady *et al*., 2014). The population that receives this immune prophylaxis varies depending on the jurisdiction (Brady *et al*., 2014).

Palivizumab prophylaxis decreased the rate of hospitalization for RSV infection by 56%, according to a recent Cochrane analysis (Garegnani *et al*., 2021). Due to the antibody's half-life, palivizumab's primary setbacks are its high cost and short half-life. The cost of the medication has prevented its widespread usage, particularly in low-income nations, and the requirement for

repeated monthly administration is linked to missed doses, which lowers the treatment's overall efficacy (Ananworanich *et al*., 2021). As a result, numerous clinical trials have evaluated more recent drugs with extended half-lives.

A mAb of the second generation with a stronger affinity for RSV is called motavizumab. However, in a phase 3 trial involving children at high risk, motavizumab did not show any advantage over palivizumab. Additionally, the United States (US) Food and Drug Administration (FDA) did not approve motavizumab due to a greater risk of skin rashes. Another monoclonal antibody suptavumab was reported to have poor activity against RSV-B strains in a phrase 3 effectiveness study (Ramilo *et al*., 2014).

Nirsevimab (Beyfortus®), a recombinant human IgG1 kappa mAb interacts with the RSV F1/F2 subunits (Venkatesan *et al*., 2022). To stop the virus from infecting the host cell, this interaction locks the RSV F protein in the prefusion conformation. A single nirsevimab injection given prior to the RSV season could reduce the incidence of medically attended RSV-associated LRTI by 70% and hospital admissions by 78% for healthy preterm infants (Venkatesan *et al*., 2022). A more recent study evaluating the impact of nirsevimab on healthy term and late-preterm newborns revealed a 75% decrease in medically attended LRTI in the nirsevimab group as opposed to the placebo group (Hammit *et al*., 2022). These variations held true for all RSV subtypes throughout the duration of the trial. Nirsevimab's safety profile is like that of palivizumab (Domachowske *et al*., 2022). The European Union recently approved nirsevimab to prevent RSV illness in neonates and infants throughout their first RSV season.

Prophylactic efforts will be guided by more research on the effectiveness of these mAbs, as it is highly desirable to have a long-half-life product that does not require repeated administration. Meanwhile, there are continuous efforts to lower the cost of mAb products and simplify their administration by needle-free administration (Gatt *et al*., 2023). In summary, numerous RSV vaccinations for mothers and infants are presently undergoing various clinical trials, in addition to ongoing assessments of more recent mAbs, some of which are yielding encouraging outcomes. Future RSV preventative management will probably integrate various active and passive immunization approaches. The immunization objectives in the newborn and early infancy stages can be met by maternal vaccines, passive mAb administration, or a combination of the two. For the older pediatric and adult age groups, active immunization through vaccinations will offer supplemental protection as passively acquired immune responses gradually diminish (Gatt *et al*., 2023).

1.2.12 Recent developments on RSV vaccine development

In 2023, the FDA authorized nirsevimab for usage by all newborns below 8 months old who are contracting RSV for the first time whereas Merck’s clesrovimab had promising results in the phase III clinical trial (Phuah *et al*.,2023). ENFLONSIA (clesrovimab-cfor) is Merck’s extended half-life monoclonal antibody (mAb) designed for passive immunization for the inhibition of respiratory syncytial virus (RSV) lower respiratory tract disease in babies and infants who are

born through or going into their initial RSV season was approved by the US FDA in June 2025 (https://www.merck.com/news/, accessed 30/07/2025). This monoclonal antibody is derived from parental RB1 (Research Biologic 1) (Tang *et al*., 2019) and it targets the conserved site IV of the RSV fusion protein. RB1 was further modified by introducing three amino acid substitutions (YTE) in the Fc domain. The YTE mutation of clesrovimab leads to high binding affinity to the neonatal Fc receptor (FcRn), which improves recycling of the antibody, leading to longer half-life in the serum. Clesrovimab reaches high levels in nasal tissue and concentrations at sites of RSV infection (Zar *et al*., 2025; Zhu *et al*., 2017). It is called an extended half-life monoclonal antibody because it was designed to stay in the body for a while compared to other antibodies. So, the longer it stays in the body, it could potentially confer extended duration of protection against RSV (Madhi *et al*., 2025; Zar *et al*., 2025). ENFLONSIA is directed as non-weight-based and is intended to provide protection against RSV disease through a 5-months long RSV season (http://d5jk.2.vu/1).

Both mAbs target the antigenic site IV, which is found in both the preF and postF conformations of the RSV F protein. Nirsevimab and clesrovimab are more effective compared to palivizumab and therefore they could be administered once per RSV season (Phuah *et al*., 2023). Two newly developed vaccines for adults; Pfizer (Abrysvo) and GSK (Arexvy) have been approved for use in elderly individuals and pregnant women (Kampmann *et al*., 2023; Melgar *et al*., 2023). The AREXVY vaccine is for the prevention of RSV-associated lower respiratory tract disease (LRTD) in adults ≥60 years of age. This adjuvanted vaccine, comprises a stable prefusion RSV-F antigen (RSVPreF3) (Foley *et al*., 2024).

1.2.13 Challenges in RSV vaccine development

Not long after it was isolated, work on developing a pediatric RSV vaccination started. A formalin-inactivated RSV vaccine candidate, FI-RSV lot 100, was injected intramuscularly into infants and children between the ages of two months and seven years in the middle of the 1960s (Fulginiti *et al*., 1969; Kapikian *et al*., 1969). However, FI-RSV increased the chance of acquiring severe respiratory disease after infection with wildtype RSV (wtRSV) virus during the ensuing RSV season, rather than providing protection against wild-type RSV infection and sickness. Two infants who received FI-RSV lot 100 sadly died because of the considerably higher rate of severe RSV disease (44%) among age-matched children with RSV disease compared to placebo recipients (6%) (Fulginiti *et al*., 1969; Kapikian *et al*., 1969). The augmented RSV sickness was characterized by severe bronchiolitis, hypoxemia, and pneumonia. The lungs of the infants who received the FI-RSV vaccine and had enhanced disease had significant eosinophilic infiltrates.

The subsequent conditions are possibly factors to the vaccine failure according to investigations: Significant viral epitopes vital for the activation of a potent neutralizing antibody response and cytotoxic T cell responses were disrupted by formalin inactivation (Fulginiti *et al*., 1969; Kapikian *et al*., 1969; Mazur *et al*., 2022). The insufficient TLR stimulation might have resulted in insufficient maturation of virus-specific antibodies. Furthermore, low antibody avidity may

have amplified the severity of the illness by triggering immune complexes to accumulate in the lungs. Moreover, an imbalance in the T-helper cell response probably made vaccinees more sensitive to mounting allergic asthma when infected naturally (Fulginiti *et al*., 1969; Kapikian *et al*., 1969; Mazur *et al*., 2022).

The requirement for a potent and robust protective immune response in addition to the possibility of vaccine-enhanced illness has impeded the development of the RSV vaccine (Mazur *et al*., 2022). A deeper comprehension of the pathophysiology of FI-RSV and the immunological correlates of RSV protection is crucial for the development of future vaccines. Due to the experience
it has not been possible to develop non-live virus vaccinations in RSV-naive youngsters up to this point with FI-RSV (Mazur *et al*., 2022).

1.2.14 Laboratory diagnostics methods

Viral culture used to be the gold standard method for determining if an RSV infection was productive, but it doesn't always yield fast enough data to guide therapeutic care (Bernstein *et al*., 2023). Consequently, reverse transcription-polymerase chain reaction in real-time (rRT-PCR) is frequently referred to as the reference/gold standard for RSV diagnosis in clinical settings since it can detect the presence of the virus (either active or inactive) with sensitivity that is either equal to or higher than that of viral culture (Bernstein *et al*., 2023). Additional RSV detection methods exist, yet their diagnostic efficacy varies. This includes electron microscopy, indirect and direct immunofluorescent antibody tests, enzyme-linked immunoassays (EIAs), and nucleic acid amplification (polymerase chain reaction [PCR]) (Bernstein *et al*., 2023).

1.2.14.1 Cell culture

For a long while, cell culture was the go-to method for identifying respiratory viral infections. Cell culture can detect viral coinfections, albeit with variable accuracy (Zwang *et al*., 2020). Furthermore, the isolated virus can be kept for use in upcoming diagnostic investigations. However, there are difficulties in cell culture as well, such as the need for specific specimen handling protocols to preserve viral vitality, a lengthy assay period (about 2-5 days), higher labor and material expenses per test, and comparatively lower sensitivity when compared to nucleic acid amplification testing (NAT) (Mesquita *et al*., 2017).

Even if more people are using recently developed diagnostic techniques, cell culture will still be crucial for examining a portion of the viral strains that are released each year for changes in genetic and antigenic makeup (e.g., to search for new mutations that enable viruses to evade detection using antigen/PCR assays) and for finding unidentified viruses, such as the novel human coronaviruses, Boca viruses, and human metapneumovirus (Mesquita *et al*., 2017; Zwang *et al*., 2020). The number of laboratories equipped with tissue culture technology will decline in tandem with the decline in the utilization of the cell culture assay. As such, the establishment of

regional centers for viral isolation might be required to ensure the availability of technical expertise and resources (Mesquita *et al*., 2017; Zwang *et al*., 2020).

1.2.14.2 Serology

Serology is typically not effective for diagnosing acute respiratory viral infections, because 10-15% of patients with proven respiratory viral infections will stay serologically negative. Research-based serologic methods do, nevertheless, yield valuable seroepidemiologic data (Zhang *et al*., 2020).

Antigen detection assays are used by most clinical laboratories to diagnose RSV infection, and several tests are available to give clinicians a quick diagnosis. Antigen-based assays, such as optical immunoassays, Enzyme Immunoassay (EIA), and indirect and direct immunofluorescent antibody tests, have been around for over 30 years. When it comes to simplicity of use, sensitivity, specificity, and convenience of use, EIAs typically offer the finest combination among the commercially available quick diagnostic tests (Mesquita *et al*., 2017). The manufacturer, the virus and strain being detected, the suitability of the samples, and other factors all affect the sensitivity and specificity of these tests. During the off-season, no assay possesses the necessary sensitivity and specificity to yield dependable outcomes. Antigen-based techniques are frequently employed due to their low cost, simplicity of usage, and ease of interpretation (Mesquita *et al*., 2017; Zhang *et al*., 2020).

Nonetheless, the assays that are presently approved by the FDA are still insufficient in terms of sensitivity and specificity, particularly in situations where the virus is uncommon (off-season) or populations like the elderly or immunocompromised. Rapid multiplex point-of-care antigen detection for numerous respiratory viruses, including RSV, is now possible thanks to recent advancements in laboratory diagnostic techniques (Petrocelli *et al*., 2023). These techniques offer higher sensitivity and enable the identification and distinction of several respiratory viruses. However, compared to molecular assays, antigen detection techniques are frequently thousands of times less sensitive (Zhang *et al*., 2020).

1.2.14.3 Molecular assays

The new benchmark for detecting respiratory viruses is molecular assays. When compared to cell culture or antigen tests, they have the benefit of being extremely sensitive and specific (~100%). Research comparing molecular tests to cell culture assays shows that if the assay includes a technique for identifying genuine positives, the sensitivity is much improved (12–50%) (Mesquita *et al*., 2017).

The BioFire Diagnostics-designed FilmArray® is a diagnostic technology used for RSV analysis. It uses a nested multiplex PCR (nmPCR) methodology to identify 16 viral and 4 bacterial targets (at gender and/or species) in a biological sample. Utilizing a disposable, small pouch, the integrated FilmArray® platform is a closed system that facilitates biological reactions

for the extraction, purification, and amplification of the nucleic acid of the pathogen contained in a single sample (Petrocelli *et al*., 2023). The analysis will take about 1 hour to complete. The Cepheid Xpert®Flu / RSV system, a molecular biology diagnostic test that enables one to identify the RSV in just twenty minutes.

An analytical platform that allows for the detection of a greater range of viruses and bacteria from a single nasopharyngeal swab has recently been presented for the diagnosis of symptomatic airway infections. The Seegene Allplex™ Respiratory Full Panel Assay kit is a multiplex One-step RT Real-time PCR assay that simultaneously detects and identifies agents of respiratory illnesses, including 16 viruses, 7 bacteria, and 3 subtypes of human influenza A viruses (Petrocelli *et al*., 2023). About four hours are spent on test setup including nucleic acid extraction, running the test and analysis of results (Petrocelli *et al*., 2023).

1.2.15 Factors affecting the sensitivity and specificity of the assay

The sensitivity and specificity of a test for viral detection might be impacted by several factors. These include specimen quality, specimen transport conditions, reagent quality, experience of the laboratory technician, assay suitability for populations (e.g., rapid antigen test in elderly versus young people), and community prevalence of the agent (Mesquita *et al*., 2017)**.**

1.15. Summary

RSV is a respiratory infection that causes lower respiratory tract infections. It is common in infants, mostly those who are born prematurely and those who are born with congenital heart disease, and adults who are immune compromised or have underlying diseases. It plays a key role in morbidity and mortality in these age groups. RSV is associated with bronchiolitis and pneumonia. There is currently no vaccine licensed for RSV disease, however there is a pipeline of vaccines candidates in clinical trials which mostly focuses on the RSV fusion protein due to its historic nature of being conserved compared to the RSV F proteins. In the absence of a vaccine, infants who are at higher risk of RSV disease are given palivizumab which is a monoclonal antibody that targets the highly conserved antigenic site II of the RSV F protein. Given that hospitalization rates peak at a very young age, maternal immunization could be an effective approach for reducing RSV-related hospitalizations. RSV can be diagnosed using different molecular assays such as rt-PCR and serological assays.

CHAPTER 2

MATERIALS AND METHODS

2.1. Study setting.

This study was conducted in the Division of Virology, University of the Witwatersrand and the National Health Laboratory Services (NHLS). Overview of all research methods described here are shown in Figure 2.1.



Figure 2.1. Overview of research methodology including all the laboratory procedures stepwise.

2.2. RSV F gene sequence data

African RSV-F gene and RSV genome nucleotide sequences were retrieved from GenBank (https://www.ncbi.nlm.nih.gov/nuccore/) and Global Initiative on Sharing All Influenza Data (GISAID) online databases. Assembled sequence contigs were exported in FASTA format. The sequences were from various African countries such as Cameroon, Cote d'Ivoire, Egypt, Gambia, Ghana, Kenya, Madagascar, Mali, Morocco, Mozambique, Senegal, and South Africa.

2.3. F gene and SP sequence analysis

BioEdit v7.2 Sequence Alignment Editor (Hall, 1999) (https://bioedit.software.informer.com/7.2/) and AliView 1.27-Alignment Viewer and Editor (https://ormbunkar.se/aliview/) were used for sequence data collation, extraction of F gene SP sequences and multiple sequence alignment with Clustal embedded in the programs. A2 long

reference strain (GenBank Accession number: M74568.1) and "strain B1" (Accession Number NC_001781.1) were used as reference sequences against RSV-A and RSV-B F gene sequences respectively. To construct phylogenetic trees, Nextclade v.2.14.1 (https://clades.nextstrain.org/) was used for clade and genotype assignment. The genotype assignment for RSV strains based on the G protein gene was done as described by Goya *et al*. (2019) and clade assignment was done as described by Otieno *et al*. (2016). The RSV surveillance server (RSVsurver) on GISAID was used to extract global data for the occurrence of the mutations identified.

2.4. Laboratory Methods

2.4.1. Expression plasmid for RSV F and control plasmid

Human respiratory syncytial virus (RSV) (subtype-A, strain long) fusion glycoprotein / RSV-F (codon optimized) ORF mammalian expression plasmid, N-HA tag as well as a control vector were obtained from Sino Biological (Houston, Texas, U.S.A). The negative control vector lacks the RSV-F open reading frame (Sino Biological: Houston, Texas, U.S.A) and were included to measure the baseline expression levels in transfected cells' supernatant fluids. Inclusion of this control during transfections helps identify whether the protein expression observed is due to the inserted F gene in the test vector or non-specific cellular proteins. The test clone or vector contained a full-length codon optimized F gene sequence (that resembles the F gene from the RSV Long strain) in a CMV expression vector (Sino Biological, Houston, Texas, U.S.A). Full details are found in Appendix B and Appendix C.

2.4.2. Preparation of RSV F protein plasmid stocks

Two LB Agar plates with kanamycin at a final concentration of 50µg/ml (Appendix A) for selection, were used for determining transformation efficiency. For the bacterial transformation 2µl of each RSV-A F gene construct and pCMV control vector which were added into 1.5ml sterile microcentrifuge tubes. The final concentration of the construct and control vector was 10ng in each tube. JM109 High Efficiency competent cells were removed from -80°C and placed in an ice bath until just thawed for five minutes.

The cells were mixed gently by flicking the tube and further transferred 50µl of cells into each 1.5ml tube containing 2µl of each, RSV-A F gene construct and pCMV vector. These tubes were gently flicked to mix and placed on ice for 20 minutes to help maintain the permeability of the cell membrane and high efficiency for DNA uptake. The cells were then removed from ice and heat shocked for 45-50 seconds in a water bath at exactly 42°C to allow the DNA to enter the cell through the disrupted membrane and immediately returned to ice for two minutes to retain the plasmid inside the bacteria. 950µl room temperature SOC medium was added into each tube with the cells and incubated for 1.5 hours at 37°C with shaking (150rpm). The transformation culture was plated through spreading using a spreader onto LB kanamycin plates. The plates were incubated overnight for at least 16 hours.

The following day after transformation, the plates were removed from the incubator and single colonies were picked from the plates, which were each inoculated into 3ml of LB broth in 15ml tubes (10 tubes) with the LB broth containing kanamycin at a final concentration of 50µg/ml. Seven of the tubes contained RSV-F and three contained pCMV transformation mix. These cultures were incubated overnight for a minimum of 16 hours at 37°C and shaking at 100rpm.

2.4.3. Plasmid DNA purification

Plasmid purification was performed using Qiagen plasmid mini purification kit (Qiagen, Hilden, Germany) according to manufacturer's instructions. The bacterial cells were harvested by centrifugation at 6000 x g for 15 minutes at 4°C. Column based purification method was used. The pelleted bacterial cells were resuspended in 3000µl buffer 1 containing Tris-Cl-maintains stable pH, EDTA weakens the bacterial cell and inactivate DNases and it is mixed with RNase A (degrades RNA, so the final product is plasmid DNA) and transferred to a microcentrifuge tube. Then 3000µl of buffer 2, the lysis buffer with high concentration of salts namely, sodium hydroxide and sodium dodecyl sulfate to disrupt the cells and denatures both proteins and nucleic acids, was added into the tube and mixed thoroughly by inverting the tube 6 times. Subsequently, 3000µl of buffer 3 (neutralization buffer containing potassium acetate) was added to neutralize the alkaline lysis mixture by mixing thoroughly by inverting the tube 6 times. This step enables renaturation of plasmid DNA. The lysate was centrifuged for 10 minutes at 16000 x g to pellet (clear) white debris.

The Qiagen-tip was equilibrated with 10000µl of buffer QBT -Equilibration buffer contains quinidine hydrochloride and ethanol which helps DNA binds to the silica membrane more tightly by creating a high-salt, chaotropic environment after centrifuging and allowed the column to empty by gravity flow. The cleared lysate supernatant was loaded onto the Qiagen filtered tip and permitted to pass through the filter resin by gravity flow; followed by washing twice with 2000µl QC Wash buffer (contains ethanol and Tris-CL) to remove residual salts, proteins and other impurities from the silica column. Ethanol helps maintain DNA binding to the membrane during wash. After washing with QC, the plasmid DNA was eluted from the tip membrane with 8000µl of buffer QF (containing 10mM Tris-CL pH 8.5) into a clean tube. To precipitate the DNA, isopropanol was added to the eluate, and the mixture was centrifuged to pellet the plasmid DNA. The supernatant was discarded, then the pellet was air-dried for 10 minutes and redissolved DNA in a 50µl TE buffer. Followed by gel electrophoresis to see the plasmid DNA recovered using 0,8% agarose gel (1.6g) in TAE buffer (200ml). The concentration of the purified plasmid DNA was determined using a nanophotometer by measuring absorbance at 260 nm and 280 nm. According to the manufacturer's instructions, when working with a high copy plasmid the expected concentrations are between 100 to 200ng/µl with absorbance 260/280 ratio of approximately 1,8 indicating high purity.

2.4.4. Agarose gel electrophoresis

To see the plasmid DNA recovered, a 0,8% agarose, Molecular Grade (Bioline, London, England), was prepared by dissolving 1,6g of agarose powder into 200 ml of 1×Tris-Acetate-EDTA (TAE) buffer to examine the results of the plasmid DNA purification. The agarose gel was stained with 1µl of a fluorescent dye called GelRed ® Nucleic Acid (Biotuim, Fremont, CA) before it was poured into a gel casting tray. The samples were prepared for loading into gel wells by mixing 5µl of the purified plasmid DNA and 1µl of loading dye (Thermo Fisher Scientific, USA). A 1kb DNA ladder was used (Promega Corporation, Madison, USA) as a reference. Then 5µl of DNA ladder was loaded into the first well, followed by 5µl of each plasmid DNA sample mixed with loading dye. The gel electrophoresis was run at 120V and 140 Amps for 60 minutes. The results were visualized under UV light using the Gel-doc system (Syngene, Frederick, USA).

2.5.Primer design and preparation

The most prevalent mutations: (I5T, A8T, T12I and L15F), were identified from multiple sequence alignment analysis. Overlapping forward and reverse primers containing the mutation of interest that are 25 to 45 nucleotides in length were designed using NEB online design software, NEBase Changer tool (https://www.neb.com/en/neb-primer-design-tools/neb-primer-design-tools) (Table 2.1). These primers were synthesized and purified using HPLC purification (Integrated DNA Technologies (Coralville, Lowa, United States). The amino acid substitutions (I to T change at position 5, A to T change at position 8, T to I change at position 12 and L to F change at position 15) were identified for introduction through mutation by site-directed mutagenesis using designed primers shown in Table 2.1. The mutation primers were reconstituted according to the manufacturer's instructions at 10µM. The mutations were introduced into the RSV F gene expression vector using a Q5 site directed mutagenesis kit (New England Biolabs, Ipswich, MA, USA).

Table 2.1: List of mutation primer sets to introduce the selected mutations using site-directed mutagenesis.

Mutation	Native sequences	Mutated sequences	Forward Primer	Reverse Primer	Melting temperature
Isoleucine to threonine change at Position 5	ATT	ACT	GGAACTGCCGactCTG AAAGCCA GC=57%	ATTTAGTGATGGTGG TGATGATGGTG GC=42%	68°C
Alanine to threonine change at position 8	GCC	ACC	GATTCTGAAAaccAAT GCCATCAC GC=42%	GGCAGTTCCATTTAG TGATG GC=45%	62°C
Threonine to isoleucine change at position 12	ACC	GCT	CAATGCCATCgctACCA TCCTGG GC=57%	GCTTTCAGAATCGGC AGTTC GC=50%	65°C

Leucine to phenylalanine change at position 15	CTG	TTC	CACCACCATCttcGCAG CAGTGA GC=57%	ATGGCATTGGCTTTC AGAATC GC=43%	64°C

2.6. Site-directed mutagenesis to mutate RSV F clone SP sequence.

2.6.1. Exponential Amplification (PCR)

To amplify the material using the Q5 site directed mutagenesis kit, (New England Biolabs, Ipswich, MA, USA) exponential amplification PCR was run, and the following reagents were assembled into one PCR tube to run the PCR: Q5 Hot start high fidelity 2X master mix- 12,5µl, 1,25µl of each primer, template DNA 1µl and nuclease free water 9,0µl (Table 2.2). These reagents were mixed completely and thermocycling was performed using conditions in Table 2.3 according to the manufacturer's instructions on an ABI 9700 thermocycler (Applied Biosystems, California, USA) with ramp speed set at maximum.

Table 2.2. Mutation PCR reagents and volumes required per reaction.

Reagents	25 µl RXN	FINAL CONC.
Q5 Hot Start High-Fidelity 2X Master Mix	12,5 µl	1X
10µM Forward Primer	1,25 µl	0,5µM
10µM Reverse Primer	1,25 µl	0,5µM
Template DNA (1–25ng/µl)	1 µl	10ng
Nuclease-free water	9,0 µl	

Table 2.3: Thermocycling conditions for site directed mutagenesis mutation PCR.

Step	Temp	Time
Initial denaturation	98ºC	30 seconds
PCR cycling: 25 cycles		
Denaturation	98ºC	10 seconds
Annealing	52ºC	15 seconds
Elongation	72ºC	30 seconds/kb
Final extension	72ºC	2 minutes
Hold	10ºC	indefinitely

2.6.2. Kinase, Ligase & Dpnl (KLD) Treatment

The PCR product was then added directly to a unique kinase-ligase-Dpnl (KLD) enzyme mix for rapid (5 minutes), room temperature circularization and template removal, for this procedure, in one tube 1 µl of PCR product. 5 µl of 2X KLD reaction buffer, 1 µl 10X KLD of enzyme mix, 3 µl of nuclease free water were all added and mixed well by tapping tubes. The roles of these enzymes in site directed mutagenesis are as follows: Kinase speeds up the reaction via an active base residue R1, which draws a proton from the substrate R3, transferring the weakly nucleophilic hydroxyl to an alkoxide ion which strikes the phosphate of ATP. Any template DNA that was still left and not mutated in the PCR is terminated by the Dpnl which cleaves the methylated plasmids (unmutated). The new fragments of the synthesized DNA are joined together by ligase for the formation of a seamless strand. The mixture was incubated at room temperature for 5 minutes.

2.6.3. Transformation

300ml of LB agar was prepared by dissolving 9,6g of LB agar powder to 300ml of distilled water. X-gal is used for differentiating between white colonies where the plasmid's lacZα gene was disrupted by a DNA insert and therefore the bacteria could not hydrolyse the X-gal and blue colonies for bacteria that could hydrolyse the X-gal as their lacZα genes remained intact due to no DNA insert. After the LB agar was prepared, the following additions were made to enable blue/white colony selection: 300 µl of IPTG (100mM), 500 µl of kanamycin (100 mg/ml) and 60 µl of X-gal (20 mg/mL) were added per 100ml LB agar. The pCMV plasmid DNA used as a control was diluted at a 1:5 ratio of DNA to total volume by adding 20 µl of the nuclease free water to 5 µl of the plasmid DNA to obtain a concentration of 20ng/µl in a total volume of 25 µl.

Following the KLD treatment, the mixture was transformed into a high efficiency NEB 5-alpha tube of competent cells which was thawed on ice to maintain the cell membranes' permeability and to stabilize the DNA-cell membrane interaction for uptake of the plasmid DNA. Furthermore, 5 µl of the KLD mix from the KLD section was added into a tube with 50 µl of the competent cells. The tube was flicked 4-5 times to mix completely and placed on ice for 30 minutes. It was removed from ice and heat shocked for 45 seconds and immediately returned to ice for 5 minutes. 400ml of SOC medium was added into the tube after being placed on ice for 5 minutes and incubated at 37ºC for 60 minutes with shaking at 250rpm. The transformation culture was then removed from the incubator and centrifuged for five minutes at maximum speed. The supernatant was discarded and spread the pellet onto a selection plate with kanamycin, X-GAL and IPTG and incubated overnight for at least 16 hours at 37ºC.

2.6.4. Bacterial culture and Plasmid DNA preparation

The LB plates with kanamycin and transformation culture were removed from the incubator after 24 hours and picked up single white colonies from each plate using inoculation loop and added the colonies into 3ml of LB broth with kanamycin at final concentration of 50µg/ml, followed by incubation overnight for at least 16 hours at 37°C.

2.6.5. Mini Plasmid DNA purification

Mini prep was performed using the Qiagen mini prep kit (according to manufacturer's instructions) followed by gel electrophoresis to see the plasmid DNA recovered using 0,8% agarose gel (1,6g) in TAE buffer (200ml). Full protocol on page 51, section 2.4.5.

2.6.6. Midi plasmid DNA purification

Midi prep was performed using the Qiagen midi prep kit (according to manufacturer's instructions) followed by gel electrophoresis to see the plasmid DNA recovered using 0,8% agarose/TAE gel (1,6g agarose in 200ml TAE buffer). Full protocol in section 2.4.5.

2.7.Sanger sequencing of mutant plasmid clones

Following ligation and transformation, colonies were picked and sequenced with T3 (5'-AATTAACCCTCACTAAAGGG) and T7 (5'- GTAATACGACTCACTATAGGGC) primers to confirm the presence of the F gene and identify bacterial cultures for extraction of F gene containing plasmid DNA. The presence of the desired mutations was confirmed by sequencing of mutated RSV-F clones' plasmid DNA of 7889 base pairs (bp) size in total (of which the F gene insert is 1725 bp) as determined by agarose (0,8%) gel electrophoresis with appropriate DNA molecular weight size markers to identify clones of the correct size (7889 bp). Plasmid DNA for transfection experiments and bacterial stocks were prepared from successfully mutated clones and stored at -20ºC.

2.8. Cell culture and transfection of 293T cells

2.8.1. Cell lines HEK293T (Human Embryonic Kidney SV40 large T antigen)

The HEK293T cells were cultured at 37° in 5% CO2**.** The adherent 293T cell line was used for cell culture due to their high reported efficiency for successful transfections and expression of heterologous proteins (Ooi *et al*., 2016). They were maintained in Dulbecco's modified Eagle medium (DMEM) (Gibco, New York, USA), supplemented with 10% fetal bovine serum (FBS) (Gibco, New York, USA) 1% L-glutamine (Gibco, New York, USA) 1% penicillin/ streptomycin (Gibco, New YORK, USA) and non-essential amino acids (Gibco, New York, USA) in a 37ºC incubator with CO_2.

The cells were maintained every two days for two weeks in this way: The flasks with the cells were removed from the incubator and discarded the previous media which the cells consumed. Furthermore, 2ml of PBS was added into the flask to rinse the cells. The PBS was then removed and added 1ml of trypsin, cell detachment solution which allowed the cells to detach completely. Then added 2ml of DMEM with 10% FBS and streptomycin/penicillin antibiotics cocktail to stop the cell detachment reaction, pipette up and down 8 times to un-clump the cells and make them singular. Afterwards, everything was removed from the flask and seeded 0,5ml of the cells and added 10ml of the media and incubated at 37°C in the CO2 incubator. Cells were viewed

under a light microscope to ensure that 80-90% confluency was reached before proceeding with transfections.

2.9. Transfection of 293T cells with mutated F clones

Following cell culture, the culture density was transfected with a plasmid mixture (I5T and T12I, mutated clones) using the Lipofectamine 3000 reagent transfection kit (Thermo Fisher Scientific, USA) in accordance with the manufacturer's instructions. The P3000 reagent plays an essential role in the Lipofectamine 3000 transfection system. While the Lipofectamine reagent facilitates membrane interaction and nucleic acid delivery, P3000 improves complexation, stability, and intracellular trafficking of the DNA mixture. The 2-tube system improves transfection efficiency (Thermo Fisher Scientific, USA).

Mixture 1 contained: 24,05µl ([58,05ng/µl]) and 12,06µl ([29,10ng/µl]) of plasmid I5T and 0,5µl ([700ng/µl]) and 15,45µl ([45,30ng/µl]) of T12I mutated clones were added into different tubes each containing 250µl of serum free media (panserin) and 10 µl of P3000 reagent. Mixture 2 was prepared by mixing 250µl of serum free media to 7,5µl of lipofectamine for each transfection reaction.

For each transfection reaction Mixtures 1 and 2were combined into one tube, mixed completely and incubated for 5 minutes at room temperature. Thereafter, 6ml of warm serum-free media was added to T75cm of cells after the 5 minutes incubation and then added the transfect mix drop wise to cells and incubated at 37ºC incubator for 48 hours.

2.9.1. Harvesting of cells and culture supernatant fluids for protein detection

After the 48 hours incubation, the culture supernatant fluids and cells were harvested in 15ml tubes and centrifuged for 10 minutes at 4000rpm. The supernatant fluids were separated from the pellet and were stored as 200µl aliquots in a -20 degrees Celsius freezer until needed for SDS-PAGE gel electrophoresis.

The cell pellets were washed with PBS and centrifuged for 10 minutes at 4000rpm, then removed the PBS and added 1 ml of lysis buffer (Appendix A) to resuspend and lyse the cells. Furthermore, the cells were incubated on ice for 10 minutes and centrifuged again this time for 5 minutes at 4000rpm. The lysate supernatant was then harvested and transferred into a new tube and centrifuged at 11000rpm for 10 minutes whereafter the lysate supernatant was again harvested. Afterwards, 200 µl aliquots of the harvested cell lysates were made and stored at -20ºC until used for SDS-PAGE gel electrophoresis.

2.10. Detection and quantification of total protein

The total protein concentration was determined using the bicinchoninic acid (BCA) protein assay kit (Thermo Fisher Scientific, USA). Reconstituted bovine serum albumin (BSA) standards were prepared as dilutions outlined in Table 2.4 using microcentrifuge tubes and a 96-well microplate.

For the working solution, 15µl of reagent A (containing sodium carbonate, sodium bicarbonate, bicinchoninic acid (BCA), and sodium tartrate in 0.1 N sodium hydroxide) which reacts with cuprous (Cu) ions. was mixed with 300µl of reagent B (containing 4% cupric sulfate solution) which contains the Cu ions needed for the biuret reaction. For assays in microplates the manufacturer recommended that smaller volumes (10–25µl) of protein sample can be used at a ratio of 1:8 for sample to working reagent but cautions to potential difficulties with interfering.

Table 2.4. BSA standard dilution scheme for the 96 well microplate procedure to determine protein quantification.

Vial	Volume of diluent (PBS)	Volume and source of BSA	Final BSA concentration
A	0	300µl of stock	2 000µg/ml
B	125µl	375µl of stock	1 500µg/ml
C	325µl	325µl of stock	1 000µg/ml
D	175µl	175µl of vial B dilution	750µg/ml
E	325µl	325µl of vial C dilution	500µg/ml
F	325µl	325µl of vial E dilution	250µg/ml
G	325µl	325µl of vial F dilution	125µg/ml
H	400µl	100µl of vial G dilution	25µg/ml
I	400µl	0	0=Blank

substances and low protein concentrations. Here, 25µl of each standard was pipetted into 96-well microplate wells and each standard solution was tested in triplicate. Subsequently added 5µl each sample (I5T and T12I) in duplicates into clean vials in the microplate well with 20µl of the PBS. Then added 200µl of the working solution into each well of both the standards and samples. The solutions were mixed well and incubated the plate at 37ºC for 30 minutes. After incubation, the absorbance was measured at 562 nm on a plate reader. The linear equation used to solve X, the protein concentration in µg/mL was Y= mX + b where the Y-axis is the absorbance readings, m= the slope and b= the Y intercept.

2.11. ELISA

ELISA (EUROIMMUN, Medizinische Labordiagnostika AG) was performed using human plasma samples to identify and select plasma which are positive for RSV IgG antibodies (ethical approval number M200902) to use as primary antibody to detect RSV F proteins by western blot. Plasma samples were diluted 1:101 in sample buffer (10µl plasma samples were added to 1,0ml sample buffer and mixed well) before addition of 200µl of each to columns 2 and 3 in order as indicated (Table 2.5).

Table 2.5. Pipetting protocol for ELISA indicates the layout used for positive control, calibrators, negative control and human plasma samples.

Column	1	2 (Plasma samples)	3 (Plasma samples)
A	Calibrator 1	29	1757D
B	Calibrator 1	44	1755D
C	Calibrator 2	50	1751D
D	Calibrator 2	35	1774D
E	Calibrator 3	1734D	1760D
F	Calibrator 3	1735D	1736D
G	Positive	1500D	1773D
H	Negative	1759D	1753D

Sample incubation: 100µl of the calibrators (standards), positive and negative controls and diluted plasma samples were transferred into individual microplate wells pre-coated with RSV F proteins and incubated for 30 minutes at room temperature to allow for antigen-antibody binding to occur. The plate was washed to remove unbound antibodies, 3 times with 450µl working strength wash buffer using the Bio-Rad plate washer (Hercules, California, USA) and tapped dry after the third was to remove excess liquid.

Subsequently, pipetted 100µl of enzyme conjugate (peroxidase-labelled anti-human IgG) into each well of the microplate wells and incubated for 30 minutes at room temperature. Then the plate was washed 3 times as described. Thereafter, 100µl of chromogen/substrate solution was pipetted into each of the microplate wells and incubated for 15 minutes at room temperature. The plate was covered with foil to protect it from direct light, which can result in early or non-specific color formation and affect assay accuracy. Then 100µl of stop solution chromogen/substrate solution was added and measurement was done within 30 minutes of adding stop solution. Photometric measurement of the color intensity was made at wavelengths of 450 nm and 650 nm.

The results were determined by calculating a ratio of the extinction value of the patient/ test sample over the extinction value of calibrator 2 and further interpreted as follows using the manufacturer's instructions: ratio <0,8: negative, ratio ≥0,8 to <1,1: borderline and ratio ≥1.1: positive.

2.12. SDS-PAGE and Western Blotting to detect mutated F clone expression.

Following transfection, to confirm that the correct gene was successfully expressed the harvested cell lysates and culture supernatant fluids were loaded for separation of proteins by sodium dodecyl sulfate polyacrylamide gel electrophoresis (SDS-PAGE) and staining with EZ blue gel staining reagent to detect the F proteins.

2.12.1. Running NuPAGE Bis-Tris mini protein gel

Protein extracts were prepared in a Laemmli sample buffer, 15µl of each sample (I5T and T12I) and 15µl of the sample buffer into different tubes. To have the final equal volume for each

sample to run western blot, we added PBS to each sample based on the calculated concentrations from the standard curve (Figure 3.9). These samples were heated on a heating block at 95ºC for 10 minutes to denature the proteins. The samples were loaded into the wells of the pre-cast gels from Invitrogen (NuPAGE Bis-Tris mini protein gels) and run the gel in 1X Tris-glycine running buffer for two hours at 300V and 50mA. The molecular mass of the protein (F1 and F2) after cleavage of F0 precursor, is 45-55kDa and 18 kDa in SDS-PAGE under reducing conditions.

2.12.2. Transfer of proteins to membrane

To confirm the presence of the recombinant RSV F protein. Proteins were transferred onto a nitrocellulose membrane. The transfer sandwich was prepared for gel transfer using the Bio-Rad semi-dry transfer blot. Two blotting papers were wetted in transfer buffer (Running buffer diluted with 20% methanol, 30ml of methanol and 120ml of the running buffer) and placed on the semi-dry transfer blot, followed by a wet nitrocellulose membrane (Whatman plc, Maidstone, United Kingdom) from the transfer buffer, which was placed on the blotting papers, added the gel on top of the membrane with two more blotting papers again.

The transfer ran overnight at 25V and 40mA. The following day the membrane was washed with PBS and stained with ponceau stain to check whether the transfer was successful. Subsequently, blocked the membrane with a blocking buffer for 1 hour. The membrane was then washed with PBS and incubated with primary antibody, 7µl of the HCV plasma positive sample and 14ml of the blocking buffer at 4ºC overnight. The membrane was then washed with TBST three times after incubation and incubated again with secondary antibody (2µl of the goat anti-human IgG conjugated to horseradish peroxidase diluted in 12ml blocking buffer) for 1 hour.

2.12.3. Detection of F protein specific bands by membrane immunoblotting

Post to 1 hour incubation, the secondary antibody was discarded, and the nitrocellulose membrane was washed three times with TBST and subsequently added the 3,3’,5,5’-Tetramethylbenzidine (TMB) membrane substrate to the nitrocellulose membrane to visually detect the presence of bound horse peroxidase conjugated antibodies after incubation for 30 minutes at room temperature in the dark.

2.14.Ethics

An application for ethical clearance waiver was submitted to Wits Human Ethics Committee (HREC) and an approval to continue with the study was granted (Reference number M230345, Appendix D). RSV sequence data was retrieved from GISAID following registration and adhering to their data sharing agreement.

CHAPTER 3

RESULTS

RSV-A and -B strains from Africa

A total of 4876 RSV sequences were available of which 330 were from GenBank and 4546 from GISAID (https://gisaid.org/; date accessed 22/08/2022). Of these, 78,8% (3841/4876) were excluded, due to lack of the F gene sequences. A total of 1035/4876 (21,3%) RSV F gene sequences with the signal peptide remained in the final dataset used for analysis. Of the 1035 sequences 10,1% (105/1035) were from the RSV-A subgroup and 89,9% (930/1035) were RSV-B. The oldest sequences included were from 2005 but most of the sequences were from 2015 to 2022.

3.1. Phylogenetic analysis of RSV-A F genes

For analysis, 105 African RSV-A F gene sequences (Figure 3.1a) were combined with reference global data provided by Nextclade. GA2.3.5 was the most prevalent genotype and GA3.0.5b the least prevalent genotype. Among the African RSV-A subgroups, the most dominant genotypes were GA2.3.5 (47,6%; 50/105) and GA2.3.3 (34,3%; 36/105) (Figure 3.1b). Genotype GA2.3.5 was detected in the following African countries: South Africa (74%; 37/50), Morocco (20%; 10/50), Gambia (6%; 3/50), and Cote d'Ivoire (2%; 1/50).

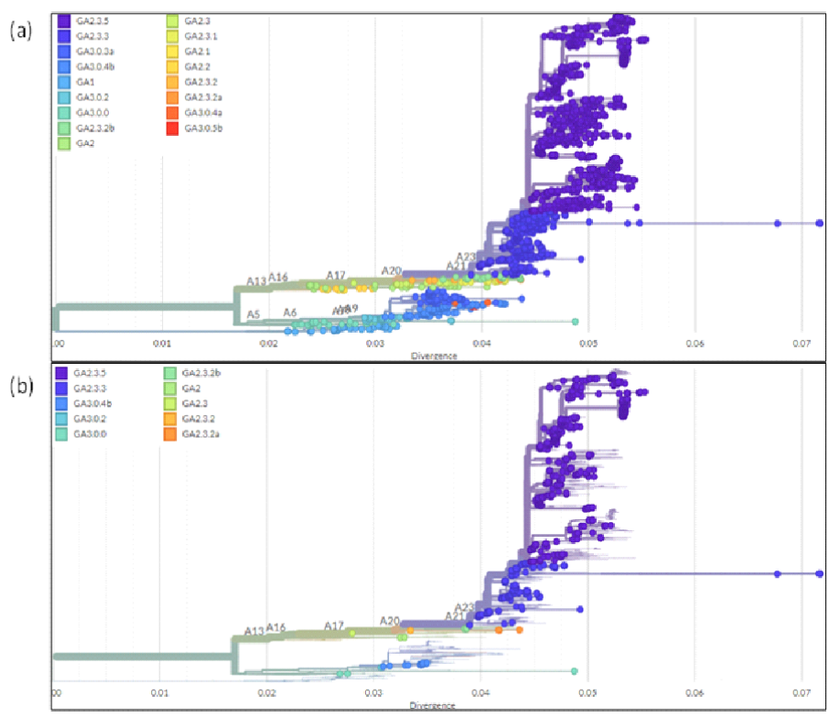


Figure 3.1. Nextclade constructs a phylogenetic tree for RSV-A with (a) showing the African sequences and reference global data combined whereas (b) shows *only* the African sequences (n=105) from this study. G genotypes are indicated by the colored round tips with clade names indicated at branch nodes. Reference strain hRSV-A England/397/2017 (EPI_ISL_412866) was used as the root on Nextclade.

The remaining two sequences were missing information on geographic origin. GA2.3.3 was seen in South Africa (36,1%; 13/36), Kenya (2%; 9/36), Morocco (22,2%; 8/36), Cote d'Ivoire (16,6%; 6/36). The most prevalent genotypes were followed by these other genotypes that were identified on the African sequences: GA3.0.0 (11,4%; 12/105) originated from Kenya (83,3%; 10/12) and Ghana (16,6%; 2/12). The GA2.3.4b genotype accounted for (4,8%; 5/105) of strains and was detected among RSV sequences originating from South Africa, whereas the two GA2.3.2 strains were identified in Egypt and Cote d'Ivoire.

3.1.1. RSV-A F genes clade assignment

The RSV-A genomes clustered predominantly into clade A23 (47,6%; 50/105) which is representative of genotype GA2.3.5 strains that circulated between 2007 and 2022 (Table 3.1). Clade A6 strains (34,3%; 36/105) circulated between 2010-2019 and were all genotype GA2.3.3. While clades A8 (11,4%; 12/105) and A12 (4,8%; 5/105) were classified as genotypes GA3.0.0 and GA3.0.4b, respectively (Table 3.1).

Table 3.1. Summary RSV-A F genes clades detected in Africa with their genotypes and the period they were detected.

Clade	n/N (%)	Genotypes	Geographic origin	Period detected
A6	36/105 (33,91%)	GA2.3.3	South Africa, Morocco, Kenya, Cote d'Ivoire,	2010 - 2019
A8	12/105 (11,43%)	GA3.0.0	Kenya and South Africa	2010 - 2018
A12	5/105 (4,76%)	GA3.0.4b	South Africa	2018
A17	2/105 (1,90%)	GA2.3.2	Egypt and Cote d'Ivoire	2017 - 2020
A23	50/105 (47,62%)	GA2.3.5	South Africa, Gambia, Morocco, Kenya, Cote d'Ivoire,	2007- 2022

3.2 Phylogenetic analysis of RSV-B F genes

Figure 3.2 shows Nextclade constructed a phylogenetic tree for (a) combined African and global reference data whereas (b) shows only the African RSV-B sequences (n=930). Among the combined RSV-B F gene sequences, GB5.0.5a was identified as the most prevalent genotype (Figure 3.2a).

The following RSV-B genotypes were represented: GB4, GB5, GB5.0.0, GB5.0.1, GB5.0.2, GB5.0.4a and GB5.0.5a (Figure 3.2b). Of these, GB5.0.5a represented (66,9%; 622/930) and GB5.0.2 (28,9%; 269/930) of the RSV-B F gene sequences. GB5.0.5a strains were from Kenya (39,4%; 245/622), South Africa (16,2%; 101/622), Mozambique (3,2%; 20/622), Senegal (2,7%; 17/622), Cote d'Ivoire (1,9%; 12/622), Egypt (1,5%; 9/622), Morocco (1,5%; 9/622), Madagascar (0,2%; 1/622), and unknown origin (33,4%; 208/622). GB5.0.2 genotype was present among African RSV-B sequences from Kenya (63,9%; 172/269), Gambia (13,4%: 36/269), Mali (4,9%; 11/269), South Africa (1,1%; 3/269), Morocco (0,5%; 5/269), Ghana (2,6%; 7/269), Cameroon (3,0%; 8/269). The remaining sequences did not have geographic

origin information (11,9%; 32/269). Only 1 GB5.0.1 genotype was among the RSV-B F sequences and geographic information was missing.

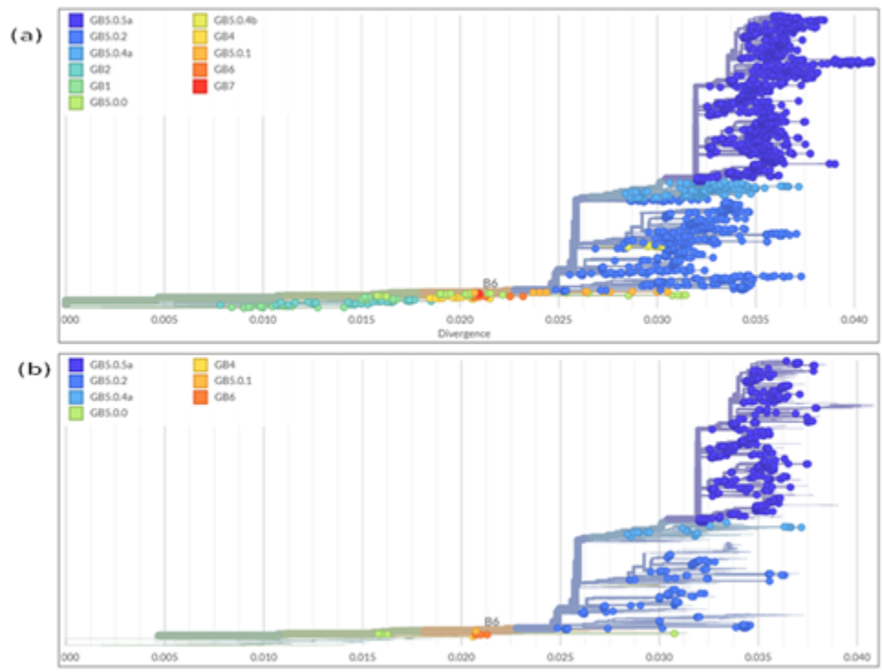


Figure 3.2. Nextclade constructs a tree for RSV-B with (a) showing the African sequences and reference global data combined whereas (b) highlights *only* the African sequences (n=930) from this study. The hRSV-B/Australia/VIC-RCH056/2019 (EPI_ISL_1653999) was used as root for both trees.

3.2.1. RSV-B F genes clade assignment

There were only three clades (B1, B2 and B6) identified among RSV-B sequences from Africa. The RSV-B F genes clustered predominantly into clade B6 at (99,0%; 921/930) represented by GB5.0.2, GB5.0.5a and GB5.0.4a genotypes that circulated between 2007 and 2022 (Table 3.2). Clade B1 only included genotype GB6 whereas clade B2 included both GB5.0.0 and GB4 genotypes (Table 3.2). There were two sequences that had missing data.

Table 3.2. Summary RSV-B F genes clades detected in Africa with their genotypes and the period they were detected.

Clades	n/N (%)	Genotypes	Geographic Origin	Period detected
B1	5/930 (0,65%)	GB6	unknown	unknown
B2	2/930 (0,21%)	GB5.0.0 and GB4	unknown	unknown
B6	921/930 (99,03%)	GB5.0.2, GB5.0.5a and GB5.0.4a	South Africa, Morocco, Kenya, Cameroon, Mali Gambia, Ghana	2007-2022

3.3 Single nucleotide polymorphisms in the signal peptide of African RSV-A F proteins

The summary of amino acid frequencies at each position across the F protein's signal peptide sequences is shown in table 3.3. Mutations were identified at seven amino acid positions among

the signal peptide sequences of African RSV-A strains occurring at frequency of <3%. At position 5, (I) isoleucine to (T) threonine change was observed in 2,9% (3/105) of RSV-A sequences. At position 6 the (L) lysine to (H) histidine mutation was present in 1,0% (1/105) of sequences. At position 8, (T) threonine changed to either (A) alanine (1,9%; 2/105) or (I) isoleucine (1,0%; 1/105). An (A) alanine to (T) threonine (1,0%; 1/105) change was seen at position 10. At position 12, amino acid substitutions were seen at frequencies of 1,9% (2/102) and 1% (1/102), respectively for T12I and T12A. The amino acid substitution T13A occurred at a frequency of 1% (1/104). Lastly, (L) lysine to (F) phenylalanine substitution was seen at position 15 at a frequency of 1,9% (2/105). Gaps were identified, at positions 1, 2 and 3 in less than 2% of sequences.

Table 3.3. Positional amino acid frequencies in RSV-A signal peptide (N=105).

Position	Wildtype Amino acid	Wildtype n (%)	V1 n (%)	V2 n (%)	GAPS n	%
1	M	103 (98,9%)			2	1,9%
2	E	104 (99,1%)			1	1,0%
3	L	104 (99,1%)			1	1,0%
4	P	105 (100%)				
5	***I***	***102 (97,1%)***	***T 3 (2,9%)***			
6	L	104 (99,1%)	H 1 (1,0%)			
7	K	105 (100%)				
8	***T***	***102 (97,1%)***	***A 2 (1,9%)***	***I 1 (1,0%)***		
9	N	105 (100%)				
10	A	104 (99,1%)	T 1 (1,0%)			
11	I	105 (100%)				
12	***T***	***102 (97,1%)***	***I 2 (1,9%)***	***A 1 (1,0%)***		
13	T	104 (99,1%)	A 1 (1,0%)			
14	I	105 (100%)				
15	***L***	***103 (98,1%)***	***F 2 (1,9%)***			

*V which stands for variant. A2 Long strain as reference (GenBank Accession number: M74568.1).

3.4. Characteristics of the most prevalent RSV-A SP amino acid mutations.

The genotype and clade that were most frequently associated with the prevalent mutations observed in the signal peptide were at positions 5, 8, 12 and 15 (Table 3.4). The I5T mutation was associated with genotype GA2.3.3 (clade A23) identified in Egypt circulating in 2018 (Table 3.2). While T12A/I and T8I/A mutations were associated with genotype GA2.3.5 of clade A23 among South African RSV-A sequences from 2018 and 2020, respectively (Table 3.2). L15F mutation was associated with genotype GA2.3 (clade A17) strains detected in Egypt circulating in 2019.

Table 3.4. Summary of genotype, geographic location, and year of detection of RSV-A strains with key signal peptide mutations.

Mutations	*Genotype	**Clade	Geographic location	Year
I5T	GA2.3.3	A23	Egypt	2018
T8A/I	GA2.3.5	A23	South Africa	2020
T12I/A	GA2.3.5	A23	South Africa	2018
L15F	GA2.3	A17	Egypt	2019

*Genotype assignment as described by (Goya *et al*., 2019) **Clade assignment as described by (Otieno *et al*. 2016)

3.5. Global frequencies of prevalent RSV-A SP mutations

Assessment of prevalent SP mutations among global data of RSV-A are provided (Table 3.5). Sequences from this study with the identified SP mutations were uploaded on GISAID to compare our data with the global data. The most prevalent mutation was T12I, prevalent at a frequency of 12,80%) (770/6016) in the global dataset representing sequences from 6 continents: Africa (7,5%; 58/770), Asia (16,9%; 130/770), Australia (0,8%; 6/770), Europe (36,5%; 281/770), North America (30,5%; 235/770) and South America (7,8%; 60/770). In Africa, this mutation was dominantly present in South Africa at a frequency of (96,6%; 56/58) and occurred in Cote d'Ivoire (Figure 3.3.c). The T12A substitution occurred only at a frequency of 0,04% (3/6016) in the global dataset and was associated with lineage GA2.3.5/A23.

Table 3.5. Global frequency of select signal peptide sequence mutations for RSV-A determined using RSVsurver GISAID.

Amino acid Position	Mutation	V1	% (n/N)	Geographic Origin	Period
5	I5T	T	0,06% (4/6785)	Africa (3) North America (1)	2018- 2019 2022
8	T8A/I	A	0,03%(2/6743)		
		I	0,59% (40/6743)	Africa (3) Asia (1) Europe (33) North America (1) South America (2)	2021-2021 2019 2019-2022 2019 2018-2019
12	T12A/I	I	12,80% (770/6016)	Africa (58) Asia (130) Australia (6) Europe (281) North America (235) South America (60)	2019-2033 2019-2023 2019 2022-2022 2019-2023 2019-2023
		A	0,04% (3/6016)		
15	L15F	F	6,73% (428/6364)	Africa (26) Asia (24) Australia (248) Europe (42) North America (42) South America (46)	2019-2022 2019-2021 2020-2022 2018-2022 2019-2022 2021-2022

Followed by L15F that occurred at a frequency of (6,73%; 428/6364) already across 6 continents: Africa 6,1% (26/428), Asia 5,6% (24/428), Australia (57,9%; 248/428), Europe 9,8% (42/428), North America 9,8% (42/428), South America (10,8%; 46/428). In Africa, it was found in Kenya 69,2% 18/26), then in Egypt 26,9% (7/26) and least common in South Africa (3,8%; 1/26) (Figure 4.3.d). L15F was associated with lineage GA2.3/A23. T8I, prevalent at (0,59%; 40/6743) and T8A at (0,03%; 2/6743) of the global dataset. The T8I substitution was present in the following continents: Africa 7,5% (3/40), Asia 2,5% (1/40), Europe (82,5%; 33/40), North America (2,5%; 1/40) and South America (5%; 2/40). In Africa it's only been seen in South

Africa (Figure 4.3.b). The least prevalent mutation was I5T at (0,06%; 4/6785) of global dataset and associated with RSV-A viruses from 2 continents: Africa (3) and North America (1). I5T only occurred in Egypt in Africa (Figure 3.3.a).

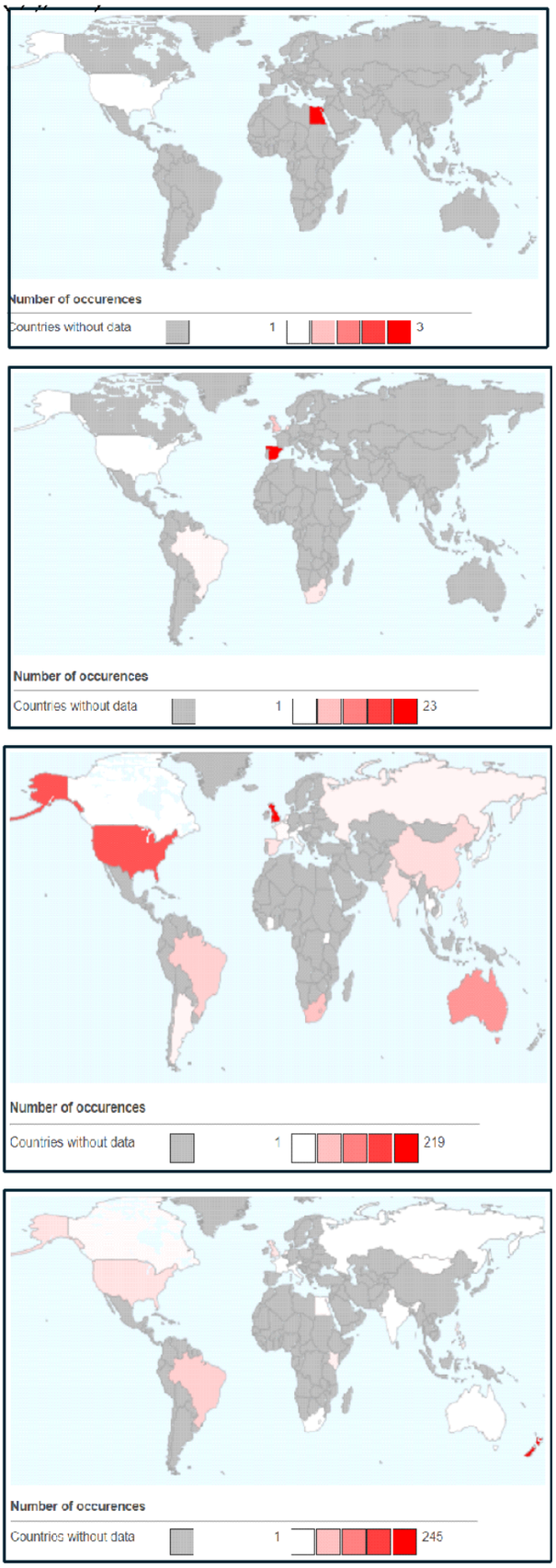


Figure 3.3. Global data from GISAID shows geographic origin of RSV-A strains with mutations as highlighted for the number of occurrences shaded in different colors (where white =1 and red= maximum number) on the global maps: (a). I5T (n=4), (b). T8I (n=40), (c) T12I (n=770), (d). L15F (n=428).

3.6. Single nucleotide polymorphisms in the signal peptide of African RSV-B F proteins

Table 3.6 shows the single nucleotide polymorphisms identified in RSV-B signal peptide sequence. The RSV-B signal peptide had 7 mutations all occurring at a frequency of <3%. Only (30,9%; 287/930) had the signal peptide sequence present from the deduced RSV-B F sequences. The remaining RSV-B F sequences (69,1%; 643/930) did not have the complete F genome and had gaps.

The mutations were observed on the signal peptide sequence as follows: At position 4 (L) lysine changed to (V) valine at a frequency of 0,35% (1/287) and to (P) proline at 2,09% (6/287). Histidine (H) changed to (Y) tyrosine at a frequency of 1,39% (4/287) at position 6. At position 8 (S) serine changed to (L) lysine at a frequency of 0,35% (1/287). Substitutions at positions 9 and 11 occurred at the same frequencies for substitutions (S) serine to (G) glycine (0,35%; 1/287) and (I) isoleucine to (V) valine (0,35%; 1/287), respectively. Furthermore, at position 12, (F) phenylalanine changed to (L) lysine (1,39%; 4/287) and lastly, at position 15, (L) lysine changed to (F) phenylalanine (0,70%; 2/287).

Table 3.6: Positional amino acid frequencies in RSV-B signal peptide, (N=287).

Position	Wildtype Amino acid	Wildtype N (%)	V1	N (%)	V2	N (%)
4	*L*	*280 (97,56%)*	*V*	*1 (0,35%)*	*P*	*6 (2,09%)*
6	*H*	*283 (98,61%)*	*Y*	*4 (1,39%)*		
8	S	286 (99,65%)	L	1 (0,35%)		
9	S	286 (99,65%)	G	1 (0,35%)		
11	I	286 (99,65%)	V	1 (0,35%)		
12	*F*	*283 (98,61%)*	*L*	*4 (1,39%)*		
15	*L*	*285 (99,30%)*	*F*	*2 (0,70%)*		

* RSV-B reference sequence “strain B1” (Accession Number NC_001781.1)

3.7. Characteristics of the most prevalent RSV-B SP amino acid mutations.

The most prevalent mutations for RSV-B are found at the following positions: 4, 6, 12, and 15. (Table 3.7) highlights the genotype, clade, geographic location, and the period in which the mutations were detected. L4P was detected in South Africa in 2018, however information regarding the genotype and clade is missing. H6Y is associated with genotype GB5.0.5a and clade B6, it was found in South Africa in 2018. Information regarding the genotype and clade of F12L is missing however it shows that it was detected in South Africa in 2018. L15F is associated with GB3 and was detected in South Africa in 2018, there is missing information regarding the clade.

3.8. Global frequencies of prevalent RSV-B SP mutations

Mutational analysis of RSV-B F global, including the geographic origin for each mutation, the frequency, and the period they occurred (Table 3.8). F12L was the most prevalent substitution among global B strains at 1,70% (82/4661) across 6 continents with dominance in Africa (10), Europe (20) and North America (36) from 201 to 2022. In Africa, it was seen in Morocco (7), South Africa (2) and only once in Ivory Coast (1) (Figure 3.4.d). The second most prevalent amino acid substitutions occurred at position 4 at a frequency of 0,77% (37/4788) in 5 continents from 2018 to 2022, with dominance among RSV-B strains from North America (24/37) (Table 3.8). Africa (3), South America (1). In Africa, it was only seen in South Africa (Figure 3.4.a). Another represented mutation, H6Y occurred at a frequency of 0,27% (13/4808) globally in 4 continents: Asia (1), Australia (1), Europe (9), North America (2) (Figure 3.4.b). L15F was the least prevalent mutation which occurred at 0,20% (10/4779) in Europe (4) and North America (6) (Figure 3.4.e).

Table 3.7: Summary of the most prevalent mutations in RSV-B with their genotypes, geographic locations, and the period they were detected.

Mutations	Genotype	Clade	Geographic location	Year
L4P	Missing information	Missing information	South Africa	2018
H6Y	GB5.0.5a	B6	South Africa	2018
F12L	Missing information	B1	South Africa	Missing information
L15F	GB3	Missing Information	South Africa	2018

Table 3.8: Global sequence data of mutations that occurred in RSV-B signal peptide acquired from GISAID.

Amino acid position	Mutation	V1	Occurrence	Geographic location	Period
4	L4P	P	0,77% (37/4788)	Africa (3) Asia (1) Europe (8) North America (24) South America (1)	2021-2022 2021 2018-2020 2018-2020 2018
6	H6Y	Y	0,27% (13/4808)	Asia (1) Australia (1) Europe (9) North America (2)	2021 2020 2018,2019, 2023 2020
12	F12L	L	1,70% (82/4661)	Africa (10) Asia (4) Australia (2) Europe (20) North America (36) South America (4)	2019 & 2021 2019-2020 2019-2020 2019-2022 2018-2022 2019
15	L15F	F	0,21% (10/4799)	Europe (4) North America (6)	2018,2021,2023 2018-2019

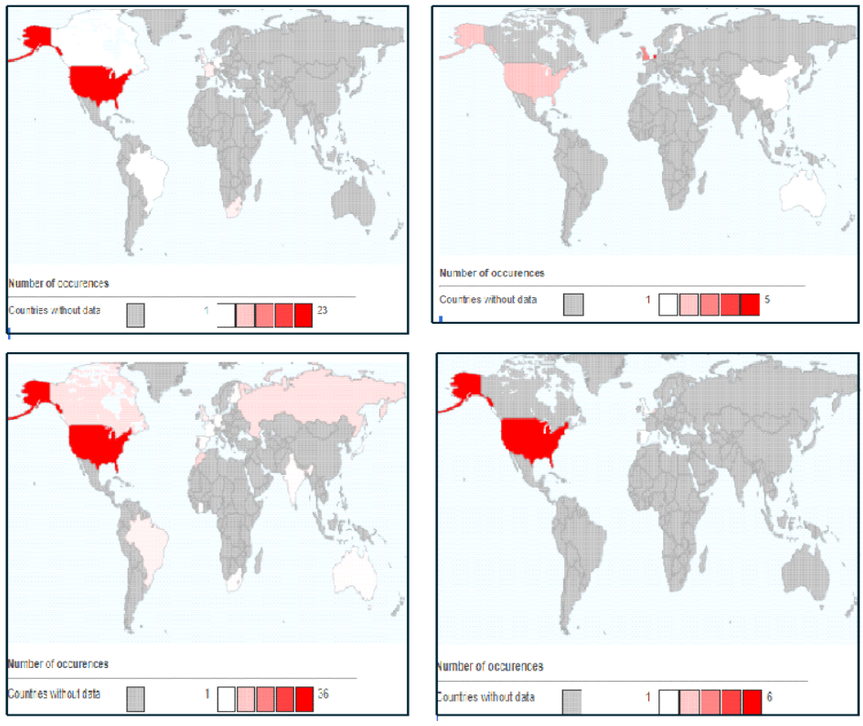


Figure 3.4. Global data from GISAID shows geographic origin of the mutations found in RSV-B, with the number of occurrences. The occurrence of the mutations for each country are highlighted in different colors on the global data: (a) L4P (n=37), (b) H6Y (n=13), (c) F12L (n=82) and (d) L15F (n=10).

3.9. Impact of signal peptide mutations on F gene expression

The most prevalent mutations were introduced into the RSV F gene after generating the plasmid that carried the desired modifications. The use of site directed mutagenesis allowed us to modify the DNA sequence of the RSV F gene by introducing target changes, while keeping the rest of the sequence unchanged. Primers to introduce the I5T and T12I mutations were used, and results are shown in Figure 3.5 for the successful clones after purification of the plasmid DNA and electrophoresis through a 2% agarose gel. Here, for example, results for I5T plasmid clones are indicated by P5.1; the P in front of the number 5 indicates that it is a "plasmid clone" and the second number (.1) is the relevant clone number. The same naming convention was used for T12I plasmid clones. The bacterial cultures from which mini plasmid DNA preparations were successful were used to inoculate 50ml LB broth to perform midi plasmid DNA preparations to increase the yield of plasmid DNA. Each plasmid DNA sample was loaded using 5µl of each sample to assess integrity and respective concentrations determined are indicated in Figure 3.5a for mini plasmid DNA samples: Lanes 1-2 were loaded in order with P12.1: 6,700 ng/µl and P12.2: 14,600 ng/µl, and lanes 3-5 were loaded in order with P5.1: 5,9500 ng/µl, P5.2: 4,800 ng/µl and P5.3 1,35 ng/µl. As also indicated by gel photo plasmid DNA recovery was poor for clone P5.2 but poorest for clone P5.3 as indicated by faint bands and the DNA concentrations and therefore the corresponding bacterial culture for clone P5.3 was not included for midi plasmid DNA preparation cultures. The midi plasmid DNA samples were loaded in order (Figure 3.5b) and the respective concentrations obtained after the purification were: P5.1: 29,100 ng/µl, P5.2: 58,050 ng/µl, P12.1: 45,300 ng/µl and P12.2: 7,000 ng/µl.

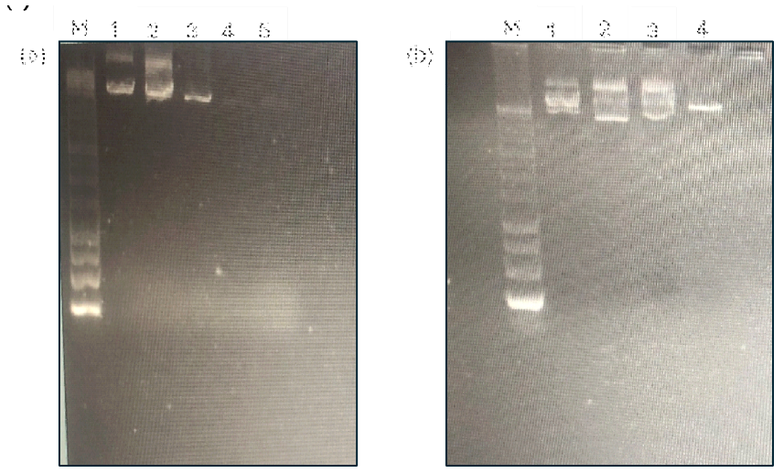


Figure 3.5: Gel electrophoresis results of the mini & midi prep for RSV F site-directed mutagenesis, analyzed by electrophoresis in 2% agarose gel. Figure (a) Lane M: 1kb DNA Ladder (Promega corporation, Madison, USA), Lanes 1-2: T12I clones P12.1: 6,700 ng/µl and P12.2: 14,600 ng/µl, Lanes 3-5: I5T clones P5.1: 5,9500 ng/µl, P5.2: 4,800 ng/µl and P5.3 1,35 ng/µl. Figure (b), Lane M: 1kb DNA Ladder, Lanes 1-2: I5T clones P5.1: 29,100 ng/µl and P5.2: 58,050 ng/µl, Lanes 3-4: T12I clones P12.1: 45,300 ng/µl and P12.2: 7,000 ng/µl.

3.10. Sequenced clones to confirm the presence of the mutations

The two mutations that were introduced into the RSV F protein signal peptide sequence were sent for sequencing to confirm whether the insertion was successful or not. The highlighted box on the sequence indicates the signal peptide sequence. The two sequences of the transformants with mutations were aligned against the RSV F protein construct (wildtype) as shown below (Figure 3.6). P5 (I5T) and P12 (T12I) are the expected mutant clones that we have sent for sequencing. However, there were no insertions identified on the sequences when compared to the RSV F protein wildtype original sequence.

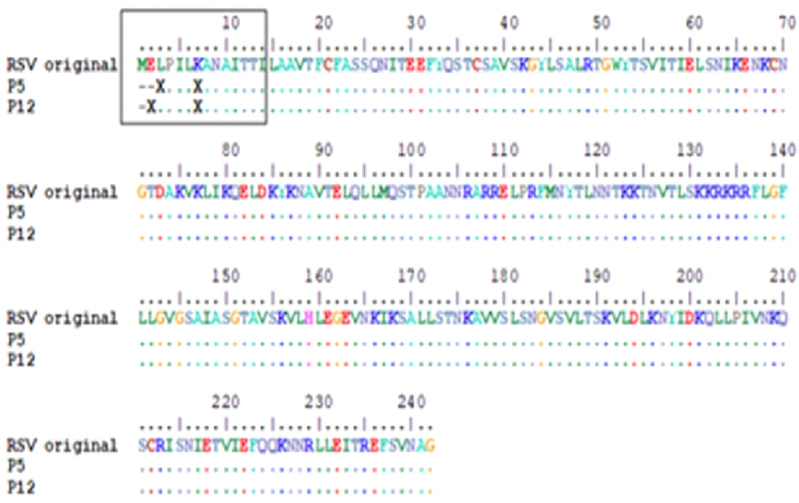


Figure 3.6. Multiple sequence alignment with the RSV F wildtype (original) amino acid sequence as reference and the two clones (P5 and P12) obtained following site-directed mutagenesis to introduce mutations I5T and T12I. X: unresolved.

3.10. Expression of RSV F protein in western blot.

3.10.1. RSV antibody ELISA

To detect and quantify antibodies against RSV to use for western blot, ELISA was performed. 16 patient's serum samples were used as described in the methods. In Table 3.9, the sample (1757D in bold italic font) with absorbance of 0,401 was the one chosen for western blot as primary antibody due to its high ratio value, (0,401/0,2815=1,43). The rest of the calculations for the other samples are shown in Table 3.9.

Table 3.9. Summary of the results from RSV antibody ELISA with absorbance extinction ratios calculated to identify positive/negative samples using the criteria: negative: ratio <0,8; borderline: ratio ≥0,8 to <1,1 and positive: ratio ≥1.1.

Samples	**Ratio**	**Result interpretation**	**Samples**	**Ratio**	**Result interpretation**
Negative Control	0,112/0,2815=0,42	Negative	Positive Control	0,529/0,2815=1,88	Positive
29	0,049/0,2815=0,17	Negative	1759D	0,392/0,2815=1,40	Positive
44	0,043/0,2815=0,15	Negative	1760D	0,397/0,2815=1,41	Positive
50	0,042/0,2815=0,15	Negative	1755D	0,349/0,2815=1,30	Positive
35	0,043/0,2815=0,15	Negative	***1757D***	***0,401/0,2815=1,43***	***Positive***
1751D	0,140/0,2815=0,50	Negative	1734D	0,328/0,2815=1,16	Positive
			1735D	0,307/0,2815=1,09	Positive
			1753D	0,325/0,2815=1,15	Positive
			1773D	0,331/0,2815=1,18	Positive
			1774D	0,332/0,2815=1,18	Positive
			1500D	0,307/0,2815=1,09	Positive
			1736D	0,338/0,2815=1,20	Positive

3.10.2. Western blot

Western blot for RSV F protein expression was performed to confirm the success of the transfection of the HEK-293T cells and expression of the RSV F protein. Figure 3.7(a) shows the results of the SDS-PAGE gel for the culture supernatants harvested post-transfection. The solubilized protein fractions identified in lane 4 (blue arrow) of approximately 18kDa corresponded to the expected size of the F2 subunit. This protein was intended to contain the T12I mutation. However, as we proceed with transfections before sequencing results were obtained due to time constraints, we only learnt afterwards that the observed results for I5T and T12I also represented the wildtype (unmutated) F proteins (Figure 3.7). Figure 3.7b shows the negative controls (lanes 1 to 5) which were just the cell lysates for which we did not expect to observe the RSV F protein bands.

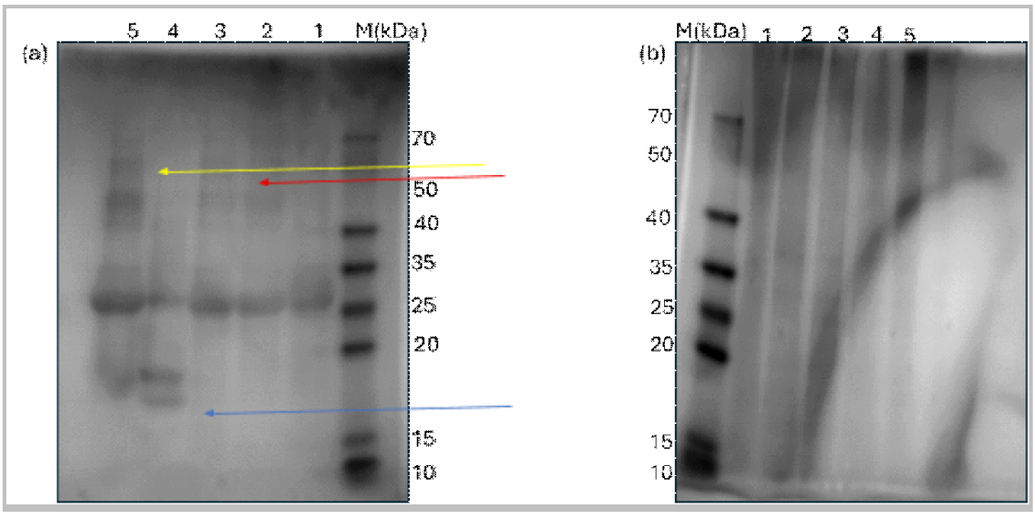


Figure 3.7. (a). Expression of the RSV F protein on SDS-PAGE using supernatants treated in HEK-293T cells and harvested 48 hours post to transfection. Lane M shows the prestained protein standards with molecular masses from 10 to 250 kDa. Lane 1 is the mock transfected cells supernatant fluid used as control (they were not transfected with RSV F). Lane 2-3 (shown by the red arrow on the gel is lane 3, approximately corresponding to the size of the F1 subunit between 45-55 kDa) is the I5T clone and lane 4-5 is the T12I clone (lane 4 shown by blue arrow, approximately 18 kDa, corresponding to the F2 subunit, while the yellow arrow shows the F0 subunit, which is between 50 and 70 kDa). Figure (b) lanes 1 to 5 shows the cell lysates. The cell lysates were not expected to contain the expressed RSV F proteins. Lane M is the protein standard.

3.11. Immunoblotting to detect the RSV F protein

To assess the conformation of the expressed protein that was detected from the SDS-PAGE, immunoblotting was performed using the HCV negative plasma sample as primary antibody against the harvested supernatant. The binding affinity between the two was observed even though the efficiency was not as high as anticipated. The F1 subunit was located at lane 1&2 indicated by the blue arrow on the gel with F2 not being detected in the other lanes (Figure 3.8a and b). Therefore, we conclude that RSV F specific protein expression was observed, but unfortunately the introduction of the intended amino acid substitutions was unsuccessful as highlighted by the plasmid clones sequencing results (Figure 3.6).

3.12. Quantification and detection of total expressed proteins

We continued to quantify the amount of expressed F proteins. The results from a plate reader were used to determine the protein concentrations of the standard and samples. Figure 3.9 shows the standard curve for BCA assay standards (calculated as per Table 2.3, Chapter 2), which was used to calculate the protein concentrations of the samples (Table 3.10). The formula for the concentrations: Y= -180,238X+ 2273,417 where X is the protein concentration (µg/mL) and Y is the absorbance value. Column 4 shows the concentration of the standards, from A to C and the rest of column 4 (D to G is the sample I5T). Column 5 from A to D and 8H (is sample T12I)

(Table 3.10). Once again, to remember that based on sequencing results for I5T and T12I clones (Figure 3.6) these F proteins all represent the original wildtype (unmutated).

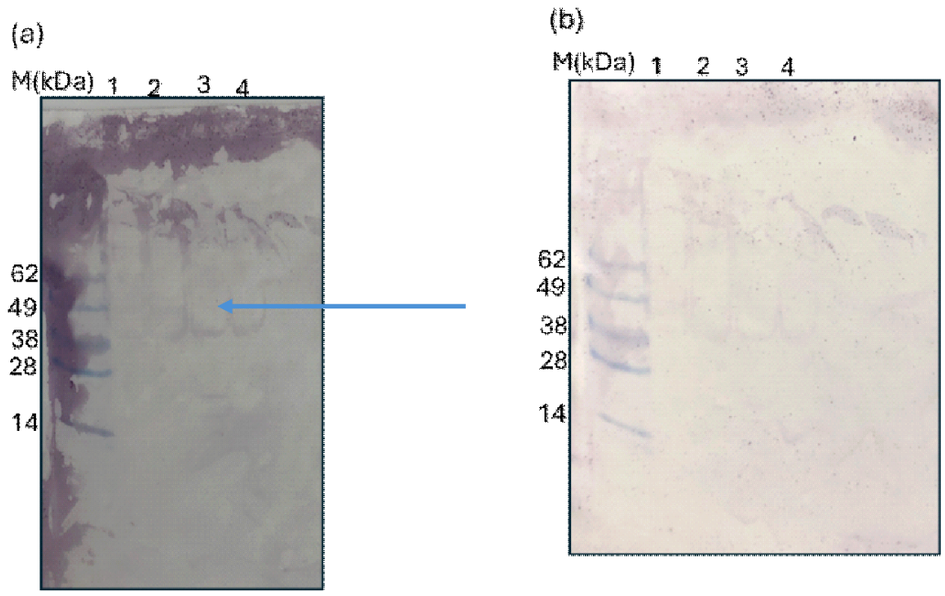


Figure 3.8.(a) and (b) shows the western blot analysis of RSV F protein expression in HEK 239T cells treated with human plasma samples as primary antibodies. Lane M is the protein standard marker (Thermo Fisher scientific, USA). Lane 2-3 is the intended I5T supernatant (Lane 2 indicated by blue arrow shows the F1 subunit which is approximately 45 kDa) and lane 4-5 is the T12I supernatant in both pictures where (a) shows protein separation from supernatant fluids and (b) protein separation from cell lysates.

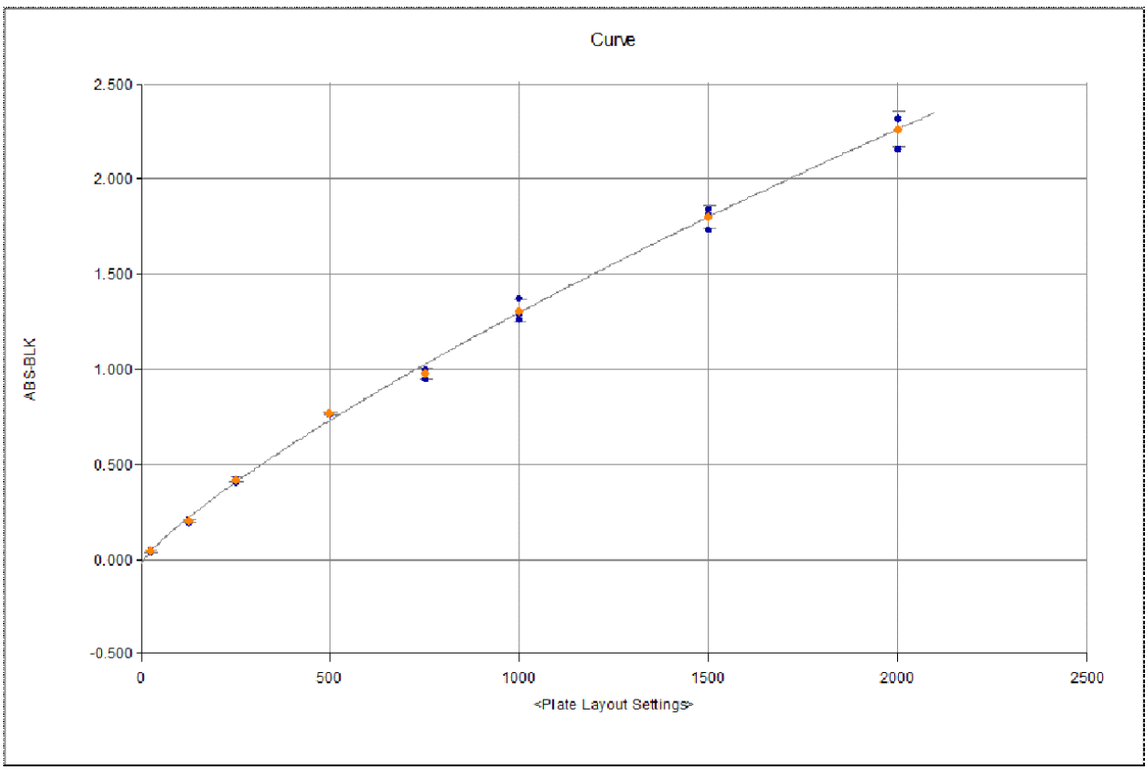


Figure 3.9. BCA protein assay. BSA standard curve using the standard microplate well protocol (37ºC/30-minute incubation). The linear equation to solve X was Y= mX + b. Y= -180,238X +

2273,417 where m= -180, 238 and b= 2273,417. The X-axis is the protein concentration in µg/mL while the Y-axis is the absorbance readings.

Table 3.10. Absorbance and protein concentrations for expressed F protein samples

Sample name	Absorbance	Protein concentration [µg/mL]
I5T	274 756	11,09
I5T	331 489	10,78
I5T	317 303	10,86
I5T	364 789	10,59
T12I	379 356	10,51
T12I	342 017	10,72
T12I	356 406	10,64
T12I	457 797	10,06
T12I	290 026	11,01

CHAPTER 4

DISCUSSION

The RSV-F protein has been identified as a candidate of vaccine research and the focus of antiviral drug or antibodies development due to its historical nature of being well conserved when compared to G glycoprotein, however it continues to evolve (Chen *et al*., 2018; Hause *et al*., 2017; Zhu *et al*., 2017). Several studies have reported on the sequence variability of RSV F genes between the two RSV subtypes (Hause *et al*., 2017: Tapia *et al*., 2014: Xia *et al*., 2014). This study aimed to report on the diversity and impact of the most prevalent signal peptide mutations on the expression of F-proteins from African RSV strains.

Genetic diversity among RSV-A and -B strains from Africa

In this study we identified GA2.3.5 (A23) 47.6% (50/105) and GA2.3.3 (A23) 34.3% (36/105) as the most prevalent genotypes from RSV-A and GB5.0.5a (B6) 66.9% (622/930) and GB5.0.2 (B6) 28.9% (269/930) as the most prevalent genotypes of the RSV-B F gene sequences. In Europe, a recent study established 96.9% of RSV-A genomes are from the GA2.3.5 (ON1) lineage (Lai *et al*., 2024). In a 2019-2022 cohort from South Korea, it was reported that 100% of RSV-A strains were identified as GA2.3.5 (Na *et al*., 2024). A South African study which had done whole genome sequencing of both RSV-A and RSV-B between 2021 and 2022, revealed that over the study period the circulating strains in South Africa were lineages GA2.3.5 (previously ON1) and GB5.0.5a (previously BA9) (Sondlane *et al*., 2024). Recent research supports earlier findings, showing that GA2.3.5 and GB5.0.5a were the dominant RSV genotypes circulating both before and after the COVID-19 pandemic in multiple countries (Goya *et al*., 2023; Jallow *et al*., 2022; Redlberger-Fritz *et al*., 2023).

Overall, the proportion of RSV subtypes differed by country as the diversity of RSV-B was dominant over RSV-A in this study. Consistent with this report, RSV-B has been identified to be a prevalent subtype when compared to RSV-A in 7 countries globally with South Africa as an exception (Tabor *et al*., 2020). RSV-B has been reported to have gone through more frequent genetic changes, especially in the G glycoprotein gene, which enables it to avoid neutralizing antibodies. Some of the RSV-B genotypes, like BA9 and BA10, have gained duplications in the G gene, increasing transmissibility and immune evasion, resulting in the dominance of RSV-B over RSV/A globally (Haider *et al*., 2018; Yu *et al*., 2021). When it comes to the dominance of RSV-A in South Africa, it occurs seasonally and it is influenced by genotype evolution (Otieno *et al*., 2018). However, after the COVID-19 pandemic it became more prevalent, especially genotype GA2.3.5 (A23) (Langedijk *et al*., 2024). There was a recent study in South Africa which also reported on seasonal dominance of GA2.3.5 (RSV-A) and GB5.0.5a (RSV-B) in different years (Sondlane *et al*., 2024).

Assessing signal peptide mutations on F gene expression

The historical RSV A2 long strain has reportedly been used in most RSV vaccine candidate development (Hause *et al*., 2017), hence it was used in this study as a reference against RSV-A

sequences. The amino acid changes observed in the signal peptide in this study occurred at a frequency ranging from 1-3% for both RSV-A and RSV-B strains from 2018-2022. These results indicate the RSV-F protein signal peptide sequences are generally conserved among strains in each subgroup. Although Tabor *et al*., (2020) reported that for 2017-2018 amino acid substitutions in the antigenic sites of the RSV-A F protein with frequencies ranging from 0,8 to 9,4% and 0.4 to 100% for RSV-B they did not highlight the frequency of substitutions in the signal peptides. Based on their results they concluded that RSV F protein sequences were generally well conserved in 2017 and 2018. The signal peptide mutations occurred at a lower prevalence in RSV-B which were the dominant subgroup in this study. A previous study alluded that adaptations in the G protein (e.g. duplications/positive selection) may contribute to RSV-B dominance (Yu *et al*., 2021). Unfortunately, in this study we were unable to assess the effect of mutations in the signal peptides of F proteins on protein expression which may impact RSV replication and transmission as our site-directed mutagenesis experiments failed.

This study supports certain previously recognized substitutions (A8T, T16A/I, T12I/A, and F20L) in South African RSV-A strains (Mabilo *et al*., 2022) and identified additional substitutions in both RSV-A and RSV-B strains, along with their genotypic associations. Mabilo *et al*., 2022 did not report on the specific substitutions in RSV-B and that shows that our research provides new data regarding RSV-B F protein signal peptide variability in African strains. These findings strengthen our understanding of the genetic diversity of RSV F protein signal peptides in African strains and emphasize the importance of continuing surveillance to enlighten vaccine and therapeutic strategies.

Some challenges and limitations of the study need to be acknowledged. Firstly, Site directed mutagenesis was not performed for RSV-B in our study due to the extensive variability when compared to RSV-A and the available F expression construct was for the RSV-A A2 strain. We then compared it to the B1 reference sequence and observed almost the same changes to when RSV-A sequences were compared to the RSV-A reference sequence. However, due to time and funding constraints we could not purchase an RSV-B F expression construct. For future studies, both RSV-A and RSV-B F expression for variant SPs should be done.

Secondly, our sequence analysis of the transformants revealed that the expected mutations were not present, with the sequences aligning with the wildtype strain. We performed transfections and western blot for the expressed F protein while waiting for the sequencing data and thus did not know beforehand that the mutagenesis was unsuccessful and that the expressed “mutant” proteins are wild-type. The mutations may have been unstable and reverted to the wildtype during selection. Additionally, the efficacy of DpnI digestion during SDM could have impacted the study outcome and in this instance suspicions were raised that the cold chain may have been broken. DpnI selectively digests the methylated parental plasmids to enrich newly synthesized mutant plasmids. If digestion is inadequate, the remaining parental plasmid can enter more efficiently than mutant DNA, resulting in the dominance of wild-type colonies (Yang *et al*., 2022). Without these mutations, our ability to illustrate conclusions about their impact on RSV

activity is compromised. While the lack of confirmed mutations presents a challenge, it highlights the obstacles of investigating viral proteins and emphasizes the necessity for continued research in this area.

In conclusion,

The genetic diversity of RSV in Africa highlighted that RSV-B was found the dominant group in the study period 2005 to 2022. However, the mutations observed in the F proteins' signal peptides were less prevalent among RSV-B than RSV-A strains. Future studies should further investigate the implications of these mutations on RSV fitness and transmission in different populations.

REFERENCES

1. Abarca, K., Rey-Jurado, E., Munoz-Durango, N., Vázquez, Y., Soto, J.A., Gálvez, N.M., Valdés-Ferrada, J., Iturriaga, C., Urzúa, M., Borzutzky, A. and Cerda, J., 2020. Safety and immunogenicity evaluation of recombinant BCG vaccine against respiratory syncytial virus in a randomized, double-blind, placebo-controlled phase I clinical trial. *EClinicalMedicine*, *27*.
2. Abo, Y.N., Clifford, V., Lee, L.Y., Costa, A.M., Crawford, N., Wurzel, D. and Daley, A.J., 2021. COVID‐19 public health measures and respiratory viruses in children in Melbourne. *Journal of Paediatrics and Child Health*, *57*(12), pp.1886-1892.
3. Agoti, C.N., Otieno, J.R., Munywoki, P.K., Mwihuri, A.G., Cane, P.A., Nokes, D.J., Kellam, P. and Cotten, M., 2015. Local evolutionary patterns of human respiratory syncytial virus derived from whole-genome sequencing. *Journal of virology*, *89*(7), pp.3444-3454.
4. Agha, R. and Avner, J.R., 2021. Delayed seasonal RSV surge observed during the COVID-19 pandemic. *Pediatrics*, *148*(3).
5. Alanezi, F., Aljahdali, A., Alyousef, S.M., Alrashed, H., Mushcab, H., AlThani, B., Alghamedy, F., Alotaibi, H., Saadah, A. and Alanzi, T., 2020. A comparative study on the strategies adopted by the United Kingdom, India, China, Italy, and Saudi Arabia to contain the spread of the COVID-19 pandemic. *Journal of healthcare leadership*, pp.117-131.
6. Aliprantis, A.O., Shaw, C.A., Griffin, P., Farinola, N., Railkar, R.A., Cao, X., Liu, W., Sachs, J.R., Swenson, C.J., Lee, H. and Cox, K.S., 2021. A phase 1, randomized, placebo-controlled study to evaluate the safety and immunogenicity of an mRNA-based RSV prefusion F protein vaccine in healthy younger and older adults. *Human vaccines & immunotherapeutics*, *17*(5), pp.1248-1261.
7. Ananworanich, J. and Heaton, P.M., 2021. Bringing preventive RSV monoclonal antibodies to infants in low-and middle-income countries: challenges and opportunities. *Vaccines*, *9*(9), p.961.
8. Avni, T., Babich, T., Nir, A., Yahav, D., Shaked, H., Sorek, N., Zvi, H.B., Bishara, J. and Atamna, A., 2020. Comparison of clinical outcomes of influenza A and B at the 2017–2018 influenza season: a cohort study. *European Journal of Clinical Microbiology & Infectious Diseases*, *39*, pp.1109-1114.
9. Baker, R.E., Park, S.W., Yang, W., Vecchi, G.A., Metcalf, C.J.E. and Grenfell, B.T., 2020. The impact of COVID-19 nonpharmaceutical interventions on the future dynamics of endemic infections. *Proceedings of the National Academy of Sciences*, *117*(48), pp.30547-30553.
10. Battles, M.B. and McLellan, J.S., 2019. Respiratory syncytial virus entry and how to block it. *Nature Reviews Microbiology*, *17*(4), pp.233-245.
11. Bents, S., Viboud, C., Grenfell, B., Hogan, A., Tempia, S., von Gottberg, A., Moyes, J., Walaza, S., Cohen, C. and Baker, R., 2022. The impact of COVID-19

non-pharmaceutical interventions on future respiratory syncytial virus transmission in South Africa. *medRxiv*.

12. Bernstein, D.I., Mejias, A., Rath, B., Woods, C.W. and Deeter, J.P., 2023. Summarizing study characteristics and diagnostic performance of commercially available tests for respiratory syncytial virus: A scoping literature review in the COVID-19 era. *The Journal of Applied Laboratory Medicine*, *8*(2), pp.353-371.
13. Bian, T., Gibbs, J.D., Örvell, C. and Imani, F., 2012. Respiratory syncytial virus matrix protein induces lung epithelial cell cycle arrest through a p53 dependent pathway. *PloS one*, *7*(5), p.e38052.
14. Black, C.P., 2003. Systematic review of the biology and medical management of respiratory syncytial virus infection. *Respiratory care*, *48*(3), pp.209-233.
15. Blanco, J.C., Fernando, L.R., Zhang, W., Kamali, A., Boukhvalova, M.S., McGinnes-Cullen, L. and Morrison, T.G., 2019. Alternative virus-like particle-associated prefusion F proteins as maternal vaccines for respiratory syncytial virus. *Journal of Virology*, *93*(23), pp.10-1128.
16. Bohmwald, K., Espinoza, J.A., Rey-Jurado, E., Gómez, R.S., González, P.A., Bueno, S.M., Riedel, C.A. and Kalergis, A.M., 2016, August. Human respiratory syncytial virus: infection and pathology. In *Seminars in Respiratory and Critical Care Medicine* (Vol. 37, No. 04, pp. 522-537). Thieme Medical Publishers.
17. Bukreyev, A., Yang, L. and Collins, P.L., 2012. The secreted G protein of human respiratory syncytial virus antagonizes antibody-mediated restriction of replication involving macrophages and complement. *Journal of virology*, *86*(19), pp.10880-10884.
18. Cao, D., Gao, Y., Chen, Z., Gooneratne, I., Roesler, C., Mera, C., D'Cunha, P., Antonova, A., Katta, D., Romanelli, S. and Wang, Q., 2024. Structures of the promoter-bound respiratory syncytial virus polymerase. *Nature*, *625*(7995), pp.611-617.
19. Carvajal, J.J., Avellaneda, A.M., Salazar-Ardiles, C., Maya, J.E., Kalergis, A.M. and Lay, M.K., 2019. Host components contributing to respiratory syncytial virus pathogenesis. *Frontiers in immunology*, *10*, p.2152.
20. Chanock, R.M., Parrott, R.H., Vargosko, A.J., Kapikian, A.Z., Knight, V. and Johnson, K.M., 1962. IV. Respiratory syncytial virus. *American Journal of Public Health and the Nations Health*, *52*(6), pp.918-925.
21. Cheng, X., Park, H., Zhou, H. and Jin, H., 2005. Overexpression of the M2-2 protein of respiratory syncytial virus inhibits viral replication. *Journal of virology*, *79*(22), pp.13943-13952.
22. Choudhary, M.L., Wadhwa, B.S., Jadhav, S.M. and Chadha, M.S., 2013. Complete genome sequences of two human respiratory syncytial virus genotype A strains from India, RSV-A/NIV1114046/11 and RSV-A/NIV1114073/11. *Genome announcements*, *1*(4), pp.10-1128.
23. Cohen, C., Walaza, S., Treurnicht, F.K., McMorrow, M., Madhi, S.A., McAnerney, J.M. and Tempia, S., 2018. In-and out-of-hospital mortality associated with seasonal and pandemic influenza and respiratory syncytial virus in South Africa, 2009–2013. *Clinical Infectious Diseases*, *66*(1), pp.95-103.

24. Collins, P.L., Fearns, R. and Graham, B.S., 2013. Respiratory syncytial virus: virology, reverse genetics, and pathogenesis of disease. In *Challenges and opportunities for respiratory syncytial virus vaccines* (pp. 3-38). Berlin, Heidelberg: Springer Berlin Heidelberg.
25. Coultas, J.A., Smyth, R. and Openshaw, P.J., 2019. Respiratory syncytial virus (RSV): a scourge from infancy to old age. *Thorax*, *74*(10), pp.986-993.
26. da Silva, R.P., Thomé, B.L. and da Souza, A.P.D., 2023. Exploring the Immune Response against RSV and SARS-CoV-2 Infection in Children. *Biology*, *12*(9), p.1223.
27. Day, N.D., Branigan, P.J., Liu, C., Gutshall, L.L., Luo, J., Melero, J.A., Sarisky, R.T. and Del Vecchio, A.M., 2006. Contribution of cysteine residues in the extracellular domain of the F protein of human respiratory syncytial virus to its function. *Virology Journal*, *3*(1), pp.1-11.
28. Domachowske, J.B., Anderson, E.J. and Goldstein, M., 2021. The future of respiratory syncytial virus disease prevention and treatment. *Infectious Diseases and Therapy*, *10*, pp.47-60.
29. Eshaghi, A., Duvvuri, V.R., Lai, R., Nadarajah, J.T., Li, A., Patel, S.N., Low, D.E. and Gubbay, J.B., 2012. Genetic variability of human respiratory syncytial virus A strains circulating in Ontario: a novel genotype with a 72 nucleotide G gene duplication. *PloS one*, *7*(3), p.e32807.
30. Falsey, A.R. and Walsh, E.E., 2000. Respiratory syncytial virus infection in adults. *Clinical microbiology reviews*, *13*(3), pp.371-384.
31. Falsey, A.R., Sobieszczyk, M.E., Hirsch, I., Sproule, S., Robb, M.L., Corey, L., Neuzil, K.M., Hahn, W., Hunt, J., Mulligan, M.J. and McEvoy, C., 2021. Phase 3 safety and efficacy of AZD1222 (ChAdOx1 nCoV-19) Covid-19 vaccine. *New England Journal of Medicine*, *385*(25), pp.2348-2360.
32. Foley, T., Moore, S., Quinn, K., Hunt, A., Stone, N., Dodwell, J., Readey, M., Williams, J., Campbell, C., Mountifield, S. and McLaughlin, J., New data for Arexvy, GSK's RSV vaccine.
33. Fuentes, S., Tran, K.C., Luthra, P., Teng, M.N. and He, B., 2007. Function of the respiratory syncytial virus small hydrophobic protein. *Journal of virology*, *81*(15), pp.8361-8366.
34. Gatt, D., Martin, I., AlFouzan, R. and Moraes, T.J., 2023. Prevention and treatment strategies for respiratory syncytial virus (RSV). *Pathogens*, *12*(2), p.154.
35. Garegnani, L., Styrmisdottir, L., Rodriguez, P.R., Liquitay, C.M.E., Esteban, I. and Franco, J.V., 2021. Palivizumab for preventing severe respiratory syncytial virus (RSV) infection in children. *Cochrane Database of Systematic Reviews*, (11).
36. Giles, B., Meredith, P., Robson, S., Smith, G. and Chauhan, A., 2021. The SARS-CoV-2 B. 1.1. 7 variant and increased clinical severity—the jury is out. *The Lancet Infectious Diseases*, *21*(9), pp.1213-1214.
37. Goya, S., Galiano, M., Nauwelaers, I., Trento, A., Openshaw, P.J., Mistchenko, A.S., Zambon, M. and Viegas, M., 2020. Toward unified molecular surveillance of RSV: A

proposal for genotype definition. *Influenza and other respiratory viruses*, *14*(3), pp.274-285.

38. Goya, S., Lucion, M.F., Shilts, M.H., Juárez, M.D.V., Gentile, A., Mistchenko, A.S., Viegas, M. and Das, S.R., 2023. Evolutionary dynamics of respiratory syncytial virus in Buenos Aires: Viral diversity, migration, and subgroup replacement. *Virus Evolution*, *9*(1), p.vead006.
39. Goya, S., Ruis, C., Neher, R.A., Meijer, A., Aziz, A., Hinrichs, A.S., von Gottberg, A., Roemer, C., Amoako, D.G., Acuña, D. and McBroome, J., 2024. Standardized Phylogenetic Classification of Human Respiratory Syncytial Virus below the Subgroup Level. *Emerging Infectious Diseases*, *30*(8), p.1631.
40. Graham, B.S., 2019. Immunological goals for respiratory syncytial virus vaccine development. *Current opinion in immunology*, *59*, pp.57-64.
41. Greinacher, A., Thiele, T., Warkentin, T.E., Weisser, K., Kyrle, P.A. and Eichinger, S., 2021. Thrombotic thrombocytopenia after ChAdOx1 nCov-19 vaccination. *New England Journal of Medicine*, *384*(22), pp.2092-2101.
42. Haider, M.S.H., Khan, W.H., Deeba, F., Ali, S., Ahmed, A., Naqvi, I.H., Dohare, R., Alsenaidy, H.A., Alsenaidy, A.M., Broor, S. and Parveen, S., 2018. BA9 lineage of respiratory syncytial virus from across the globe and its evolutionary dynamics. *PLoS One*, *13*(4), p.e0193525.
43. Hall, T.A. 1999. BioEdit: a user-friendly biological sequence alignment editor and analysis program for Windows 95/98/NT. *Nucl. Acids. Symp. Ser.* 41:95-98.
44. Hammitt, L.L., Dagan, R., Yuan, Y., Baca Cots, M., Bosheva, M., Madhi, S.A., Muller, W.J., Zar, H.J., Brooks, D., Grenham, A. and Wählby Hamrén, U., 2022. Nirsevimab for prevention of RSV in healthy late-preterm and term infants. *New England Journal of Medicine*, *386*(9), pp.837-846.
45. Hause, A.M., Henke, D.M., Avadhanula, V., Shaw, C.A., Tapia, L.I. and Piedra, P.A., 2017. Sequence variability of the respiratory syncytial virus (RSV) fusion gene among contemporary and historical genotypes of RSV-A and RSV-B. *PLoS One*, *12*(4), p.e0175792.
46. Hotard, A.L., He, B., Nichol, S.T., Spiropoulou, C.F. and Lo, M.K., 2017. 4′-Azidocytidine (R1479) inhibits henipaviruses and other paramyxoviruses with high potency. *Antiviral research*, *144*, pp.147-152.
47. Hsu C-H. Prolonged seasonality of respiratory syncytial virus infection among preterm infants in a subtropical climate. PLoS ONE 2014; 9: e110166.
48. http://d5jk.2.vu/1
49. IMpact-RSV Study Group, 1998. Palivizumab, a humanized respiratory syncytial virus monoclonal antibody, reduces hospitalization from respiratory syncytial virus infection in high-risk infants. *Pediatrics*, *102*(3), pp.531-537.
50. Ijaz, M.K., Nims, R.W., Rubino, J.R., McKinney, J. and Gerba, C.P., 2022. Lessons learned from the SARS-CoV-2 pandemic: Preparing for the next outbreak of respiratory and enteric viral infections. *Appl. Microbiol. Open Access*, *8*, p.100229.

51. Jallow, M.M., Diagne, M.M., Sagne, S.N., Tall, F., Diouf, J.B.N., Boiro, D., Mendy, M.P., Ndiaye, N.K., Kiori, D., Sy, S. and Goudiaby, D., 2023. Respiratory syncytial virus in pediatric patients with severe acute respiratory infections in Senegal: Findings from the 2022 sentinel surveillance season. *Scientific Reports*, *13*(1), p.20404.
52. Jha, A., Jarvis, H., Fraser, C. and Openshaw, P., 2016. Respiratory syncytial virus. *SARS, MERS and other viral lung infections*.
53. Jones, J.M., 2023. Use of nirsevimab for the prevention of respiratory syncytial virus disease among infants and young children: recommendations of the Advisory Committee on Immunization Practices—United States, 2023. *MMWR. Morbidity and mortality weekly report*, *72*.
54. Kaler, J., Hussain, A., Patel, K., Hernandez, T. and Ray, S., 2023. Respiratory syncytial virus: A comprehensive review of transmission, pathophysiology, and manifestation. *Cureus*, *15*(3).
55. Kampmann, B., Madhi, S.A., Munjal, I., Simões, E.A., Pahud, B.A., Llapur, C., Baker, J., Pérez Marc, G., Radley, D., Shittu, E. and Glanternik, J., 2023. Bivalent prefusion F vaccine in pregnancy to prevent RSV illness in infants. *New England Journal of Medicine*, *388*(16), pp.1451-1464.
56. Kaushik, S., He, H. and Dalbey, R.E., 2022. Bacterial signal peptides-navigating the journey of proteins. *Frontiers in Physiology*, *13*, p.933153.
57. Karron, R.A., Atwell, J.E., McFarland, E.J., Cunningham, C.K., Muresan, P., Perlowski, C., Libous, J., Spector, S.A., Yogev, R., Aziz, M. and Woods, S., 2021. Live-attenuated vaccines prevent respiratory syncytial virus–associated illness in young children. *American journal of respiratory and critical care medicine*, *203*(5), pp.594-603.
58. Klok, F.A., Pai, M., Huisman, M.V. and Makris, M., 2022. Vaccine-induced immune thrombotic thrombocytopenia. *The Lancet Haematology*, *9*(1), pp.e73-e80.
59. Koivisto, K., Nieminen, T., Mejias, A., Capella, C., Ye, F., Mertz, S., Peeples, M., Ramilo, O. and Saxén, H., 2021. RSV Specific Antibodies in Pregnant Women and Subsequent Risk of RSV Hospitalization in Young Infants. *The Journal of Infectious Diseases*.
60. Lai, A., Bergna, A., Fabiano, V., Ventura, C.D., Fumagalli, G., Mari, A., Loiodice, M., Zuccotti, G.V. and Zehender, G., 2024. Epidemiology and molecular analyses of respiratory syncytial virus in the 2021–2022 season in northern Italy. *Frontiers in Microbiology*, *14*, p.1327239.
61. Langedijk, A.C., Vrancken, B., Lebbink, R.J., Wilkins, D., Kelly, E.J., Baraldi, E., Mascareñas de Los Santos, A.H., Danilenko, D.M., Choi, E.H., Palomino, M.A. and Chi, H., 2024. The genomic evolutionary dynamics and global circulation patterns of respiratory syncytial virus. *Nature communications*, *15*(1), p.3083.
62. Law, B.J., Carbonell-Estrany, X. and Simoes, E.A.F., 2002. An update on respiratory syncytial virus epidemiology: a developed country perspective. *Respiratory medicine*, *96*, pp. S1-S7.
63. Lee, S.H., Chu, K.B., Kim, M.J., Mao, J., Eom, G.D., Yoon, K.W., Ahmed, M.A., and Quan, F.S., 2023. Virus-like particle vaccine expressing the respiratory syncytial virus

pre-fusion and G proteins confers protection against RSV challenge infection. *Pharmaceutics*, *15*(3), p.782.

64. Li, Y., Wang, X., Blau, D.M., Caballero, M.T., Feikin, D.R., Gill, C.J., Madhi, S.A., Omer, S.B., Simões, E.A., Campbell, H. and Pariente, A.B., 2022. Global, regional, and national disease burden estimates of acute lower respiratory infections due to respiratory syncytial virus in children younger than 5 years in 2019: a systematic analysis. *The Lancet*, *399*(10340), pp.2047-2064.
65. Liang, X., Liu, D.H., Chen, D., Guo, L., Yang, H., Shi, Y.S., Wang, Y.J., Wang, W.K., Xie, Z.P., Gao, H.C. and Duan, Z.J., 2019. Gradual replacement of all previously circulating respiratory syncytial virus A strain with the novel ON1 genotype in Lanzhou from 2010 to 2017. *Medicine*, *98*(19), p.e15542.
66. Liljeroos, L., Krzyzaniak, M.A., Helenius, A. and Butcher, S.J., 2013. Architecture of respiratory syncytial virus revealed by electron cryotomography. *Proceedings of the National Academy of Sciences*, *110*(27), pp.11133-11138.
67. Lin, G.L., Drysdale, S.B., Snape, M.D., O'Connor, D., Brown, A., MacIntyre-Cockett, G., Mellado-Gomez, E., De Cesare, M., Bonsall, D., Ansari, M.A. and Öner, D., 2021. Distinct patterns of within-host virus populations between two subgroups of human respiratory syncytial virus. *Nature Communications*, *12*(1), p.5125.
68. Luna, M.S., Manzoni, P., Paes, B., Baraldi, E., Cossey, V., Kugelman, A., Chawla, R., Dotta, A., Fernández, R.R., Resch, B. and Carbonell-Estrany, X., 2020. Expert consensus on palivizumab use for respiratory syncytial virus in developed countries. *Paediatric respiratory reviews*, *33*, pp.35-44.
69. Mabilo, P., Mthiyane, H., Simane, A., Subramoney, K. and Treurnicht, F.K., 2022. Characterisation of RSV fusion proteins from South African patients with RSV disease, 2019 to 2020. *Viruses*, *14*(11), p.2321.
70. Madhi, S.A., Simões, E.A., Acevedo, A., Novoa Pizarro, J.M., Shepard, J.S., Railkar, R.A., Cao, X., Maas, B.M., Zang, X., Krick, A. and Roadcap, B., 2025. A phase 1b/2a trial of a half-life extended respiratory syncytial virus neutralizing antibody, clesrovimab, in healthy preterm and full-term infants. *The Journal of Infectious Diseases*, *231*(3), pp.e478-e487.
71. Malasao, R., Chaiut, W., Tantipetcharawan, W., Tongphung, R., Charoensri, N., Takarn, P., Sudjaritruk, T. and Maneekarn, N., 2023. Predominance of ON1 and BA9 genotypes of human respiratory syncytial virus in children with acute respiratory infection in Chiang Mai, Thailand, 2020–2021. *Journal of Infection and Public Health*, *16*(9), pp.1418-1426.
72. Marzi, A., Akhavan, A., Simmons, G., Gramberg, T., Hofmann, H., Bates, P., Lingappa, V.R. and Pöhlmann, S., 2006. The signal peptide of the ebolavirus glycoprotein influences interaction with the cellular lectins DC-SIGN and DC-SIGNR. *Journal of virology*, *80*(13), pp.6305-6317.
73. Mazur, N.I., Terstappen, J., Baral, R., Bardají, A., Beutels, P., Buchholz, U.J., Cohen, C., Crowe, J.E., Cutland, C.L., Eckert, L. and Feikin, D., 2023. Respiratory syncytial virus prevention within reach: the vaccine and monoclonal antibody landscape. *The Lancet Infectious Diseases*, *23*(1), pp.e2-e21.

74. McMorrow, M.L., Tempia, S., Walaza, S., Treurnicht, F.K., Moyes, J., Cohen, A.L., Pretorius, M., Hellferscee, O., Wolter, N., Von Gottberg, A. and Nguweneza, A., 2019. The role of human immunodeficiency virus in influenza-and respiratory syncytial virus–associated hospitalizations in South African children, 2011–2016. *Clinical Infectious Diseases*, *68*(5), pp.773-780.
75. Melgar, M., 2023. Use of respiratory syncytial virus vaccines in older adults: recommendations of the Advisory Committee on Immunization Practices—United States, 2023. *MMWR. Morbidity and Mortality Weekly Report*, *72*.
76. Meng, J., Stobart, C.C., Hotard, A.L. and Moore, M.L., 2014. An overview of respiratory syncytial virus. *PLoS pathogens*, *10*(4), p.e1004016.
77. Mesquita, F.D.S., Oliveira, D.B.L.D., Crema, D., Pinez, C.M.N., Colmanetti, T.C., Thomazelli, L.M., Gilio, A.E., Vieira, S.E., Martinez, M.B., Botosso, V.F. and Durigon, E.L., 2017. Rapid antigen detection test for respiratory syncytial virus diagnosis as a diagnostic tool. *Jornal de Pediatria*, *93*, pp.246-252.
78. Midulla, F., Di Mattia, G., Nenna, R., Scagnolari, C., Viscido, A., Oliveto, G., Petrarca, L., Frassanito, A., Arima, S., Antonelli, G. and Pierangeli, A., 2020. Novel variants of respiratory syncytial virus A ON1 associated with increased clinical severity of bronchiolitis. *The Journal of infectious diseases*, *222*(1), pp.102-110.
79. Mihaltan, F., RSV Burden of Disease in Adults-a new threat. *Pneumologia*, *71*(4), pp.195-201.
80. Mitra, R., Baviskar, P., Duncan-Decocq, R.R., Patel, D. and Oomens, A.G., 2012. The human respiratory syncytial virus matrix protein is required for maturation of viral filaments. *Journal of virology*, *86*(8), pp.4432-4443.
81. Mufson, M.A., Örvell, C., Rafnar, B. and Norrby, E., 1985. Two distinct subtypes of human respiratory syncytial virus. *Journal of general virology*, *66*(10), pp.2111-2124.
82. Mullard, A., 2024. FDA approves mRNA-based RSV vaccine. *Nature reviews. Drug discovery*.
83. Muñoz-Escalante, J.C., Comas-García, A., Bernal-Silva, S. and Noyola, D.E., 2021. Respiratory syncytial virus B sequence analysis reveals a novel early genotype. *Scientific reports*, *11*(1), p.3452.
84. Na, B., Park, Y.J., Seo, J., Park, M., Baek, J.Y., Lee, J.Y., Kim, M., Ahn, J.G., Lee, S.T. and Kang, J.M., 2024. Genotype Analysis of Respiratory Syncytial Virus Before and After the COVID-19 Pandemic Using Whole-Genome Sequencing: A Prospective, Single-Center Study in Korea From 2019 to 2022. *Journal of Korean Medical Science*, *39*(28).
85. Nduaguba, S.O., Tran, P.T., Choi, Y. and Winterstein, A.G., 2023. Respiratory syncytial virus reinfections among infants and young children in the United States, 2011–2019. *PLoS One*, *18*(2), p.e0281555.
86. Nam, H.H. and Ison, M.G., 2021, December. Respiratory syncytial virus. In *Seminars in Respiratory and Critical Care Medicine* (Vol. 42, No. 06, pp. 788-799). Thieme Medical Publishers, Inc.

87. Network, R.V.G.E., Li, Y., Wang, X., Blau, D.M., Caballero, M.T., Feikin, D.R., Gill, C.J., Madhi, S.A., Omer, S.B., Simões, E.A. and Campbell, H., 2022. Global, regional, and national disease burden estimates of acute lower respiratory infections due to respiratory syncytial virus in children younger than 5 years in 2019: a systematic analysis. *The Lancet*, *399*(10340), pp.2047-2064.
88. Ngwuta, J.O., Chen, M., Modjarrad, K., Joyce, M.G., Kanekiyo, M., Kumar, A., Yassine, H.M., Moin, S.M., Killikelly, A.M., Chuang, G.Y. and Druz, A., 2015. Prefusion F–specific antibodies determine the magnitude of RSV neutralizing activity in human sera. *Science translational medicine*, *7*(309), pp.309ra162-309ra162.
89. Nowalk, M.P., D'Agostino, H., Dauer, K., Stiegler, M., Zimmerman, R.K. and Balasubramani, G.K., 2022. Estimating the burden of adult hospitalized RSV infection including special populations. *Vaccine*, *40*(31), pp.4121-4127.
90. Ogunsemowo, O., Olaleye, D.O. and Odaibo, G.N., 2018. Genetic diversity of human respiratory syncytial virus circulating among children in Ibadan, Nigeria. *PLoS One*, *13*(1), p.e0191494.
91. Ooi, A., Wong, A., Esau, L., Lemtiri-Chlieh, F. and Gehring, C., 2016. A guide to transient expression of membrane proteins in HEK-293 cells for functional characterization. *Frontiers in physiology*, *7*, p.300.
92. Olsen, S.J., Winn, A.K., Budd, A.P., Prill, M.M., Steel, J., Midgley, C.M., Kniss, K., Burns, E., Rowe, T., Foust, A. and Jasso, G., 2021. Changes in influenza and other respiratory virus activity during the COVID‐19 pandemic—United States, 2020–2021. *American Journal of Transplantation*, *21*(10), pp.3481-3486.
93. Onwuchekwa, C., Moreo, L.M., Menon, S., Machado, B., Curcio, D., Kalina, W., Atwell, J.E., Gessner, B.D., Siapka, M., Agarwal, N. and Rubbrecht, M., 2023. Underascertainment of respiratory syncytial virus infection in adults due to diagnostic testing limitations: a systematic literature review and meta-analysis. *The Journal of infectious diseases*, *228*(2), pp.173-184.
94. Oraby, A.K., Stojic, A., Elawar, F., Bilawchuk, L., McClelland, R., Erwin, K., Granoski, M., Arutyunova, E., Lemieux, M.J., West, F. and Ramilo, O., 2024. A Single Amino Acid Mutation Alters the Neutralization Epitopes in the Respiratory Syncytial Virus Fusion Glycoprotein.
95. Otieno, J.R., Kamau, E.M., Oketch, J.W., Ngoi, J.M., Gichuki, A.M., Binter, Š., Otieno, G.P., Ngama, M., Agoti, C.N., Cane, P.A. and Kellam, P., 2018. Whole genome analysis of local Kenyan and global sequences unravels the epidemiological and molecular evolutionary dynamics of RSV genotype ON1 strains. *Virus evolution*, *4*(2), p. vey027.
96. Owji, H., Nezafat, N., Negahdaripour, M., Hajiebrahimi, A. and Ghasemi, Y., 2018. A comprehensive review of signal peptides: Structure, roles, and applications. *European journal of cell biology*, *97*(6), pp.422-441.
97. Peng, C., Shi, C., Cao, X., Li, Y., Liu, F. and Lu, F., 2019. Factors influencing recombinant protein secretion efficiency in gram-positive bacteria: signal peptide and beyond. *Frontiers in Bioengineering and Biotechnology*, *7*, p.139.

98. Petrocelli, P.A., Cunsolo, V., Melito, M., Scuderi, G., Testa, R., Messina, S., Tucci, F., Sardone, L., Colligiani, D., Nardone, M. and Rapi, S., 2023. Diagnosis of Syncytial Respiratory Virus (RSV) infection in children by Respiratory Panel utilized during the Covid-19 pandemic. *Annali dell'Istituto Superiore di Sanità*, *59*(1), pp.31-36.
99. Polack, F.P., Thomas, S.J., Kitchin, N., Absalon, J., Gurtman, A., Lockhart, S., Perez, J.L., Pérez Marc, G., Moreira, E.D., Zerbini, C. and Bailey, R., 2020. Safety and efficacy of the BNT162b2 mRNA Covid-19 vaccine. *New England journal of medicine*, *383*(27), pp.2603-2615.
100. Pretorius, M.A., van Niekerk, S., Tempia, S., Moyes, J., Cohen, C., Madhi, S.A., Venter, M. and SARI Surveillance Group, 2013. Replacement and positive evolution of subtype A and B respiratory syncytial virus G-protein genotypes from 1997–2012 in South Africa. *The Journal of infectious diseases*, *208*(suppl_3), pp. S227-S237.
101. Ramilo, O., Rodriguez-Fernandez, R. and Mejias, A., 2023. Respiratory syncytial virus infection: old challenges and new approaches. *The Journal of Infectious Diseases*, *228*(1), pp.4-7.
102. Redlberger‐Fritz, M., Springer, D.N., Aberle, S.W., Camp, J.V. and Aberle, J.H., 2023. Respiratory syncytial virus surge in 2022 caused by lineages already present before the COVID‐19 pandemic. *Journal of medical virology*, *95*(6), p.e28830.
103. Regev-Yochay, G., Gonen, T., Gilboa, M., Mandelboim, M., Indenbaum, V., Amit, S., Meltzer, L., Asraf, K., Cohen, C., Fluss, R. and Biber, A., 2022. Efficacy of a fourth dose of Covid-19 mRNA vaccine against Omicron. *New England Journal of Medicine*, *386*(14), pp.1377-1380.
104. Rezende, W., Neal, H.E., Dutch, R.E. and Piedra, P.A., 2023. The RSV F p27 peptide: Current knowledge, important questions. *Frontiers in Microbiology*, *14*, p.1219846.
105. Reicherz, F., Xu, R.Y., Abu-Raya, B., Majdoubi, A., Michalski, C., Golding, L., Stojic, A., Vineta, M., Granoski, M., Cieslak, Z. and Chacko, A., 2022. Waning immunity against respiratory syncytial virus during the coronavirus disease 2019 pandemic. *The Journal of infectious diseases*, *226*(12), pp.2064-2068.
106. Reimers, K., Buchholz, K. and Werchau, H., 2005. Respiratory syncytial virus M2-1 protein induces the activation of nuclear factor kappa B. *Virology*, *331*(2), pp.260-268.
107. Rios Guzman, E. and Hultquist, J.F., 2022. Clinical and biological consequences of respiratory syncytial virus genetic diversity. *Therapeutic Advances in Infectious Disease*, *9*, p.20499361221128091.
108. Rixon, H.W.M., Brown, G., Aitken, J., McDonald, T., Graham, S. and Sugrue, R.J., 2004. The small hydrophobic (SH) protein accumulates within lipid-raft structures of the Golgi complex during respiratory syncytial virus infection. *Journal of general virology*, *85*(5), pp.1153-1165.
109. Russell, C.J. and Govorkova, E.A., 2022. Novel Vaccines and Drugs That Target the Surface Glycoproteins of Influenza Viruses, RSV, Parainfluenza Viruses, and SARS-CoV-2. *Viruses*, *14*(6), p.1160.
110. Rodriguez-Fernandez, R., Tapia, L.I., Yang, C.F., Torres, J.P., Chavez-Bueno, S., Garcia, C., Jaramillo, L.M., Moore-Clingenpeel, M., Jafri, H.S., Peeples, M.E. and Piedra, P.A.,

2018. Respiratory syncytial virus genotypes, host immune profiles, and disease severity in young children hospitalized with bronchiolitis. *The Journal of Infectious Diseases*, *217*(1), pp.24-34.

111. Rodriguez-Fernandez, R., Mejias, A. and Ramilo, O., 2021. Monoclonal antibodies for prevention of respiratory syncytial virus infection. *The Pediatric infectious disease journal*, *40*(5S), pp.S35-S39.
112. Samy, N., Reichhardt, D., Schmidt, D., Chen, L.M., Silbernagl, G., Vidojkovic, S., Meyer, T.P., Jordan, E., Adams, T., Weidenthaler, H. and Stroukova, D., 2020. Safety and immunogenicity of novel modified vaccinia Ankara-vectored RSV vaccine: A randomized phase I clinical trial. *Vaccine*, *38*(11), pp.2608-2619.
113. Savic, M., Penders, Y., Shi, T., Branche, A. and Pirçon, J.Y., 2023. Respiratory syncytial virus disease burden in adults aged 60 years and older in high‐income countries: A systematic literature review and meta‐analysis. *Influenza and other respiratory viruses*, *17*(1), p.e13031.
114. Snapp, E.L., McCaul, N., Quandte, M., Cabartova, Z., Bontjer, I., Källgren, C., Nilsson, I., Land, A., Von Heijne, G., Sanders, R.W. and Braakman, I., 2017. Structure and topology around the cleavage site regulate post-translational cleavage of the HIV-1 gp160 signal peptide. *Elife*, *6*, p.e26067.
115. Sondlane, H., Ogunbayo, A., Donato, C., Mogotsi, M., Esona, M., Hallbauer, U., Bester, P., Goedhals, D. and Nyaga, M., 2024. Whole genome molecular analysis of respiratory syncytial virus pre and during the Covid-19 pandemic in free state province, South Africa. *Virus Research*, *347*, p.199421.
116. Sun, Z., Pan, Y., Jiang, S. and Lu, L., 2013. Respiratory syncytial virus entry inhibitors targeting the F protein. *Viruses*, *5*(1), pp.211-225.
117. Smyth, M., Khamina, K., Popa, A., Gudipati, V., Agerer, B., Lercher, A., Kosack, L., Endler, L., Baazim, H., Viczenczova, C. and Huppa, J.B., 2021. Characterization of CD8 T Cell-Mediated Mutations in the Immunodominant Epitope GP33-41 of Lymphocytic Choriomeningitis Virus. *Frontiers in Immunology*, *12*, p.22Shobugawa, Y., Saito, R., Sano, Y., Zaraket, H., Suzuki, Y., Kumaki, A., Dapat, I., Oguma, T., Yamaguchi, M. and Suzuki, H., 2009. Emerging genotypes of human respiratory syncytial virus subgroup A among patients in Japan. *Journal of clinical microbiology*, *47*(8), pp.2475-2482.
118. Streng, A., Goettler, D., Haerlein, M., Lehmann, L., Ulrich, K., Prifert, C., Krempl, C., Weißbrich, B. and Liese, J.G., 2019. Spread and clinical severity of respiratory syncytial virus A genotype ON1 in Germany, 2011–2017. *BMC Infectious Diseases*, *19*, pp.1-10.
119. Tabor, D.E., Fernandes, F., Langedijk, A.C., Wilkins, D., Lebbink, R.J., Tovchigrechko, A., Ruzin, A., Kragten-Tabatabaie, L., Jin, H., Esser, M.T. and Bont, L.J., 2020. Global molecular epidemiology of respiratory syncytial virus from the 2017− 2018 INFORM-RSV Study. *Journal of Clinical Microbiology*, *59*(1), pp. e01828-20.
120. Tada, H., Nohara, A. and Kawashiri, M.A., 2019. Monogenic, polygenic, and oligogenic familial hypercholesterolemia. *Current Opinion in Lipidology*, *30*(4), pp.300-306.

121. Taleb SA, Al Thani AA, Al Ansari K, Yassine HM. Human respiratory syncytial virus: pathogenesis, immune responses, and current vaccine approaches. European Journal of Clinical Microbiology & Infectious Diseases. 2018 Oct;37(10):1817-27.

122. Tang, J.W. and Loh, T.P., 2014. Correlations between climate factors and incidence—a contributor to RSV seasonality. *Reviews in medical virology*, *24*(1), pp.15-34.

123. Tapia, L.I., Shaw, C.A., Aideyan, L.O., Jewell, A.M., Dawson, B.C., Haq, T.R. and Piedra, P.A., 2014. Gene sequence variability of the three surface proteins of human respiratory syncytial virus (HRSV) in Texas. *PLoS One*, *9*(3), p.e90786.

124. Tejada, S., Martinez-Reviejo, R., Karakoc, H.N., Peña-López, Y., Manuel, O. and Rello, J., 2022. Ribavirin for treatment of subjects with respiratory syncytial virus-related infection: a systematic review and meta-analysis. *Advances in therapy*, *39*(9), pp.4037-4051.

125. Tempia, S., Walaza, S., Bhiman, J.N., McMorrow, M.L., Moyes, J., Mkhencele, T., Meiring, S., Quan, V., Bishop, K., McAnerney, J.M. and von Gottberg, A., 2021. Decline of influenza and respiratory syncytial virus detection in facility-based surveillance during the COVID-19 pandemic, South Africa, January to October 2020. *Eurosurveillance*, *26*(29), p.2001600.

126. Thornhill, E.M. and Verhoeven, D., 2020. Respiratory syncytial virus's non-structural proteins: masters of interference. *Frontiers in cellular and infection microbiology*, *10*, p.225.

127. Tran, T.L., Castagné, N., Dubosclard, V., Noinville, S., Koch, E., Moudjou, M., Henry, C., Bernard, J., Yeo, R.P. and Eléouët, J.F., 2009. The respiratory syncytial virus M2-1 protein forms tetramers and interacts with RNA and P in a competitive manner. *Journal of Virology*, *83*(13), pp.6363-6374.

128. Van Niekerk, S. and Venter, M., 2011. Replacement of previously circulating respiratory syncytial virus subtype B strains with the BA genotype in South Africa. *Journal of virology*, *85*(17), pp.8789-8797.

129. Van Royen, T., Rossey, I., Sedeyn, K., Schepens, B. and Saelens, X., 2022. How RSV proteins join forces to overcome the host innate immune response. *Viruses*, *14*(2), p.419.

130. van Summeren, J., Meijer, A., Aspelund, G., Casalegno, J.S., Erna, G., Hoang, U., Lina, B., study group in Lyon, V.R.S., de Lusignan, S., Teirlinck, A.C. and Thors, V., 2021. Low levels of respiratory syncytial virus activity in Europe during the 2020/21 season: what can we expect in the coming summer and autumn/winter? *Eurosurveillance*, *26*(29), p.2100639.

131. Venkatesan, P., 2022. Nirsevimab: a promising therapy for RSV. *The Lancet Microbe*, *3*(5), p.e335.

132. Wang, X., Shen, Y., Qiu, Y., Shi, Z., Shao, D., Chen, P., Tong, G. and Ma, Z., 2010. The non-structural (NS1) protein of influenza A virus associates with p53 and inhibits p53-mediated transcriptional activity and apoptosis. *Biochemical and biophysical research communications*, *395*(1), pp.141-145.

133. Williams, K., Bastian, A.R., Feldman, R.A., Omoruyi, E., de Paepe, E., Hendriks, J., van Zeeburg, H., Godeaux, O., Langedijk, J.P., Schuitemaker, H. and Sadoff, J., 2020. Phase

1 safety and immunogenicity study of a respiratory syncytial virus vaccine with an adenovirus 26 vector encoding prefusion F (Ad26. RSV. preF) in adults aged≥ 60 years. *The Journal of infectious diseases*, *222*(6), pp.979-988.

134. Wise, J., 2023. First RSV vaccine for older adults is approved in Europe. BMJ. 2023 Apr 28:381:978. doi: 10.1136/bmj.p978.
135. Yang, Z., Chen, Z. and Zhang, Y., 2022. A simple and economical site-directed mutagenesis method for large plasmids by direct transformation of two overlapping PCR fragments. *Biotechniques*, *73*(5), pp.227-233.
136. Yeoh, D.K., Foley, D.A., Minney-Smith, C.A., Martin, A.C., Mace, A.O., Sikazwe, C.T., Le, H., Levy, A., Blyth, C.C. and Moore, H.C., 2021. Impact of coronavirus disease 2019 public health measures on detections of influenza and respiratory syncytial virus in children during the 2020 Australian winter. *Clinical Infectious Diseases*, *72*(12), pp.2199-2202.
137. Yu, J.M., Fu, Y.H., Peng, X.L., Zheng, Y.P. and He, J.S., 2021. Genetic diversity and molecular evolution of human respiratory syncytial virus A and B. *Scientific Reports*, *11*(1), p.12941.
138. Zar, H.J., Bont, L.J., Manzoni, P., Munoz, F.M., Ramilo, O., Chen, P.Y., Novoa Pizarro, J.M., Ordonez, G.A., Tsolia, M., Tapiero, B. and Acuña, M., 2025, February. 167. Phase 3, Randomized, Controlled Trial Evaluating Safety, Efficacy, and Pharmacokinetics (PK) of Clesrovimab in Infants and Children at Increased Risk for Severe Respiratory Syncytial Virus (RSV) Disease. In *Open Forum Infectious Diseases* (Vol. 12, No. Supplement_1, pp. ofae631-004). US: Oxford University Press.
139. Zhang, N., Wang, L., Deng, X., Liang, R., Su, M., He, C., Hu, L., Su, Y., Ren, J., Yu, F. and Du, L., 2020. Recent advances in the detection of respiratory virus infection in humans. *Journal of medical virology*, *92*(4), pp.408-417.
140. Zheng, Z., Pitzer, V.E., Shapiro, E.D., Bont, L.J. and Weinberger, D.M., 2021. Estimation of the timing and intensity of reemergence of respiratory syncytial virus following the COVID-19 pandemic in the US. *JAMA network open*, *4*(12), pp.e2141779-e2141779.
141. Zhu, Q., McLellan, J.S., Kallewaard, N.L., Ulbrandt, N.D., Palaszynski, S., Zhang, J., Moldt, B., Khan, A., Svabek, C., McAuliffe, J.M. and Wrapp, D., 2017. A highly potent extended half-life antibody as a potential RSV vaccine surrogate for all infants. *Science translational medicine*, *9*(388), p.eaaj1928.

Appendices

Appendix A: Media, buffer and reagent

1. **LB Agar media preparation from powder**

16g of LB Agar medium into 500ml of distilled water was autoclaved at 121ºC and 15psi for 20 minutes. After the medium has cooled down, 500µl of kanamycin (100mg/ml) per 100ml prepared LB Agar was added. The final concentration of the kanamycin in the media was 50µg/ml.

2. **Preparing LB Agar from tablets**

10 tablets of the LB Agar (tablets) were added into 500ml of distilled water and autoclaved for 20 minutes.

3. **Preparation of LB medium broth for culturing (To pick single colonies)**

25g of LB broth was added into 1000ml of distilled water and autoclaved for 20 minutes. Then 500µl of kanamycin (100mg/ml) was added per 100ml of LB broth after cooling down. The broth was then poured into 15ml tubes at 3ml each as needed for miniprep bacterial cultures. Remaining broth with antibiotics was stored in the fridge.

4. **5M of NaCl**

Prepared by dissolving 146,1g of NaCl in 500ml distilled water

45. 1M Tris-HCl, pH 6,8

Dissolve 75,69g of Tris-base in 500ml of distilled water, then add 5ml of HCl.

5. **Lysis buffer preparation, 10ml**

1ml of 1M Tris-HCl, pH 6,8
2ml of 10% SDS
600µl of 5M NaCl
6.4ml sterile nuclease-free water, mix
Add 1 tablet protease inhibitor (Merck, Darmstadt, Germany) before use and store at 4ºC.

6. **Preparation of 1X running buffer from 10x.**

To make 1L of 1X running buffer, 100ml of 10X transfer buffer (Tris-Glycine 10X) was mixed with 900ml of deionized water.

7. **Transfer buffer**

To make 1L of 1X transfer buffer, 100ml of 10X transfer buffer, 200ml of methanol and 700ml of distilled water were mixed and stored at 4ºC.

8. Blocking buffer preparation

1X TBS, 0,1% Tween-20 with 5% of nonfat dry milk for 150ml

15ml of 10X TBS was added to 135ml distilled water and mixed, subsequently added 7.5g of nonfat dry milk and mixed well. While stirring, 0,15ml of Tween-20 (100%) was added and mixed. The buffer was stored at 4ºC until used for blocking.

9. Preparation of TBST (Tris-buffered saline, 0,1% Tween 20)

To make 1L of TBST wash buffer, 100ml of 10X TBS and 1ml of Tween 20 detergent were added to 900ml of distilled water.

10. Ponceau Stain preparation

0.1g of ponceau stain was added to 95ml of distilled water and 5ml of glacial acetic acid was added.

APPENDIX B: General information of the RSV-A fusion glycoprotein ORF mammalian expression plasmid.

Human respiratory syncytial virus (RSV) (subtype A, strain Long) Fusion glycoprotein / RSV-F (Codon Optimized) ORF mammalian expression plasmid, N-HA tag

Sino Biological Inc.
Biological Solution Specialist

Catalog Number: VG40039-NY

General Information

Gene : Human RSV (subtype A, strain Long) Fusion glycoprotein / RSV-F

Official Symbol : RSV-F

Synonym : F, HRSVgp08

Source : RSV

cDNA Size: 1725bp

Plasmid pCMV3-HA-RSV-F(A-long)

Description

Lot : Please refer to the label on the tube

Sequence Description :

A number of silent mutations were introduced into the DNA sequence in order to increase its protein expression level in mammalian cell system. The translated amino acid sequence is identical with P12568.1.

Restriction site : KpnI + XbaI (6kb + 1.75kb)

Vector : pCMV3-SP-N-HA

Shipping carrier :

Each tube contains approximately 10 μg of lyophilized plasmid.

Storage :

The lyophilized plasmid can be stored at ambient temperature for three months.

Quality control :

The plasmid is confirmed by full-length sequencing with primers in the sequencing primer list.

Sequencing primer list :

pCMV3-F↓	5' CAGGTGTCCACTCCCAGGTCCAAG 3'
pcDNA3-R↓	5' GGCAACTAGAAGGCACAGTCGAGG 3'
Or	
Forward T7↓	5' TAATACGACTCACTATAGGG 3'
ReverseBGH↓	5' TAGAAGGCACAGTCGAGG 3'

pCMV3-F and pcDNA3-R are designed by Sino Biological Inc.
Customers can order the primer pair from any oligonucleotide supplier.

Plasmid Resuspension protocol

1.Centrifuge at 5,000×g for 5 min.

2.Carefully open the tube and add 100 μl of sterile water to dissolve the DNA.

3.Close the tube and incubate for 10 minutes at room temperature.

4.Briefly vortex the tube and then do a quick spin to concentrate the liquid at the bottom. Speed is less than 5000×g.

5.Store the plasmid at -20℃.

The plasmid is ready for:

- Restriction enzyme digestion
- PCR amplification
- *E. coli* transformation
- DNA sequencing

E.coli strains for transformation (recommended but not limited)

Most commercially available competent cells are appropriate for the plasmid, e.g. TOP10, DH5α and TOP10F'.

Human respiratory syncytial virus (RSV) (subtype A, strain Long) Fusion glycoprotein / RSV-F (Codon Optimized) ORF mammalian expression plasmid, N-HA tag

Sino Biological Inc.
Biological Solution Specialist

Catalog Number: VG40039-NY

Vector Information

All of the pCMV vectors are designed for high-level stable and transient expression in mammalian hosts. High-level stable and non-replicative transient expression can be carried out in most mammalian cells. The vectors contain the following elements:

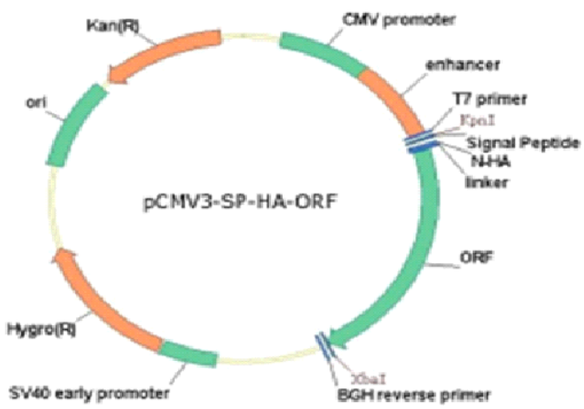
•Human enhanced cytomegalovirus immediate-early (CMV) promoter for high-level expression in a wide range of mammalian cells.

• Hygromycin resistance gene for selection of mammalian cell lines.

• A Kozak consensus sequence to enhance mammalian expression.

Vector Name	pCMV3-SP-N-HA
Vector Size	6146bp
Vector Type	Mammalian Expression Vector
Expression Method	Constiutive, Stable / Transient
Promoter	CMV
Antibiotic Resistance	Kanamycin
Selection In Mammalian Cells	Hygromycin
Protein Tag	HA

Physical Map of Plasmid :

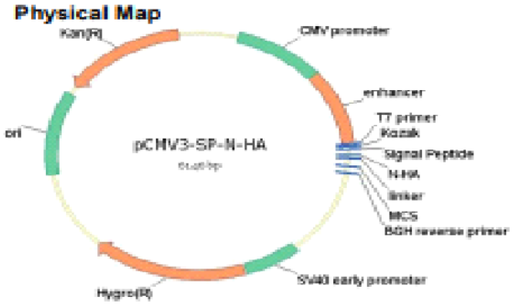


APPENDIX C: Control pCMV expression plasmid

pCMV3-SP-N-HA (suitable for secretary and membane protein expession)

Sino Biological Inc.
Biological Solution Specialist

Physical Map



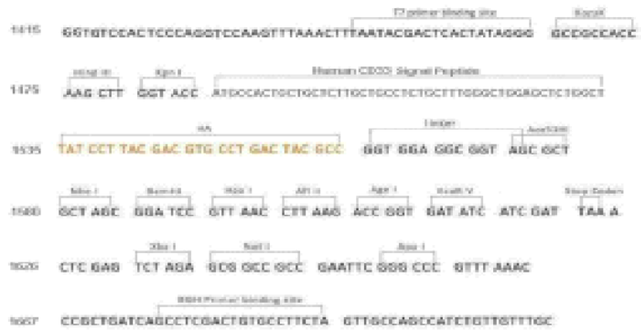
Comments for pCMV3-SP-N-HA:

CMV promoter: bases 250-837
enhancer: bases 838-1445
SV40 early promoter: bases 2387-2756
Hygromycin ORF: bases 2774-3799
pUC origin: bases 4442-5115
Kanamycin ORF: bases 5189-6004

Description

Vector Name	pCMV3-SP-N-HA
Vector Size	6146bp
Vector Type	Mammalian Expression Vector
Expression Method	Constitutive, Stable / Transient
Promoter	CMV
Antibiotic Resistance	Kanamycin
Selection In Mammalian Cells	Hygromycin
Protein Tag	HA
Sequencing Primer	Forward:T7(TAATACGACTCACTATAGGG) Reverse:BGH(TAGAAGGCACAGTCGAGG)

Schematic of pCMV3-SP-N-HA Multiple Cloning Sites



pCMV3-SP-N-HA is recommended for constructing the N-HA tag secretary and membrane proteins expression vector which containing a naïve signal peptide. An universal signal peptide is used to instead the naïve signal peptide.

APPENDIX D: Ethical clearance waiver approval letter

UNIVERSITY OF THE WITWATERSRAND JOHANNESBURG

R49 Ms T Mogawane

HUMAN RESEARCH ETHICS COMMITTEE (MEDICAL)
CLEARANCE CERTIFICATE NO. M230345

NAME: (Principal Investigator)	Ms T Mogawane
DEPARTMENT:	School of Pathology Department of Virology Medical School University
PROJECT TITLE:	*Impact of F proteins signal peptide mutations prevalent amongst African RSV strains on expression in vitro*
DATE CONSIDERED:	Ad hoc
DECISION:	Approved unconditionally
CONDITIONS:	
NOTE:	If contact information regarding student study participants is required, please contact the Registrar's office - <Nicoleen.Potgieter@wits.ac.za>
SUPERVISOR:	Dr F Treurnicht
APPROVED BY:	Dr CB Penny, Chairperson, HREC (Medical)
DATE OF APPROVAL:	2023/03/27

This Clearance Certificate is valid for 5 years from the date of approval. An extension may be applied for.

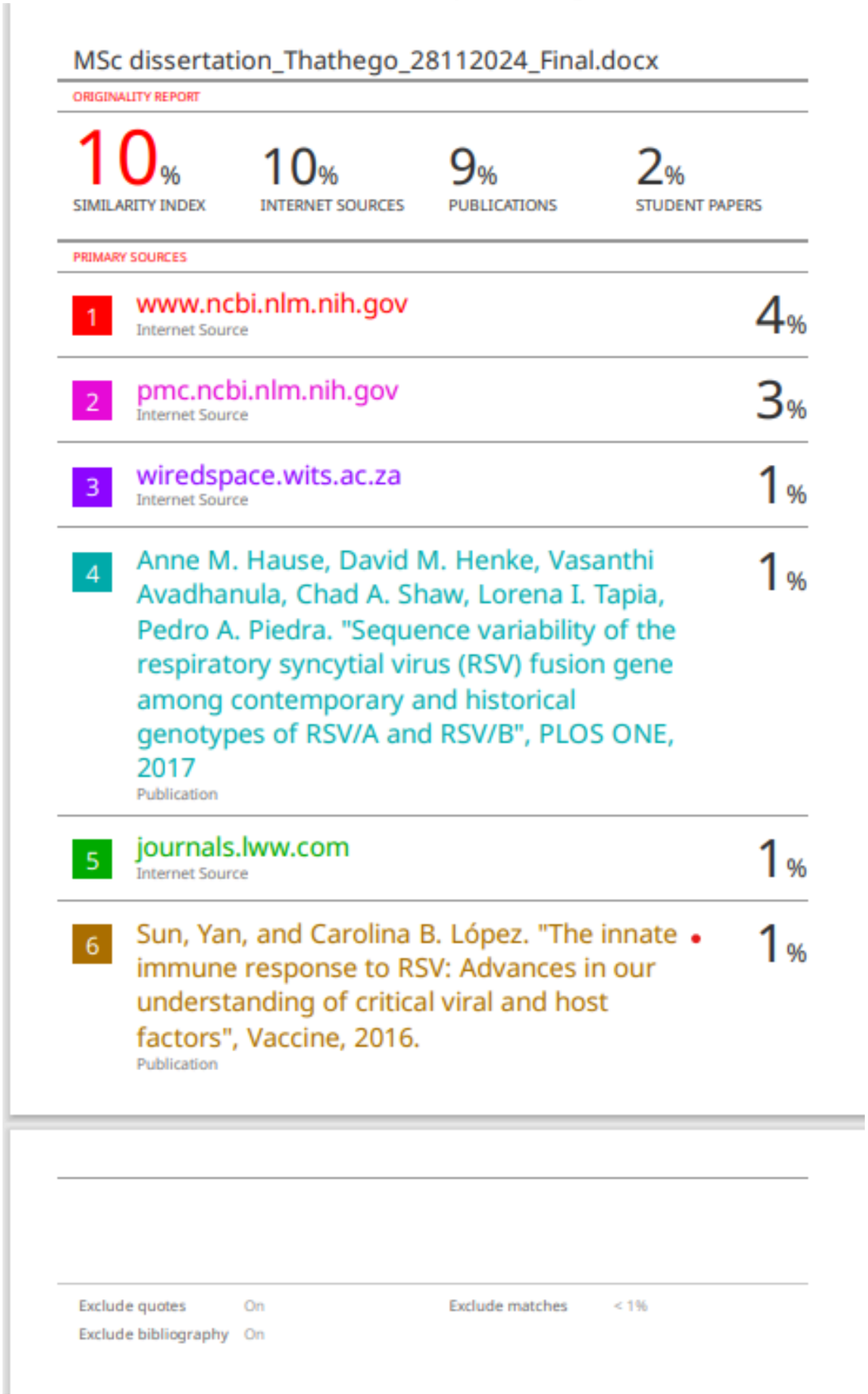
DECLARATION OF INVESTIGATORS

To be completed in duplicate and **ONE COPY** returned to the Research Office secretariat on the 3rd floor, Phillip Tobias Building, Parktown, University of the Witwatersrand, Johannesburg.

I/we fully understand the conditions under which I am/we are authorized to carry out the above-mentioned research and I/we undertake to ensure compliance with these conditions. Should any departure be contemplated from the research protocol as approved, I/we undertake to submit details to the Committee. **I agree to submit a yearly progress report.** When a funder requires annual re-certification, the application date will be one year after the date when the study was initially reviewed. In this case, the study was initially reviewed in **2023/02/01** and therefore reports and re-certification will be due in the month of **2023/02/01** each year. Unreported changes to the study may invalidate the clearance given by the HREC (Medical).

Signature of Principal Investigator _____ Date _____

APPENDIX E: Word count and Plagiarism report



MSc dissertation_Thathego_28112024_Final.docx

ORIGINALITY REPORT

10%	10%	9%	2%
SIMILARITY INDEX	INTERNET SOURCES	PUBLICATIONS	STUDENT PAPERS

PRIMARY SOURCES

1	www.ncbi.nlm.nih.gov Internet Source	4%
2	pmc.ncbi.nlm.nih.gov Internet Source	3%
3	wiredspace.wits.ac.za Internet Source	1%
4	Anne M. Hause, David M. Henke, Vasanthi Avadhanula, Chad A. Shaw, Lorena I. Tapia, Pedro A. Piedra. "Sequence variability of the respiratory syncytial virus (RSV) fusion gene among contemporary and historical genotypes of RSV/A and RSV/B", PLOS ONE, 2017 Publication	1%
5	journals.lww.com Internet Source	1%
6	Sun, Yan, and Carolina B. López. "The innate immune response to RSV: Advances in our understanding of critical viral and host factors", Vaccine, 2016. Publication	1%

Exclude quotes	On	Exclude matches	< 1%
Exclude bibliography	On		